EXPLORING THE UTILITY OF SEVERAL EVALUATION METHODS IN DISTINGUISHING CANNON BONES FROM FRACTURE-AFFLICTED AND SKELETALLY INTACT RACEHORSES

by

Jonathan E. Gaide

A Thesis

Submitted to the Faculty of Purdue University

In Partial Fulfillment of the Requirements for the degree of

Master of Science in Biomedical Engineering

Weldon School of Biomedical Engineering

West Lafayette, Indiana

December 2019

THE PURDUE UNIVERSITY GRADUATE SCHOOL
STATEMENT OF COMMITTEE APPROVAL

Dr. Russell P. Main, Chair
Department of Basic Medical Sciences, Weldon School of Biomedical Engineering

Dr. Timothy B. Lescun
Department of Veterinary Clinical Sciences

Dr. Thomas Siegmund
School of Mechanical Engineering

Approved by:
Dr. George R. Wodicka

Dedicated to my parents, Carrie and Bert, for their endless support

ACKNOWLEDGMENTS

First and foremost, I'd like to thank Dr. Russell Main for the years of support and guidance. I'm very grateful to have played a role in the remarkable research being conducted in his lab, and the time I've spent there has not only fortified my passion for research and science, but has championed my growth into the engineer I am today.

I'd also like to thank Dr. Tim Lescun for being an endlessly valuable resource and contributor to the project, and for continually challenging me to think critically and view things from different perspectives.

Xiaoyu Xu and Bayram Süzer formed a wonderful support system and were excellent role models throughout my time on this project. I'm grateful for their bright minds and helpful demeanors, and I'm excited to see the impact they continue to make on medicine in the future!

Lastly, I'd like to thank Tony Corsten, the PVM Diagnostic Imaging staff, Brennan Flannery, Max Hammond, Dr. Hsin-Yi Weng, Dr. Dianne Little, and Dr. Thomas Siegmund for the roles they've played in this experience. The project and my journey toward my degree would not have been possible without the gracious lending of time and talent from these individuals.

TABLE OF CONTENTS

LIST OF TABLES

LIST OF FIGURES

LIST OF ABBREVIATIONS

Abbreviation	Meaning
MC3	Third Metacarpal
SSMD	(Proximal Forelimb) Sesamoid
LB	Long Bone
C	Control
RPI	Reference Point Indentation
BMSi	Bone Material Strength Index
BMD	Bone mineral density
BMC	Bone mineral content
1st ID / ID1	First Indentation Distance
TID	Total Indentation Distance
avgED	Average Energy Dissipated
IDI	Indentation Distance Increase
CID	Creep Indentation Distance
avgCID	Average Creep Indentation Distance
ED	Energy Dissipated
US	Unloading Slope
avgUS	Average Unloading Slope
LS	Loading Slope
TDD	Touchdown Distance

ABSTRACT

Stress fractures are common in the limb bones of human and equine athletes alike. Repetitive skeletal loading can lead to remodeling and the accumulation of microdamage in bone, which only becomes grossly evident during catastrophic fracture of the bone due to the accumulated microdamage. Though various metrics attempting to quantify bone health exist, none have distinguished themselves as early predictors of the susceptibility of bone to fracture. In this exploratory study, we examine the ability of several evaluation methods to distinguish between third metacarpal (MC3) bones from racehorses that have experienced a limb-bone fracture and from those that have not. Third metacarpal bones were harvested from deceased Thoroughbred racehorses and categorized into four groups: MC3 bones from horses whose cause of death was not related to skeletal fracture (Control group, n = 20), MC3 bones form horses that were euthanized after fracturing proximal sesamoid bones (Sesamoid group, n = 20), MC3 bones from horses that were euthanized after fracturing a non-MC3 long bone (Long Bone group, n = 19), and MC3 bones from horses that were euthanized after fracturing an MC3 (MC3 group, n = 5). Each MC3 bone underwent testing using a variety of tools and methods at the proximal, midshaft, and distal levels of the lateral, dorsal, and medial surfaces. All tools and methods (OsteoProbe reference point indentation, BioDent reference point indentation, x-ray, micro-CT, and pQCT) exhibited some capability in differentiating between control and fracture groups. The long-term objective of this project is to create a model that will utilize data from a set of evaluations and output the susceptibility of the horse to fracture a bone, a long bone, or the MC3, specifically. Although the sample size in this study is not sufficient to create a reliably predictive logistic regression model, promising results from preliminary models provide incentive to further explore the possibility of creating one. While clinical practicality will be a vital consideration for a model in the future, establishing this basis for the capability of each evaluation at hand is a necessary first step in predicting and preventing fracture in bone.

1. INTRODUCTION

1.1 Background

The limbs of racehorses are subjected to a large number of high-magnitude loading events during their early lives. In full gallop, the forelimbs in the average Thoroughbred racehorse can experience compressive forces up to 26 N / kg, or approximately 2,870 lbf [1]. Healthy bones undergo modeling and remodeling during training to better withstand these forces; however, it's estimated that up to 2% of racing starts result in fracture [2], with between 0.3 and 1.7 in 1,000 starts resulting in fatal musculoskeletal injury [3-6]. These musculoskeletal failures contribute to the approximately 1,600 jockey injuries sustained at US racetracks each year, and the often resultant euthanasia of the horse sheds negative light on the $100 billion dollar horseracing industry from the public perspective [69].

Wolff's law asserts that healthy bone adapts to the loading conditions under which it is placed [7]. Though some details and derivations within this axiom have since been updated [8,9], the outlined principles have remained crucial to modern skeletal biomechanics research. Numerous theories have been proposed in an attempt to explain the mechanisms behind these geometric adaptations, including skeletal microdamage stimulating osteonal remodeling [70], piezoelectricity produced by collagen fibers [10], and, perhaps most widely-accepted, shear stress caused by interstitial fluid flowing through the lacunar-canalicular network in bone [11].

The modeling and remodeling processes that allow bones to be better suited to their loading conditions, however, are not instantaneous. A bone undergoing remodeling undergoes the resorption phase in 2 to 4 weeks, while bone deposition occurs more slowly over a span of multiple months [12]. Repetitive loading on an elastic material such as bone leads to material fatigue within the bone—the stresses experienced during high-force, cyclic loading can lead to microdamage in the bone tissue. Over time, this damage can accumulate into macroscopic cracks which may then lead to catastrophic fracture of the material. This fatigue can happen in any bone subjected to cyclical loading, and bone tissue left vulnerable due to the slow timeline inherent to the remodeling process may be even more susceptible to the formation of stress fractures or progression to catastrophic failure [13].

While there are proposed training regimens that promote healthy bone remodeling and reduce the rate of bucked shins or stress fracture by allowing adequate time for microdamage to heal and osteoblasts to deposit new tissue [14,15], the incidence of limb fracture in racehorses remains common. Though current clinical metrics and methods such as bone mineral density and radiography can provide a collection of information about the state of a bone's health, the predictive power in assessing the susceptibility of fracture is still rather low.

In humans, bone mineral density measurements standard for assessing bone health have been shown to correctly identify approximately 10% of fractured bones and 91% of non-fractured bones. A different method known as statistical shape and density modeling has been found to correctly identify 55% of fractured bones and nearly 95% of non-fractured bones [71]. When multiple factors are considered together, the predictive power increases. An assessment tool that utilizes a multivariable logistic regression models called the FRACTURE Index boasts an area under a receiver operating characteristic curve of almost 77%, nearing the 90% or 95% typically sought after in medical diagnostic tools [72].

1.2 Radiography

The relationship between bone mineral content (BMC), bone mineral density (BMD), and physical activity have long been studied [16,17]. In the mid-to-late 1900s, the gold standard in quantifying BMC in human clinical settings was x-ray spectrophotometry [18,19]; since then, however, multiple methods of characterizing the inorganic components of bone have arisen. Well-collimated scintillation detectors were implemented to improve upon the traditional x-ray approach [20], and multiple energies of x-ray were utilized to parse out soft tissue absorption in a method known as dual energy x-ray absorptiometry (DXA) [21]. DXA has since become a staple in diagnosing and monitoring osteoporosis [22], assessing the effects of drugs on the bones of postmenopausal women [23], or even quantifying a patient's visceral fat to predict his or her susceptibility to diabetes or heart disease [24]. Peripheral quantitative computed tomography (pQCT) measures volumetric bone mineral density (vBMD) rather than areal bone mineral density (aBMD) as in DXA. While vBMD is able to better adjust for different bone sizes (such as those in children) and can also provide geometric information about the bone that DXA cannot [25], its design inherently limits it to use in the appendicular skeleton, which has been shown to be a poor predictor of mineral density in sites of common fracture such as the proximal femur or spine [26].

Sound-based methods such as quantifying broadband ultrasonic attenuation and ultrasonic velocity have been developed, with apparent increasing effectiveness over time, as alternatives to methods dependent on radiation [27-29].

Various studies have attempted to quantify bone mineral parameters to assess bone health in racehorses. Horses that had undergone training were found to have significantly higher distal epiphyseal subchondral sagittal groove vBMD values than their untrained counterparts [30,31]. Additionally, trabecular BMD has been shown to significantly correlate with whole-bone breaking strength in the proximal phalanx [32]. BMD in bones from horses with or without fracture, however, show conflicting results. Some studies that examined the third metacarpal and proximal phalanx have reported no significant differences in BMD between control and fracture groups [31,33], while others have found that both the BMD and stiffness are significantly higher in bones from fracture groups than from control groups [34].

In human medicine, radiography is a staple of the diagnostic imaging field. X-ray imaging is used to locate and diagnose fractures, examine lung health, and even find cavities in teeth. In equine research, x-rays are often utilized as a noninvasive way to measure geometric properties of bone, particularly those of cortical bone. Finding bone length [35], cortical bone thickness [36,37], location and severity of fracture [38,39], or even history of fracture [40] are common uses of x-rays. Studies performed using x-rays have characterized geometric values in the appendicular bones of healthy thoroughbred racehorses [41]. These radiographic studies have also found correlations between exercise speed and cortical bone modeling [36] and have explored the effects of exposing bones to exogenous growth hormones [42]. Radiography is excellent at detecting fracture, osteoarthritis, and other visually-discernable maladies. However, radiology falls short of technologies such as magnetic resonance imaging to detect early stages of osseous disease or dysfunction [43], and limitations such as superimposition can inhibit accurate anatomic imaging or density measurements.

1.3 Reference Point Indentation

Reference point indentation (RPI) is an emerging technology that creates microindentations on the surface of a sample to gather information about its material properties. Determining the hardness of a material via indentation has been used for decades [44], often in metals and other engineered materials. Indentation techniques come in a variety of forms, from spherical to conical

& pyramidal indenters [45,46] and even nanometer-scale indentations [47]. While various methods for gathering information about bone using indentation have been proposed or performed [48-50], many would be difficult to utilize *in vivo*. Nanoindentation testing requires extremely precise contact angles and microscopic evaluation, both of which may be prohibitively difficult in a clinical setting and would likely require biopsies to be collected [51]. Many researchers have lately turned to one of two microindentation systems produced by Active Life Scientific, Inc. that have a greater potential clinical relevance than previously-used nanoindentation techniques. The OsteoProbe, a handheld single-impact device that has recently been approved for clinical use in Europe [52], returns a single parameter: bone material strength index (BMSi). Studies utilizing the OsteoProbe have elucidated differences between the bones of postmenopausal women with type 2 diabetes versus those without [53,54], have found correlations between BMSi in patients with a history of fragility fracture and those without [55,56], and have even discovered a relationship between low BMSi and chronic kidney disease [57]. The BioDent, a benchtop cyclic-RPI system, measures a number of parameters related to a bone's ability to resist microfracture than BMSi (Table 1.1).

Table 1.1. The BioDent system calculates parameters based on distance, stiffness, and plasticity. Listed below are each of the parameters and what a low outputted value for each indicates about the material properties of the sample [58].

Parameter	**↓ value means…**
1st-cycle Indentation Distance (1st ID)	Hard, dense, highly-mineralized
Total Indentation Distance (TID)	Resistant to crack propagation; tough*; high bone quality
Indentation Distance Increase (IDI)	Resistant to fracture; low brittleness of bone
Creep Indentation Distance (CID)	Tissue has low viscoelasticity, high damage susceptibility
Unloading Slope (US)	Low elastic modulus
Loading Slope (LS)	Low resistance to plastic deformation; not stiff
Average Energy Dissipated (ED)	Material resistant to plastic deformation

** Note: conflicting conclusions have been drawn on the degree of correlation between TID and material toughness*

Of the multiple BioDent parameters, IDI is considered to best correlate with whole-bone mechanical behavior [3]. Studies have found that IDI and TID were significantly decreased in tibiae from human patients that had experienced osteoporotic femoral fractures compared to control patients [59,68]. In horses, IDI has been found to be associated with training and fracture history. In a study in which the medial condyles of third metacarpal bones from 31 Thoroughbred racehorses were examined, IDI was found to be higher in untrained horses compared to horses undergoing race training, and higher in horses that had died as a result of a musculoskeletal injury compared to those with other causes of death [60]. These results suggest an increased resistance to indentation on the articular surface in horses that had undergone training and in those that were skeletally intact at the time of death, potentially indicating successful bone adaptation as a response to repetitive loading in accordance with Wolff's law in these groups.

1.4 Multivariable Regression Models

Many regression analyses take multiple explanatory or response variables into consideration. While one factor may correlate well with an outcome, the statistical model may be improved by introducing more explanatory variables, especially when the explanatory variables themselves do not correlate with one another [61]. One study in human cadavers compared fracture strength of the femoral neck to other clinical measurements such as areal bone mineral density, cortical porosity, RPI, and advanced glycation end-products. Each of these parameters alone proved to correlate well with fracture strength; however, when the same data were analyzed using a multiple linear regression model, it was found that combinations of BMD with any other parameter resulted in a higher correlation to fracture strength than any one variable alone [2]. Another study examining risk factors for proximal sesamoid fractures in Thoroughbred racehorses utilized a multivariable logistic regression to predict fracture risk based on a horse's sex, number and type of workouts, and distance run prior to death. It was discovered that fracture risk was higher in sexually-intact males than females and in horses that had run greater cumulative distances prior to their deaths [62].

1.5 Study Aims and Hypotheses

The primary purpose of this study was to explore and compare against one another multiple clinical and preclinical tools used in imaging or otherwise measuring bones. We first examined whether or not any tools or methods could be used to distinguish between third metacarpal bones from horses that have experienced a skeletal fracture and those that have not. Moving forward, we aimed to see if this distinction could be detected using only clinically relevant methods that may be suitable on a standing horse. These aims were undertaken to provide a basis for the ultimate goal of the project: to select a series of tests whose measurements can be used in a statistical model to compare a sample to known "intact" and "fractured" populations, effectively predicting the sample's susceptibility to fracture.

Multiple hypotheses have been formulated based on previously published results. Prior studies have found that bone mineral density correlates to whole-bone breaking strength in horse limbs [32], resistance to indentation correlates with training and fracture histories [60], and geometric parameters such as cross-sectional area correlate with training history [30]. Based on these results, we hypothesized that reference point indentation, CT, and x-ray imaging may provide powerful insight into the extent of healthy adaptation to loading and general health of a bone.

While a higher resistance to indentation on the surface of bone may seem to intuitively indicate a strong bone, it was hypothesized that high resistance to indentation may indicate higher susceptibility to fracture. Because the deposition of woven bone on the periosteal surface of bone is an indicator of healthy adaptation to loading, and because woven bone would presumably resist indentation less than lamellar bone, higher indentation distances were predicted to be seen in the control group than in the fracture groups.

More intuitively, greater BMD and geometric parameters such as cross-sectional area or cortical thickness were hypothesized to be associated with bones from horses that had not experienced fracture based on general mechanical principles. As bone is subjected to repetitive compression, apposition and mineralization are natural mechanisms to better support these forces.

Because third metacarpal bones tend to undergo modeling on the dorsal surfaces during training [30], it was hypothesized that this surface would be particularly conclusive in distinguishing between bones that were adapting properly to training and those that were not. Similarly, because distal condylar fractures are common in third metacarpal bones, it was hypothesized that the distal region (75% length or, in pQCT, 90% length) may be of interest when examining bone properties.

Ultimately, it was hypothesized that a number of clinically relevant tests could be used in concomitance to achieve the aim of the study: distinguishing with considerable power between bones from horses with a history of skeletal fracture or those without.

2. METHODS

2.1 Sample Collection and Selection

Thoroughbred racehorses from Indiana racetracks, when euthanized due to skeletal injury or died of causes not related to skeletal fracture, were sent to the Animal Disease Diagnostic Laboratory at Purdue University. Third metacarpal (MC3) bones were harvested during autopsy, wrapped in saline-soaked gauze, and frozen at -20° C. Horses were often transported to Purdue a day after death, resulting in a typical 24 – 30 hour time period between death and freezing of the third metacarpal bones. If a horse was autopsied on the same day on which it died, the third metacarpal bones would be refrigerated for approximately 24 hours prior to freezing to maintain consistency between horses.

Each set of MC3s was classified into one of four fracture groups based upon the reasons for euthanasia: Control (C), from horses that had died of causes not related to skeletal fracture; third metacarpal (MC3), from horses that had been euthanized due to MC3 fracture; Long Bone (LB), from horses that had been euthanized due to a non-MC3 fracture such as a tibial fracture; and Sesamoid (SSMD), from horses that had been euthanized due to a proximal sesamoid fracture. Among these groups, sample sizes for the present study were chosen based upon the data from a previous study and from the availability of bones. For C, LB, and SSMD groups, a sample size of n=20 for each group was selected. A sample size of n=5 was acquired for the MC3 group, as fewer horses with this specific fracture type were available. We had an additional n=5 that could be considered for the MC3 group, but MC3 fracture often coincided with fracture of neighboring bones as well. These samples were excluded from this study to minimize confounding factors within experimental groups.

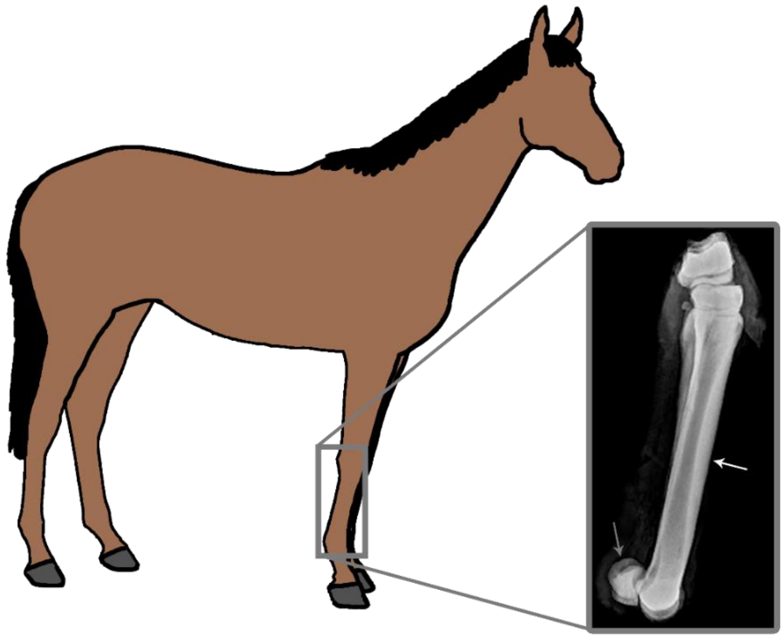

Figure 2.1. Third metacarpal bones (white arrow) were collected from deceased Thoroughbred racehorses. Proximal sesamoids (gray arrow) are a common site of fracture in racehorses.

The experimental groups were age- and sex-matched. When a one-way ANOVA test was performed, neither age (p = 0.069) nor mass (p = 0.329) returned significant differences. To accommodate for the small sample size of the MC3 group, a separate one-way ANOVA was performed between the C and SSMD groups and a combined LB / MC3 group. This resulted in a significant difference in age (p = 0.028), but not in mass (p = .284). Though the difference in age was considered statistically significant, the largest discrepancy of average age between groups was approximately 9 months—given the variation within the data and intuitive discretion, it was concluded that age would not be necessary to include as a confounding factor.

During the study, it was discovered that a pair of bones belonging to the LB group were 13% longer than the average MC3 in the study and nearly 2 cm longer than the next longest bone. Although variation is to be expected, these bones were deemed as a likely mislabeled set of third metatarsals and were disqualified from the study (LB group: n = 19).

2.2 X-ray

X-ray imaging was utilized to measure the cortical thickness in each bone being studied. Two dimensional digital radiographic images of the third metacarpal bones were taken by technicians in the Diagnostic Imaging Department at the Purdue Veterinary Teaching Hospital using x-ray equipment by GE. X-rays were taken while the bones were frozen. The bones being x-rayed may have undergone 0 – 2 freeze-thaw cycles prior to imaging, though this is not expected to significantly affect cortical thickness. Two images were taken of each pair of bones: one in the dorsal / palmar view, and one in the medial / lateral view. Prior to imaging, radiopaque "left" and "right" markers were used to differentiate the bones, and a 10-mm scale ball was positioned between or beside the bones to assist in later analysis (Figure 2.2).

Keystone software (Asteris, Inc.) was used to analyze the thickness of cortical bone at 25%, 50%, and 75% of the length of the bone along the dorsal, palmar, lateral, and medial surfaces, where 25% is near the proximal end of the MC3. The software's "Calibrate" capability was utilized with the 10-mm scale ball, followed by use of the "Length" tool to find locations at 25%, 50%, and 75% of the bone's length (in the proximal-to-distal direction). Finally, the "Length" tool was used to measure the cortical thickness at each site. Medial and lateral cortical thicknesses were determined using images taken in the dorsal / palmar view, and dorsal and palmar cortical thickness were determined using the medial / lateral view.

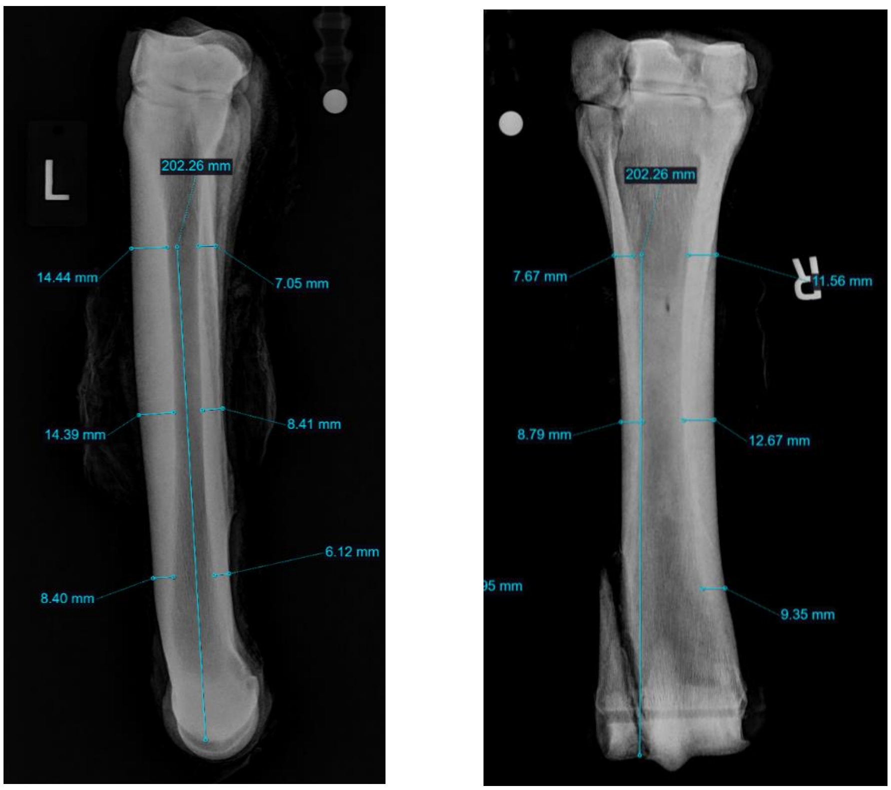

Figure 2.2. Cortical thickness measurements taken where possible at 25%, 50%, and 75% lengths from x-ray images taken from medial-lateral (left) and anterior-posterior (right) views. 10mm scale ball and left/right markers can also be seen. The annotation running down the length of the bone, shown here at the 25% position, was used to visualize where to take cortical thickness measurements.

2.3 OsteoProbe

Impact microindentation to determine the bone material strength index (BMSi) at 12 different sites along each bone was achieved using the OsteoProbe handheld microindentation tool (Active Life Scientific, Inc.).

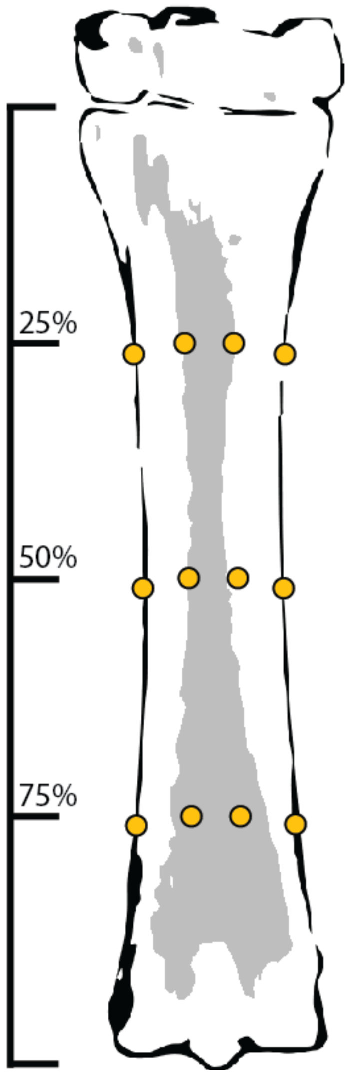

Figure 2.3. OsteoProbe indentations are made at 12 sites on each bone. The dorsal surface is avoided to simulate avoiding the digital extensor tendon *in vivo.*

When bones were harvested with skin still intact, initial OsteoProbe testing was performed through the skin to simulate clinical use. Ten percutaneous indentations, followed by 5 indentations on a block of polymethyl methacrylate (PMMA) for normalization purposes, were performed on the lateral, medial, dorsolateral, and dorsomedial surfaces at 25, 50, and 75% of the length of the bone. Indentations were taken at dorsolateral and dorsomedial surfaces, rather than on the dorsal surface, to avoid the common digital extensor tendon spanning the dorsal surface of the third metacarpal bone (Figure 2.3). OsteoProbe testing was typically performed after 1 freeze-thaw cycle, though the number of cycles at the time of testing for samples in this dataset ranges from 0 to 2.

During testing, the third metacarpal bones were held in place by a bench vice padded with paper towels, with the dorsal surface facing upright while collecting measurements on the dorsolateral and dorsomedial surfaces, the lateral surface upright while collecting measurements on the lateral surface, and the medial surface upright while collecting measurements along the medial surface. Holding the OsteoProbe in one hand, the skin at the site of indentation was held taut during testing by the operator's other hand. Ten 5 N indentations approximately 1 mm apart were made at each testing site, immediately followed by five 5 N indentations on a block of homogeneous PMMA for use in data normalization performed by OsteoProbe software.

After percutaneous OsteoProbe measurements were performed at all 12 sites of a bone, the skin and tendons were removed using a dissecting knife and scalpel. At the planes of 25, 50, and 75% of the bone length, areas approximately 1 inch wide and spanning the dorsal surface from the lateral to the medial surface were cleared of periosteum and remaining connective tissue using a scalpel and periosteal elevator.

OsteoProbe testing was then repeated on the exposed bone surface at each site on the third metacarpal, following the previous protocol with the exception of the skin being held taut. Sites of indentations made during percutaneous testing were visually located and avoided by at least 1 – 2 mm.

2.4 BioDent

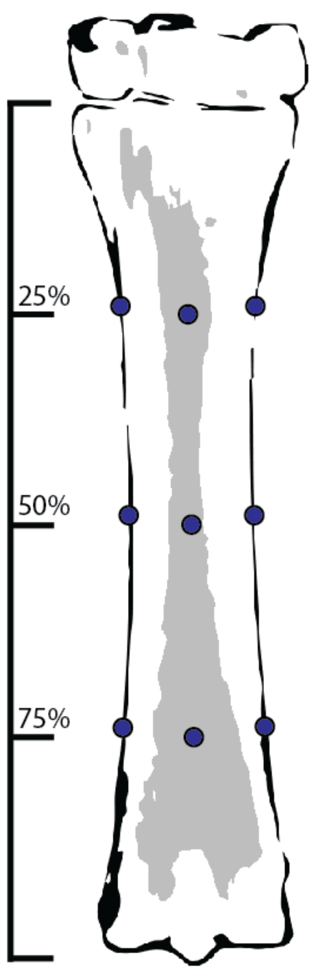

Figure 2.4. BioDent indentations are made at 9 locations on each bone. The dorsal surface is not avoided because the BioDent's benchtop setup is not considered clinically relevant.

Immediately following OsteoProbe measurements taken directly on the bone, cyclic reference point indentation testing was performed using the BioDent benchtop microindentation system (Active Life Scientific, Inc.). Where possible, BioDent testing was performed during the same freeze-thaw cycle as OsteoProbe testing. This was achieved in all but 6 samples in this study. In all bones except anomalous cases in this data set, indentation testing was performed on thawed bones after they had been frozen once. Though it has been shown that the number of freeze-thaw cycles does not have a significant effect on RPI measurements [73], consistency was striven for throughout the study. Testing was performed at the 25, 50, and 75% length sites along the dorsal, medial, and lateral surfaces of the bones. Unlike OsteoProbe testing, the dorsal surface was measured in place of the dorsolateral and dorsomedial surfaces. Because of the benchtop restrictions of the BioDent equipment, percutaneous measurements were not deemed clinically relevant and avoidance of the common digital extensor tendon was therefore not considered.

Prior to testing each bone, measurements on a homogeneous PMMA block were made in "tuning mode" until a Touchdown Distance of 150 – 200 microns was achieved. Bones were placed inside a stainless-steel pan for stability and sanitation purposes during testing, and the distal end of the bone was propped up on wetted paper towels when necessary for the testing surface to be perpendicular to the indentation probe. When testing the medial and lateral surfaces, bones were propped up using a sand-filled zipper-lock sandwich bag and secured to the metal pan using a C-clamp.

At each site, the "BP2" reference probe was lowered onto the surface of the bone until a force between 1,300 and 1,350 grams was achieved. BP2 probes are described by the manufacturer as semi-sharp probes with blunt ends, and are recommended for testing done on excised bone. The testing protocol was then cycled, with the test probe first initiating 4 pre-load cycles of 1 N at 5 Hz to penetrate any periosteum that may have remained on the bone's surface. 10 cycles at 40 N at a frequency of 2 Hz were then performed to collect and calculate data with parameters regarding distance, stiffness, and plasticity. Each indentation could be broken into three phases: a loading phase, a holding phase, and an unloading phase. The holding phase described when the probe maintained a constant, maximum force (40 N) for one-third of the measurement cycle (approximately 0.17 seconds). Three (or up to 6, depending on variability of data collected) sets of cycles were performed at each testing location, each at least 1 mm away from prior indentation sites.

As outlined in Table 1.1, seven types of metrics are automatically collected during indentation: 1st cycle indentation distance, total indentation distance, indentation distance increase, creep indentation distance, loading slope, unloading slope, and average energy dissipated. Total indentation distance (TID) and indentation distance increase (IDI) have been used widely in existing literature due to their potential ability to express the overall quality of bone and bone brittleness, respectively. Active Life Scientific also asserted that average energy dissipated (avg ED) may have been closely associated with the formation of microdamage in bone, which made this parameter also particularly relevant to the nature of this study. While parameters aside from TID, IDI, and avg ED were collected and examined, little emphasis was placed on their analysis due to the lack of reported results in previous studies and the consideration of what information they conveyed about the bone tissue.

2.5 Peripheral Quantitative Computed Tomography (pQCT)

pQCT measurements were taken using XCT 3000 equipment produced by Stratec, SE. Data was collected at five planes along the bone: the 25%, 50%, and 75% lengths as used in x-ray and indentation measures, as well as the 10% and 90% lengths to capture the metaphyses of the bone (Figure 2.5).

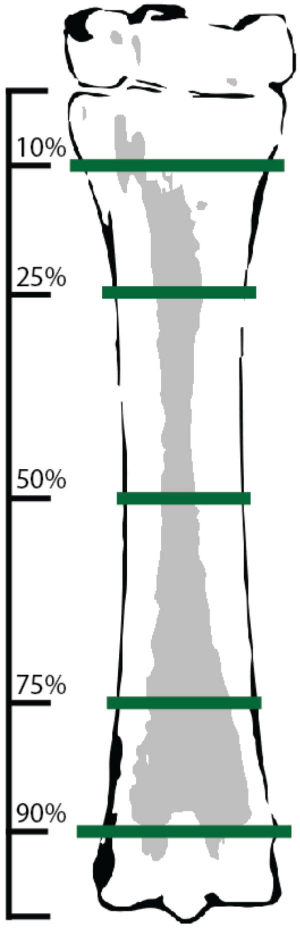

Figure 2.5. pQCT scans were taken at the planes corresponding to 10%, 25%, 50%, 75%, and 90% the length of each bone.

The locations of the planes were determined using length measurements obtained from x-rays taken previously. Voxel size was 0.1 mm × 0.1 mm × 2.2 mm, with the 2.2 mm side running parallel to the length of the bone. Bone was differentiated from surrounding tissue using a macro (courtesy of Dan Schiferl; Bone Diagnostics, Inc.) utilizing user-defined thresholding based on the magnitude of attenuation at each voxel. The thresholding assumes that fat has a density of 0 mg/mm^3, water and soft tissue have a density of 60 mg/mm^3, trabecular bone has a density of 700 mg/mm^3, and cortical bone has a density of 1,200 mg/mm^3. The macro used these defined values to measure 25 parameters from each image (Table 3.1).

The degree of attenuation, translated to density for the purposes of our study, was used to distinguish between cortical bone, trabecular bone, and surrounding material or tissue. At the 10%, 25%, 50%, and 75% levels, trabeculae were automatically contoured using a threshold value of 711 mg/mm^3. At the 90% level, a value of 169 mg/mm^3 was used. To locate the endosteal surface, a similar algorithm utilized thresholds of 900 mg/mm^3 at the 10% and 75% levels, 600 mg/mm^3 at 25% and 50% levels, and 1,200 mg/mm^3 at the 90% level. To ensure that no cortical bone was included in the trabecular measurements, the endosteal perimeter was contracted by 5%.

When imaging bones from the MC3 experimental group, medical tape was used to secure fractured pieces of the bone together, where possible. Values at sites affected by comminuted fracture were imputed.

2.6 Micro-Computed Tomography (μCT)

μCT images were taken using Quantum GX equipment produced by PerkinElmer Inc. Data was collected along the lateral, medial, and dorsal surfaces at 50% the length of each right-side bone in randomly selected samples from the C and LB experimental groups (n_C = 10, n_{LB} = 6) (Figure 2.6). The number of samples tested were determined primarily by financial restrictions, and exclusion of the MC3 and SSMD groups allowed for sample sizes adequate for statistical comparison between the C and LB groups. Factors such as difficultly in imaging fractured or fragmented bones in the MC3 group and the pathogenesis of proximal sesamoid fractures and their relevance to third metacarpal bones were also taken into consideration.

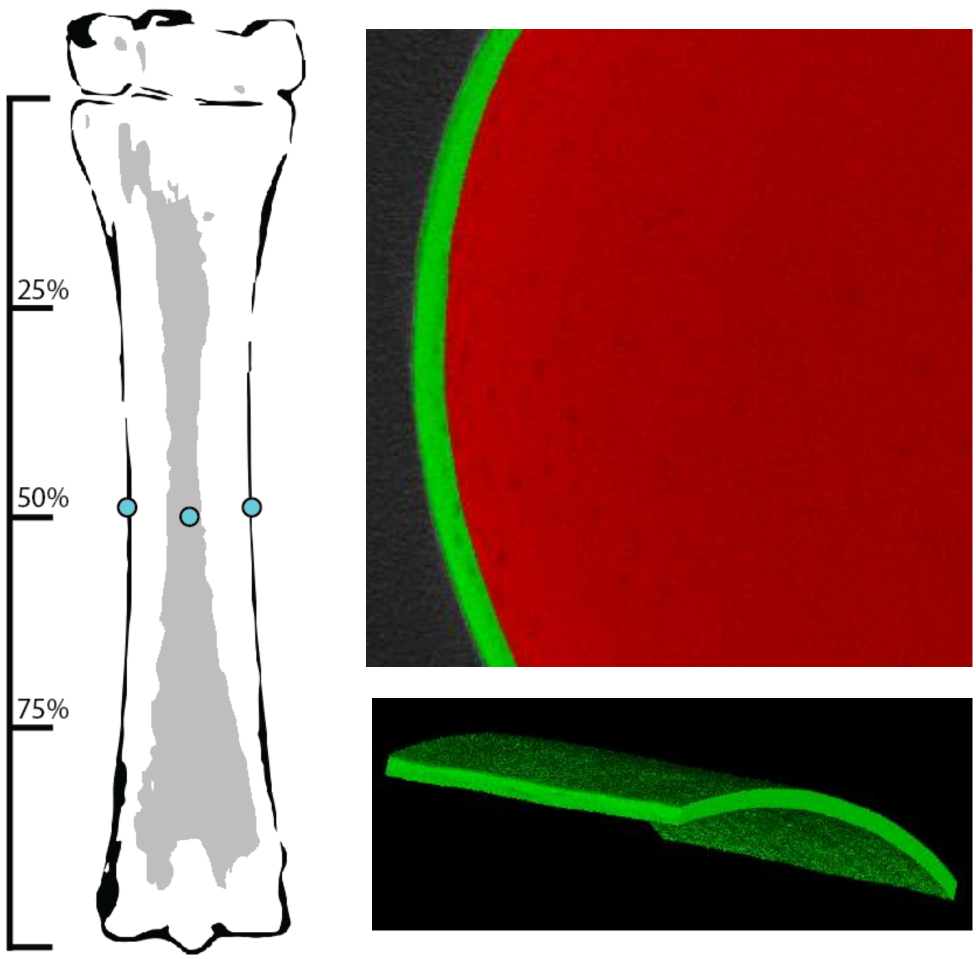

Figure 2.6. Left: μCT images were taken at the plane corresponding to 50% of the length of each bone, and BMD measurements were made at the corresponding dorsal, medial, and lateral surfaces. Top right: the outer 550 μm of the bone was eroded in AnalyzePro software. Bottom right: isolated example 15 mm2 region of analysis.

Room-temperature bones were secured to the bed with medical tape and scanned at the 50% length plane at 90 kV and 88 mA, a process taking approximately 14 minutes per bone. A voxel resolution of 11 microns was achieved for each image. After this initial scan, 15 mm^2 areas were selected at the dorsal, medial, and lateral surfaces on which to take subvolume images and bone mineral density measurements.

AnalyzePro software produced by AnalyzeDirect, Inc. was used to analyze the subvolume images. The bone surface was eroded 550 μm and isolated in order to analyze only the periosteal surface of each sample (Figure 2.6). This surface was of interest because of its physiological relevance in bone modeling and because it was the same approximate tissue on which indentation testing was performed. Subvolume images were also examined visually to inspect for potential signs of bone modeling such as woven bone along the periosteal surfaces.

2.7 Statistics

Statistical tests were carried out using IBM SPSS Statistics 24, unless otherwise noted. Before inter-group analysis was performed, measurements from right and left limbs in each horse were compared against one another via paired t-test. To avoid unnecessary confounding variation, samples were grouped by experimental group and location: for example, each cortical thickness value on the dorsal surface at the 75% length location in the Control group was included in one test.

It was necessary to consider Family-wise error rates when dealing with a large volume of comparisons. The likelihood of type I errors, or false positives, increases as multiple hypothesis tests are performed at once due to the nature of the tests themselves. Controlling procedures such as Bonferroni or Šidák corrections can be implemented to account for this phenomenon. Here, Bonferroni corrections for multiple comparisons were implemented in each paired t-test by dividing the critical p-value by the number of comparisons being performed with each test. If the test found no relevant significant ($p < 0.05 / n$) differences between measurements taken on right and left limbs of a given horse, the contralateral measurements were averaged together in an attempt to provide a more complete picture of each horse without the need to manage two sets of data or arbitrarily selecting a single limb. If significant differences were discovered, logical discretion was used to dictate whether left and right values should be averaged together for analysis.

A custom syntax was created for comparing data by site and experimental group: a linear fixed effect model with site, group, and site * group interactions as fixed effects and individual horses as random effects (with default covariance type for random effects, *variance components*, selected). The model utilizes restricted maximum likelihood (REML) methods as opposed to ANOVA, as REML is able to more effectively manage unbalanced experimental designs and also allows for inferences about covariance factors in the model. Bonferroni adjustments were implemented to control for the multiple comparisons being made in each test. A critical p-value of 0.05 selected for use with the linear model. The syntax with an example parameter of interest is shown in Figure 2.7.

```
MIXED BMSi BY site group horseno
  /CRITERIA=CIN(95) MXITER(100) MXSTEP(5) SCORING(1) SINGULAR(0.000000000001) HCONVERGE(0,
    ABSOLUTE) LCONVERGE(0, ABSOLUTE) PCONVERGE(0.000001, ABSOLUTE)
  /FIXED=site group site*group | SSTYPE(3)
  /METHOD=REML
  /RANDOM=horseno  | COVTYPE(VC)
  /EMMEANS=TABLES(site) compare(site) ADJ(BONFERRONI)
 /EMMEANS=TABLES(group) compare(group) ADJ(BONFERRONI)
 /EMMEANS=TABLES(site*group) compare(site) ADJ(BONFERRONI)
 /EMMEANS=TABLES(site*group) compare(group) ADJ(BONFERRONI)
```

Figure 2.7. A linear mixed model was created in SPSS Statistics to analyze data (here, BMSi) with effects being test location (site), experimental group (group), and individual horse (horseno).

For each test, each of the four experimental groups were initially included in the linear mixed model. After obtaining these results, the LB and MC3 groups were combined into one group and the test was run again. This was done to account for the small sample size of the MC3 group and because third metacarpal bones are a type of long bones. Mann-Whitney tests were performed for each metric between bones in the LB and MC3 groups to determine if they were functionally equivalent for the purposes of this study.

If an individual comparison was to be made between more than two fracture groups, one-way ANOVA tests were performed in SPSS. Post-hoc Tukey and Bonferroni tests were utilized to gain further insights into the results, when appropriate.

To explore observed intra-bone differences in percutaneous BMSi between different experimental groups, a proxy variable obtained by taking the differences in BMSi between the medial and dorsolateral surfaces at each length was created. These surfaces were selected based on the medial surfaces being the apparent sites of highest BMSi and the dorsolateral surface tending to have lower values. The dorsomedial surface could have also acted as the surface to which the medial surface was compared. The values obtained by taking the differences at the midshaft of the bones, where the strongest trend of this pattern was observed, were compared using one-way ANOVA.

2.8 Multivariable Regression Model

At the time of this study, the predictive statistical model was still in its infancy. MedCalc statistical software was used to perform logistic regression analyses on collections of data based primarily on educated discretion rather than sensitivity analyses. Due to the perceived physiological relevance of and observed intergroup differences at the 50% dorsal site on third metacarpal bones, all included data was collected from this location unless otherwise noted.

First, all variables were analyzed using a logistic regression model in isolation to determine their capability in distinguishing between bones from horses with or without fracture and whether or not they might be of use in models including multiple variables. Because regression models only allow dichotomous outputs, experimental groups were divided into Control and Fracture (SSMD, LB, and MC3 consolidated into one group). Receiver operating characteristic (ROC) curves were built from the logistic regression data, with the area under the curve (AUC) serving as an indicator of how much predictive power the model may possess.

When moving forward with selecting which variables to include in the next iteration of the model, the perceived utility, collinearity with other variables, and clinical relevance were considered. The first multivariable model was assembled prior to complete collection of pQCT data and included TID, avg ED, no-skin BMSi, and cortical thickness due to promising results seen throughout this study. A next iteration of the model, containing only clinically relevant parameters (percutaneous BMSi, cortical thickness, and mass of the horse) was then compiled. After completion of pQCT data collection, a final iteration was produced that included parameters selected for their perceived uniqueness, clinical relevance, and capability: BMD at 90% length, the difference in BMSi at the dorsolateral and medial sites at 50% length, and cortical thickness at the mid-dorsal surface. Each of these parameters could feasibly be measured in a standing horse, each examined a different property of bone, and each detected significant differences between experimental groups in this study.

3. RESULTS

3.1 Left & Right Limb Comparison

In this study, measurements were taken on both left and right third metacarpal bones in each horse when possible. However, in a clinical setting, testing would be more cost- and time-efficient if only one leg was measured. Additionally, being able to average left and right measurements together would make the data analysis in this study more concise and discernable. To validate that measurements from right and left limbs do not significantly differ from one another, paired t-tests were performed at each test location within each fracture group with Bonferroni correction of the p-value for multiple comparisons. Bonferroni corrections were performed by dividing the standard p-value of 0.05 by the number of statistical tests being performed simultaneously. If no significant differences were not discovered, the mean of the values from the left and right bones were used in analysis. If significant differences were discovered, logical discretion was used to dictate whether left and right values should be averaged together for analysis.

The MC3 fracture group was not subjected to left-right paired t-tests due to a lack of intact left / right pairs (n=1) leading to prohibitively small sample sizes. Left / right testing was also not performed with μCT data because only right limbs were tested.

3.1.1 X-ray

No significant differences were discovered between left and right bones in any of the experimental groups after the Bonferroni correction ($p < 0.006$) for multiple comparisons was implemented. Contralateral MC3 bones were rarely found to have the exact same length, though no significant differences existed when left and right limbs were compared via paired t-test or independent sample t-test. When cortical thicknesses were normalized by the length of the bone itself, there remained no significant differences between left and right limbs in any experimental group.

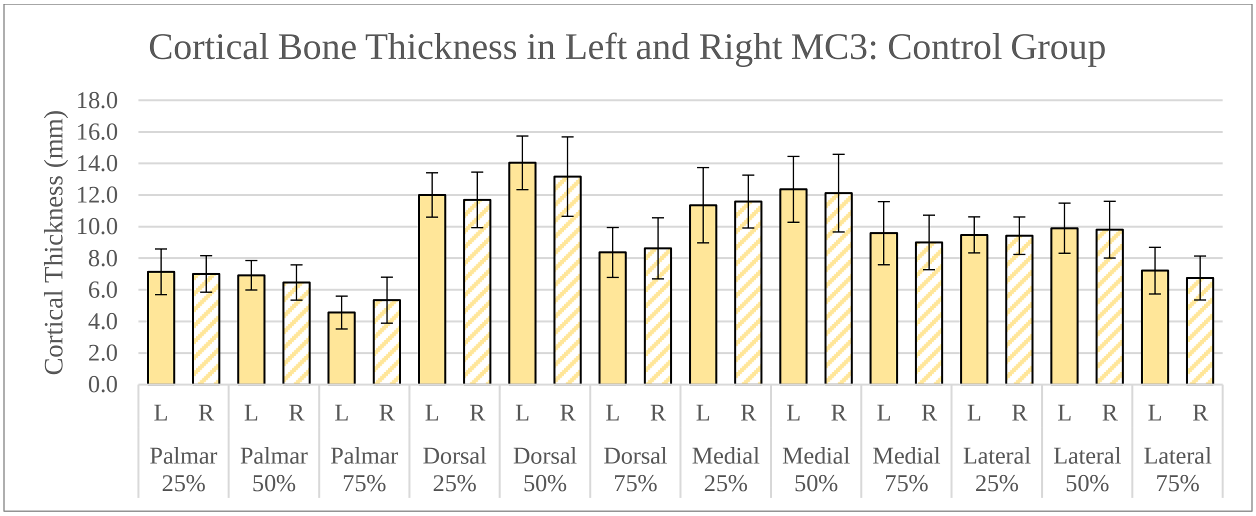

Figure 3.1. No significant ($p < 0.006$) differences between left and right MC3 cortical thickness in C group. ($n = 20$). Bar and error bars represent mean ± 1 standard deviation. Paired t-test.

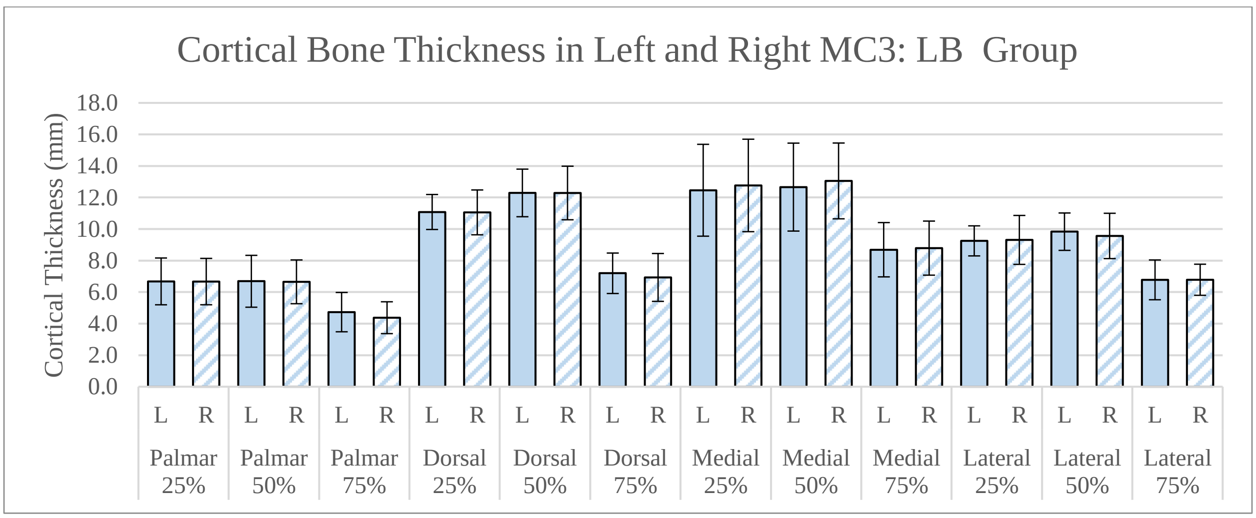

Figure 3.2. No significant ($p < 0.006$) differences between left and right MC3 cortical thickness in LB group. ($n = 19$). Bar and error bars represent mean ± 1 standard deviation. Paired t-test.

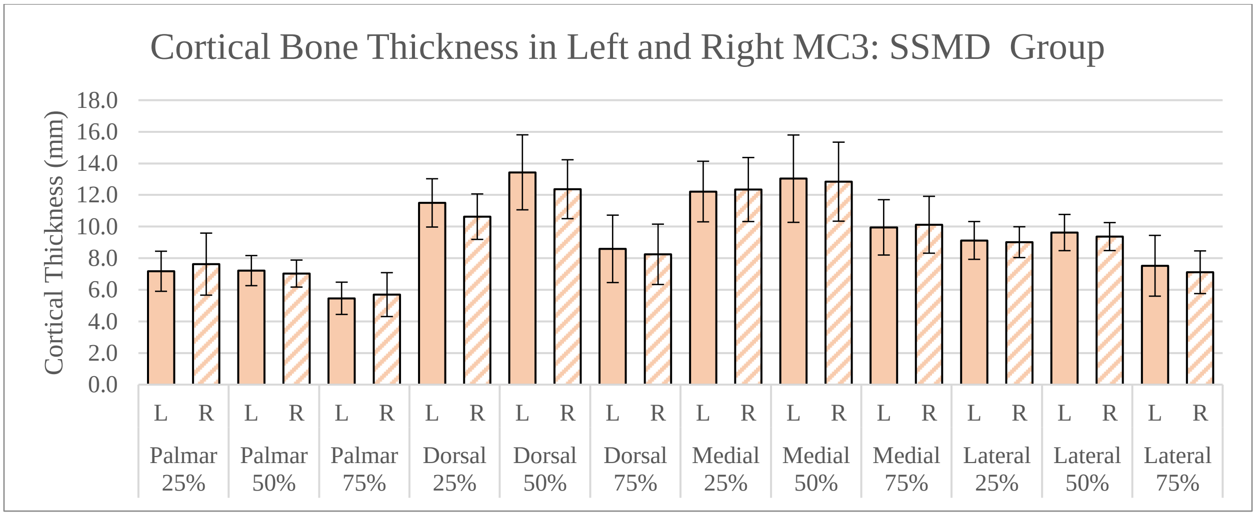

Figure 3.3. No significant (p < 0.006) differences between left and right MC3 cortical thickness in SSMD group.. (n = 19). Bar and error bars represent mean ± 1 standard deviation. Paired t-test.

3.1.2 OsteoProbe

Skin-on

Paired t-tests with Bonferroni correction for multiple comparisons were performed at each site within each experimental group. No significant (p < 0.004) differences in percutaneous BMSi between left and right third metacarpal bones existed.

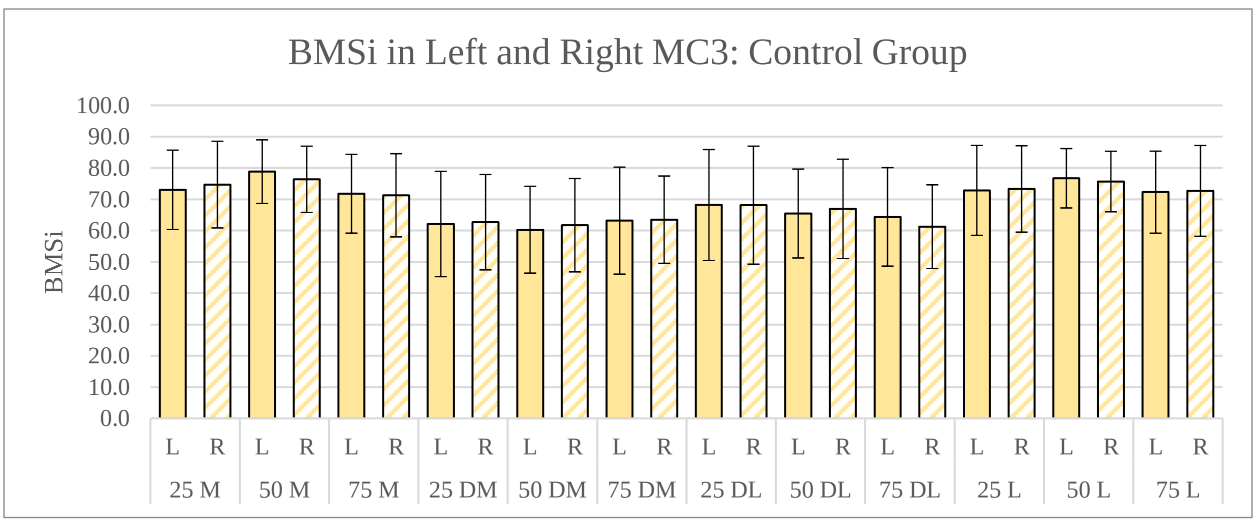

Figure 3.4. No significant (p < 0.004) differences between left and right MC3 BMSi in Control group. (n = 16 – 18, depending on site). Bar and error bars represent mean ± 1 standard deviation. Paired t-test. M = medial, DM = dorsomedial, DL = dorsolateral, L = lateral.

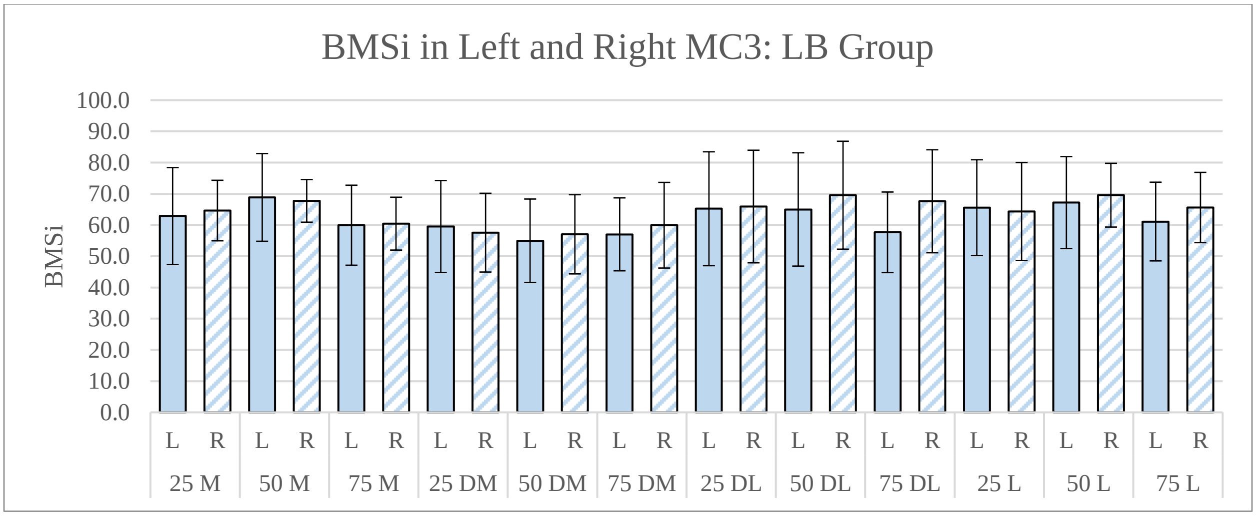

Figure 3.5. No significant ($p < 0.004$) differences between left and right MC3 BMSi in LB group. ($n = 14 – 15$, depending on site). Bar and error bars represent mean ± 1 standard deviation. Paired t-test. M = medial, DM = dorsomedial, DL = dorsolateral, L = lateral.

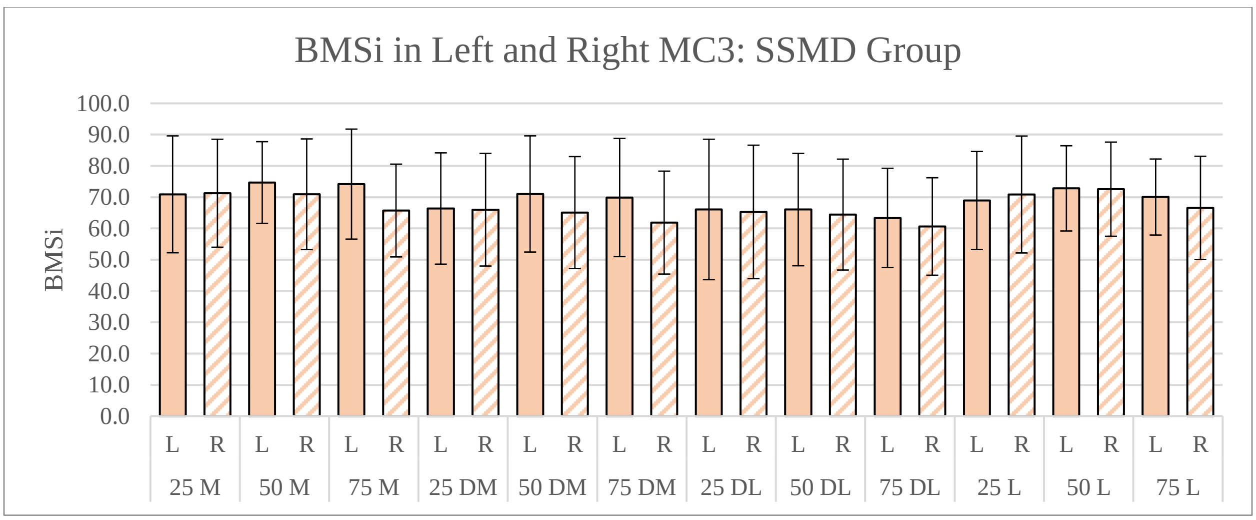

Figure 3.6. No significant ($p < 0.004$) differences between left and right MC3 BMSi in SSMD group. . ($n = 15 – 16$, depending on site). Bar and error bars represent mean ± 1 standard deviation. Paired t-test. M = medial, DM = dorsomedial, DL = dorsolateral, L = lateral.

No Skin

Paired t-tests with Bonferroni correction for multiple comparisons were performed at each site within each experimental group. No significant ($p < 0.004$) differences in no-skin BMSi between left and right third metacarpal bones existed.

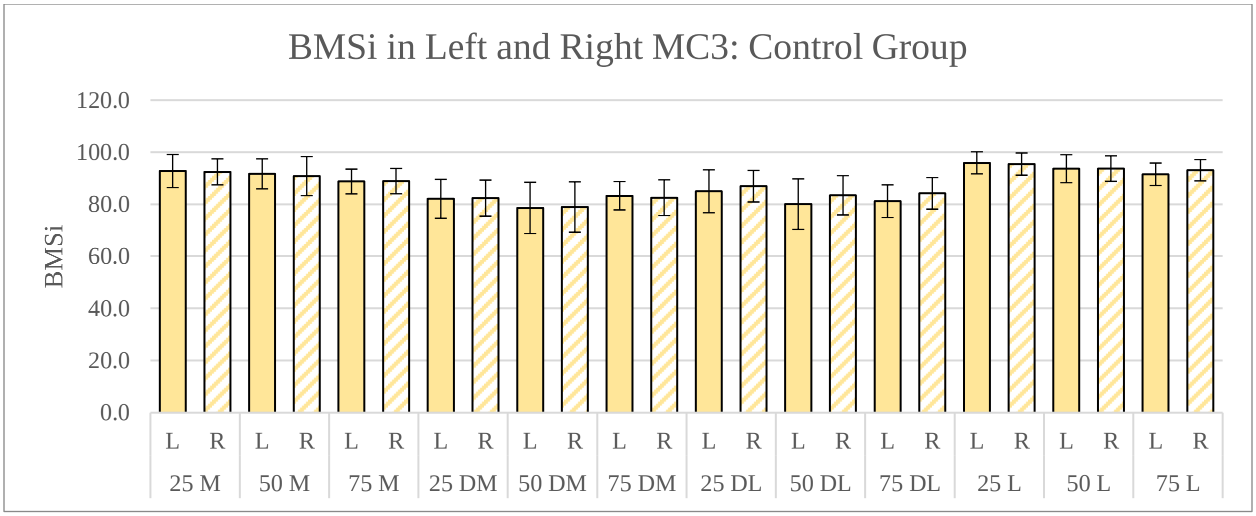

Figure 3.7. No significant ($p < 0.004$) differences between left and right MC3 BMSi in Control group. (n = 19 – 20, depending on site). Bar and error bars represent mean ± 1 standard deviation. Paired t-test. M = medial, DM = dorsomedial, DL = dorsolateral, L = lateral.

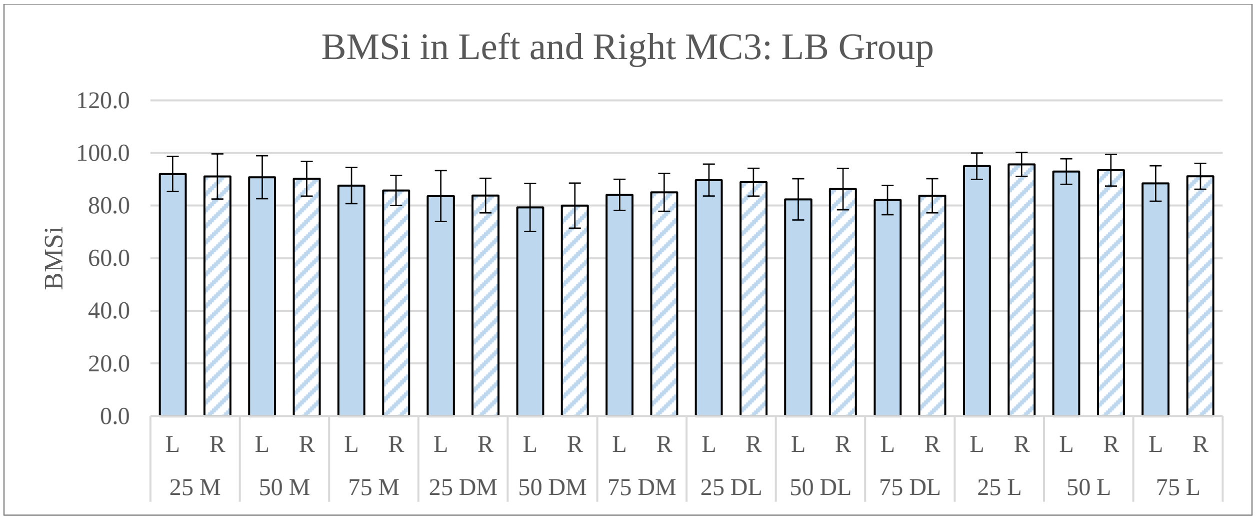

Figure 3.8. No significant ($p < 0.004$) differences between left and right MC3 BMSi in LB group . (n = 18). Bar and error bars represent mean ± 1 standard deviation. Paired t-test. M = medial, DM = dorsomedial, DL = dorsolateral, L = lateral.

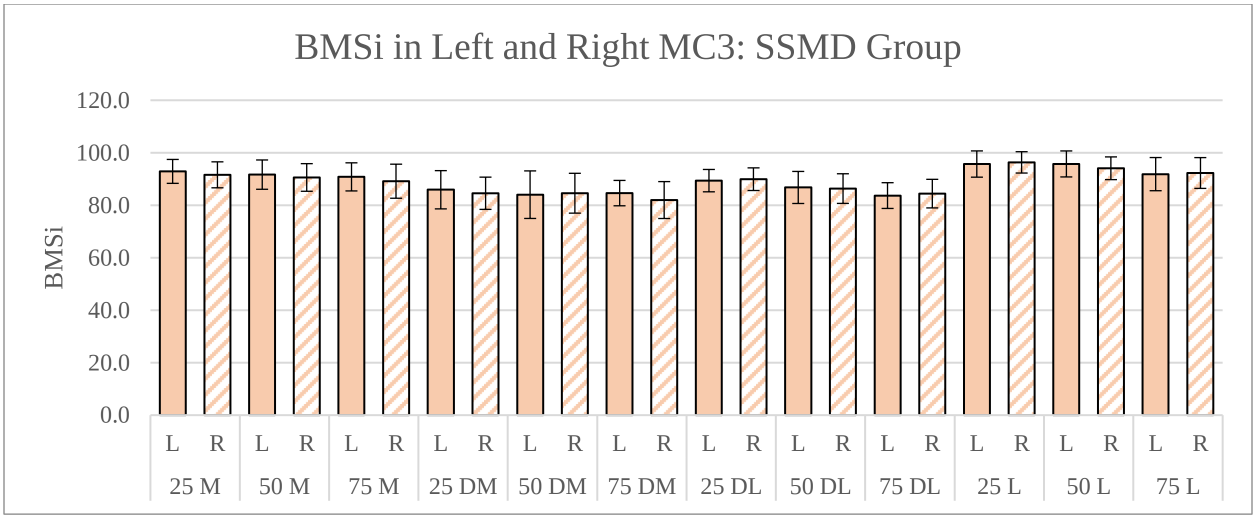

Figure 3.9. No significant (p < 0.004) differences between left and right MC3 BMSi in SSMD group. (n = 19 – 20, depending on site). Bar and error bars represent mean ± 1 standard deviation. Paired t-test. M = medial, DM = dorsomedial, DL = dorsolateral, L = lateral.

3.1.3 BioDent

When comparing BioDent parameters from right and left limbs among each of the fracture groups after Bonferroni correction, five significant (p < 0.005) differences were discovered. Four of these differences regarded loading or unloading slopes, indicating potential differences in stiffness or elastic moduli, and one regarded average energy dissipated. These discrepancies were not seen as a compelling argument to perform all left- and right-limb analyses separately, so left and right data was averaged together for the remaining analyses.

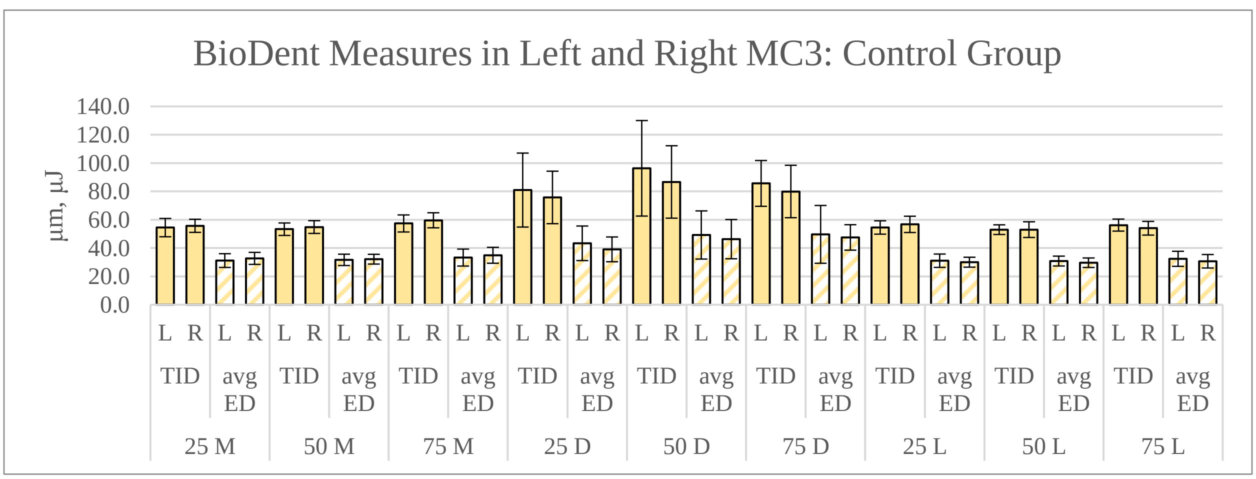

Figure 3.10. No significant (p < 0.005) TID or avgED differences between left and right limbs in the Control group. (n = 16 – 20, depending on site). Bar and error bars represent mean ± 1 standard deviation. Paired t-test. TID = total indentation distance, avg ED = average energy dissipated, M = medial, D = dorsal, L = lateral.

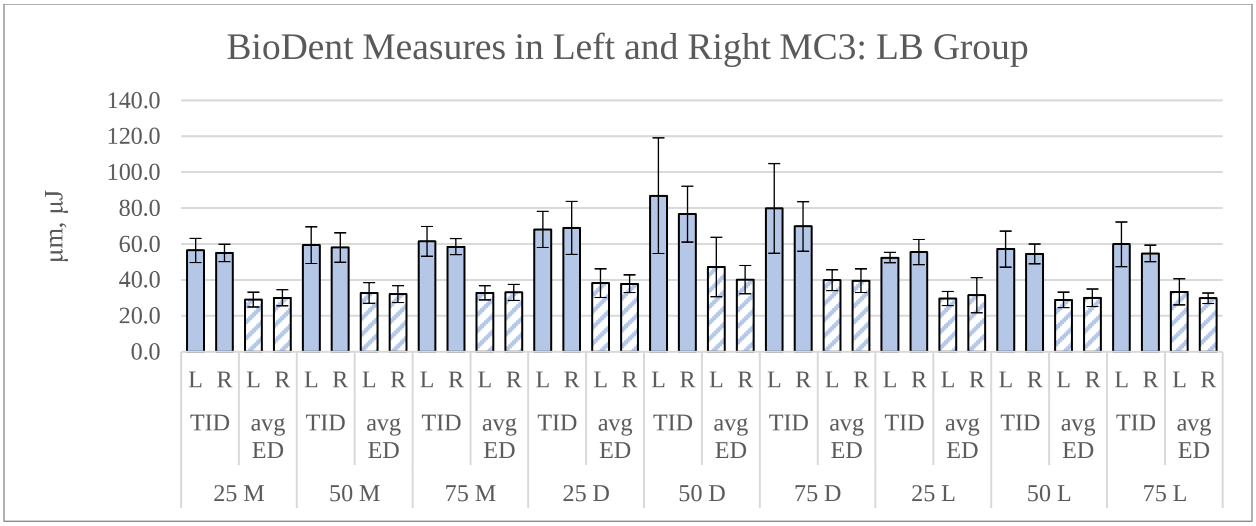

Figure 3.11. No significant (p < 0.005) TID or avgED differences between left and right limbs in the LB group. (n = 17 – 18, depending on site). Bar and error bars represent mean ± 1 standard deviation. Paired t-test. TID = total indentation distance, avg ED = average energy dissipated, M = medial, D = dorsal, L = lateral.

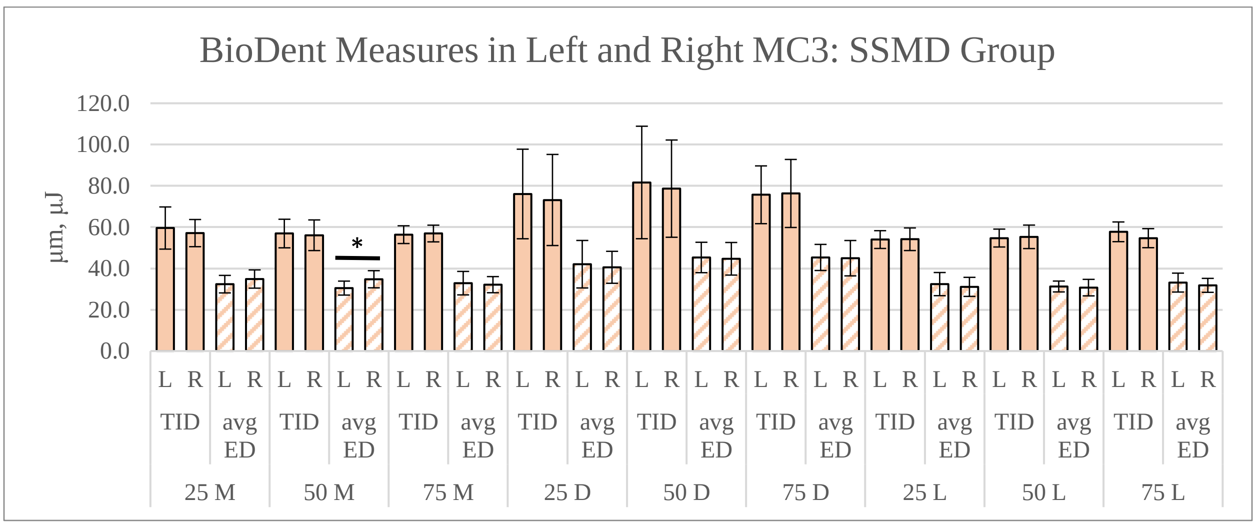

Figure 3.12. Significant (p < 0.005) avgED difference detected between left and right limbs at the 50% medial site in the SSMD group. (n = 16 – 20, depending on site). Bar and error bars represent mean ± 1 standard deviation. Paired t-test. TID = total indentation distance, avg ED = average energy dissipated, M = medial, D = dorsal, L = lateral.

Five significant (p < 0.005) differences existed between left and right limbs (Table 3.1), four of which belonged to parameters that would likely not be included in the final predictive model due to reasons outlined in Section 2.4.

Table 3.1. Significant differences between left and right third metacarpal bones are outlined below, with the value of the left mean or standard deviation in the top row for each instance and the value of the right in the bottom row.

Group	Site	Parameter	Mean (Left / Right)	Standard Deviation (Left / Right)	p-value
C	50% lateral	US1	0.71	0.052	0.003
			0.761	0.064	
C	25% lateral	US1	0.698	0.04	0.001
			0.752	0.059	
C	25% lateral	avg US	0.753	0.036	0.002
			0.801	0.059	
SSMD	50% medial	avg ED	30.48	3.39	0.003
			34.77	4.15	
SSMD	25% medial	avg LS	0.564	0.036	0.001
			0.532	0.039	

Though select differences remained after Bonferroni corrections were applied to BioDent data, there were no consensus on left bones having greater values than right or vice versa. The control group was not lacking in significant left / right differences compared to the fracture groups, suggesting that significantly different values between limbs does not necessarily forecast a fracture. Additionally, because stiffness and elastic modulus at this scale are not perceived to be critical considerations for our purposes and because a discrepancy in avgED was only observed in one location among one fracture group, these differences were not seen as compelling reasons to not average all left and right data together in each pair of bones.

Therefore, data from the left and right limbs were averaged together to create one set of values for each horse during the proceeding data analysis.

3.1.4 pQCT

Among the 26 parameters measured via pQCT on the 5 sites in each of the experimental groups (excluding MC3 due to lack of intact pairs of bones), one significant difference emerged. At the 25% length plane of bones in the SSMD experimental group, periosteal circumference was found to be significantly larger in left bones ($p = 0.029$). However, the circumference is reported to be approximately twice as large in the left bones in this location as it is in the right—this difference would be visibly discernable and obvious. Upon further inspection, it appears as if software settings may be misaligned in regards to this parameter, as many bones are reported as having a circumference of zero. Periosteal circumference will not be used in this study.

3.2 Fracture Group Comparisons

3.2.1 X-Ray

When an ANOVA was performed to compare the length of third metacarpal bones between the experimental groups, no significant differences existed.

Cortical thicknesses were analyzed using a linear mixed model with site, group, and site-group interactions as fixed effects and horse ID as a random effect. No significant differences between groups or significant site * group interactions were discovered. Results did not differ when data were normalized by mass of the horse.

Because of the small sample size of the MC3 group and the possibility that third metacarpal bones are not distinct from other long bones, data belonging to the MC3 and LB groups were then combined into one group. A Mann-Whitney U test performed between the two groups determined that there are no significant differences between their cortical thicknesses at any site on the bones, supporting the decision to combine the groups. When analyzed using the linear model, site * group interactions were significant ($p = 0.049$). Post-hoc analyses indicate that the cortical thickness of the LB-MC3 group was significantly less than that of the C group at the 50% dorsal site and significantly less than both C and SSMD groups at the 75% dorsal site. It was also found that the cortex of the LB-MC3 group is significantly less thick than the SSMD group at the 75% medial site.

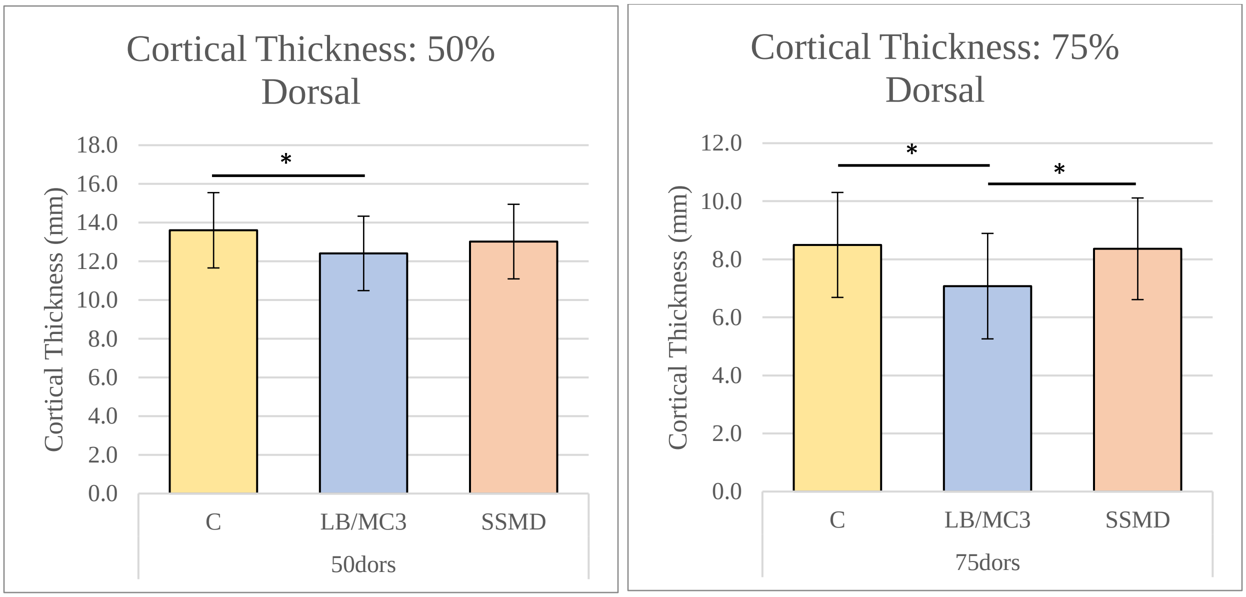

Figure 3.13. Cortical thickness significantly ($p < 0.05$) varied between fracture groups at the mid- and distal-dorsal surfaces. ($n_C = 20$, $n_{SSMD} = 20$, $n_{LB/MC3} = 24$). Bar and error bars represent mean ± 1 standard deviation.

Further consolidating the fracture groups, the data were analyzed using the mixed model with all of the fracture groups combined into one. A significant site * group interaction was discovered, and pairwise comparisons revealed significant differences between the C group and new Fx group at the 50% and 75% dorsal sites.

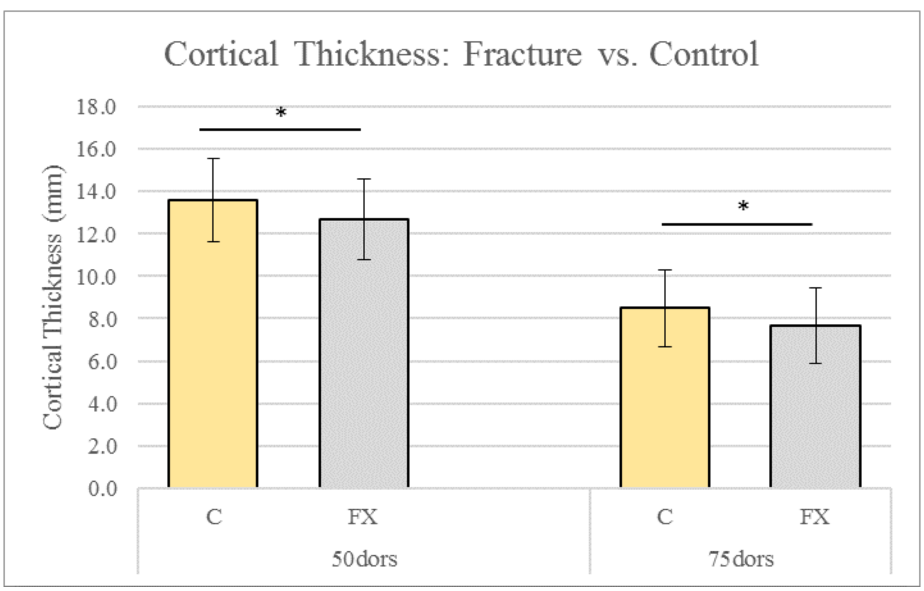

Figure 3.14. Cortical thickness was found to be significantly ($p < 0.05$) greater in the Control group than the combined Fracture group along the mid- and distal-dorsal surfaces. ($n_C = 20$, $n_{FX} = 44$). Bar and error bars represent mean ± 1 standard deviation.

3.2.2 OsteoProbe

Skin-on

When skin-on OsteoProbe data was analyzed using the linear mixed model, it returned no significant differences between groups or significant site * group interactions. A Mann-Whitney U test determined no significant differences in BMSi at any site between the LB and MC3 groups, and when LB and MC3 data were consolidated into one group, there remained no significant differences.

When all fracture data was consolidated into one fracture group to be compared against the Control group, a significant site * group interaction was reported. Upon investigation of the pairwise comparisons, it was evident that this significance was driven by differences by site within groups, not differences by group at a given site.

No significant differences in BMSi were found at any site between C and Fx groups, though some trends did appear: bones in the C group had higher BMSi values than the Fx group along the medial and lateral surfaces ($p = 0.002$ and $p = 0.015$, respectively), whereas on the dorsolateral and dorsomedial surfaces, the opposite appeared to tend to be true ($p = 0.785$ and $p = 0.726$, respectively). When values of the difference between dorsolateral and medial BMSi values at the midshaft of each bone are treated as a distinct "proxy" variable, the values from the Control group are found to be significantly ($p < 0.05$) greater than that of the LB group and MC3 groups when tested via one-way ANOVA (Figure 3.15).

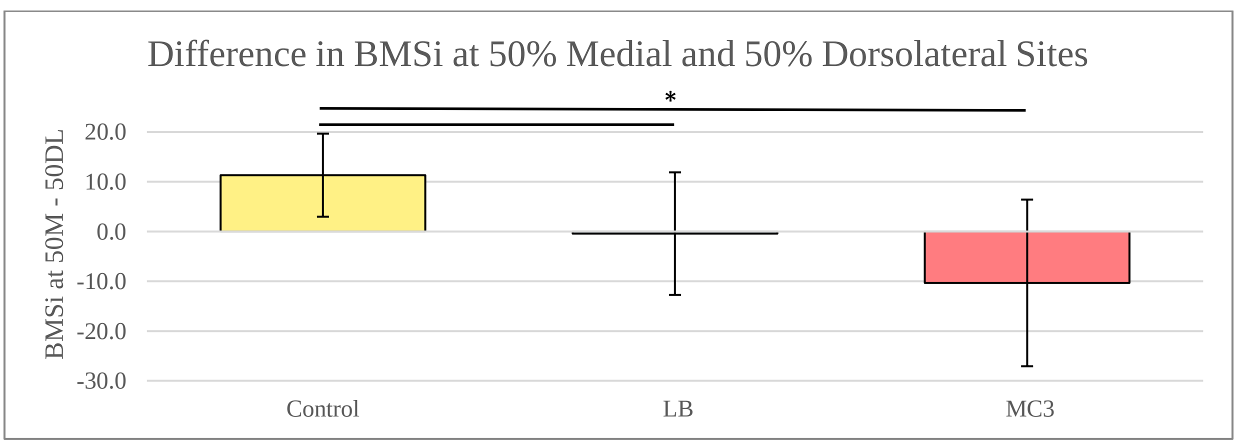

Figure 3.15. The Control group displays a pattern of higher BMSi values along the medial surface than the dorsal, while the LB and MC3 groups do not. The proxy variable obtained by taking the difference in BMSi between the 50% medial and 50% dorsolateral surfaces is significantly ($p < 0.05$) greater in the C group than in the LB or MC3 groups. Note the high standard deviation. ($n_C = 20$, $n_{LB} = 19$, $n_{MC3} = 5$). Bar and error bars represent mean ± 1 standard deviation.

No Skin

When the same tests are performed on the no-skin OsteoProbe data, no significant group differences, site * group interactions, or medial-minus-dorsolateral differences are observed when all four fracture groups are compared or when LB and MC3 are grouped together. A Mann-Whitney U test determined a significant ($p = 0.044$) difference between the LB and MC3 groups at the 25% dorsolateral level, though this discovery bears little relevance since no positive results were found by combining these two groups.

When the control group is compared against all the combined fracture groups, no significant differences or interactions are observed. However, the same phenomenon from skin-on testing held true: on medial and lateral surfaces, the control group tends to have higher BMSi values, whereas on dorsolateral and dorsomedial surfaces, the opposite is true.

3.2.3 BioDent

When BioDent data for each parameter was analyzed using the mixed model, no significant differences between groups or site * group interactions were discovered. Trends were noticed in parameters such as Total Indentation Distance, though relatively high variation in the data or the small sample size of the MC3 group may have barred any differences from being deemed significant.

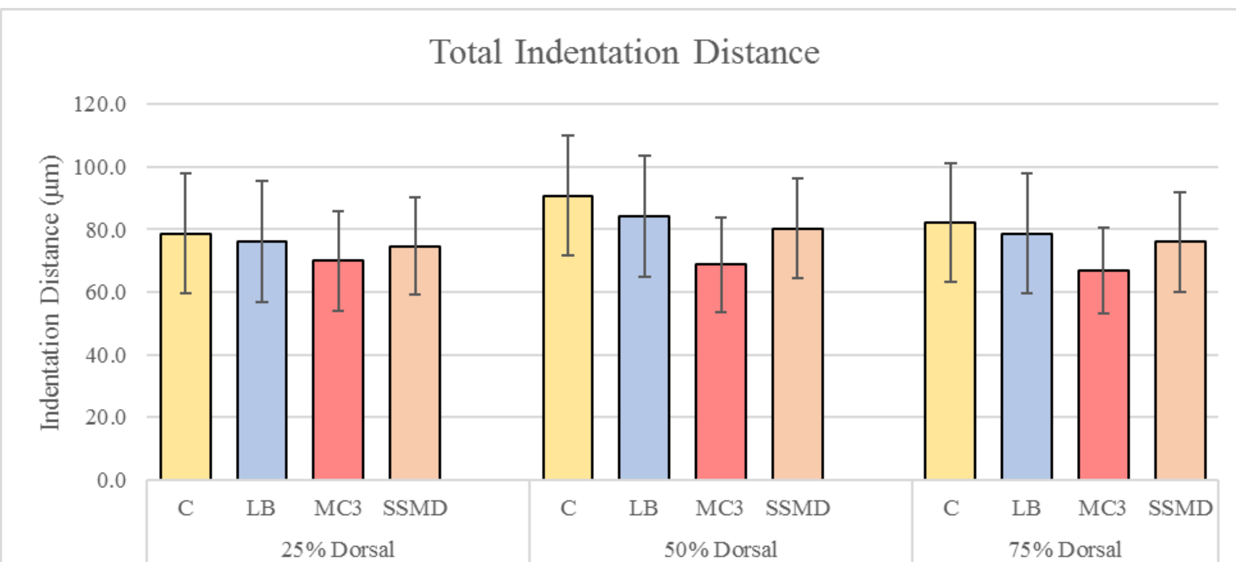

Figure 3.16. Though no significant differences arose, the MC3 group trended lower than the other experimental groups, particularly the Control group. ($n_C = 20$, $n_{LB} = 19$, $n_{MC3} = 3$, $n_{SSMD} = 20$). Bar and error bars represent mean ± 1 standard deviation.

A Mann-Whitney U test detected differences in 1st-cycle unloading slope ($p = 0.003$) and average unloading slope ($p = 0.001$) between the LB and MC3 groups at the 50% medial location, but no differences in other parameters or locations. When LB and MC3 groups are combined, no significant differences emerged. When all fracture groups are combined and compared against the Control group, a significant site * group interaction exists in Average Energy Dissipated at the 75% dorsal site. See Tables A.20 – A.22 in the Appendix for a summary of all p-values across parameters and experimental setups.

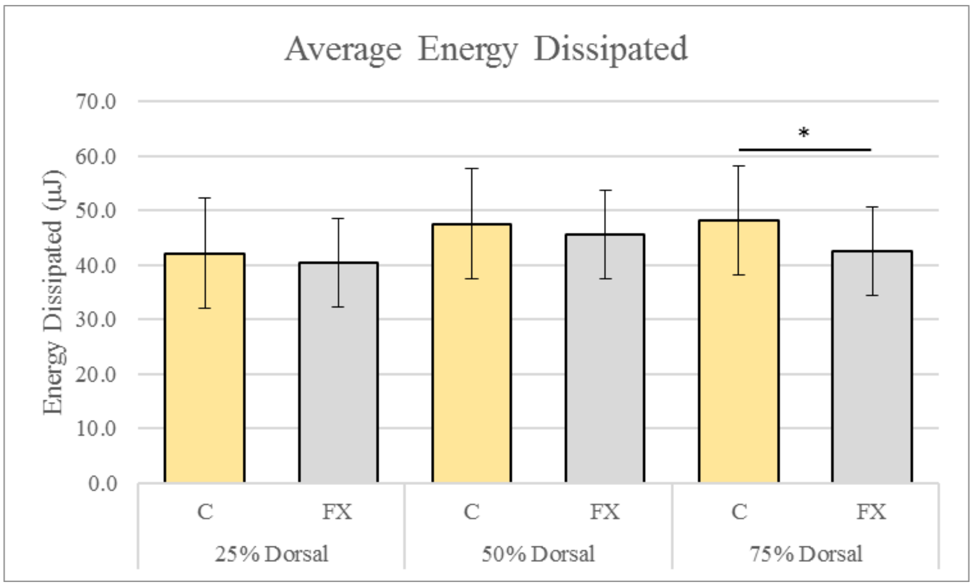

Figure 3.17. Average energy dissipated was found to be significantly ($p < 0.05$) greater in the Control group than the combined Fracture group at the 75% dorsal site. ($n_C = 20$. $n_{FX} = 42$). Bar and error bars represent mean ± 1 standard deviation.

3.3 OsteoProbe versus BioDent Correlations

Correlations between BMSi and each of the BioDent's parameters existed in in varying degrees. TID, IDI, and avgED shared some of the strongest correlations with BMSi.

To validate the relationship between BioDent and OsteoProbe microindentation testing methods, each parameter was compared against the other modality. The 50% dorsal site was examined first due to it being perhaps the most clinically-relevant location on the third metacarpal bone. Because OsteoProbe testing was performed only on the dorsolateral and dorsomedial surfaces and not the dorsal surface itself, both were initially tested against the BioDent parameter at hand. Next, the dorsolateral and dorsomedial values were averaged together in an attempt to interpolate what the BMSi value on the dorsal surface may be. These averaged data resulted in stronger correlations with most BioDent parameters, and were thus selected as the OsteoProbe data to be utilized in the comparison calculations.

The 50% dorsal site was found to consistently have the highest R^2 values across most BioDent parameters. Despite the medial and lateral measurements being taken on the same surface between instruments, as opposed to averaging two sites together, the distance-based parameters show nearly no correlation with one another (Table A.23).

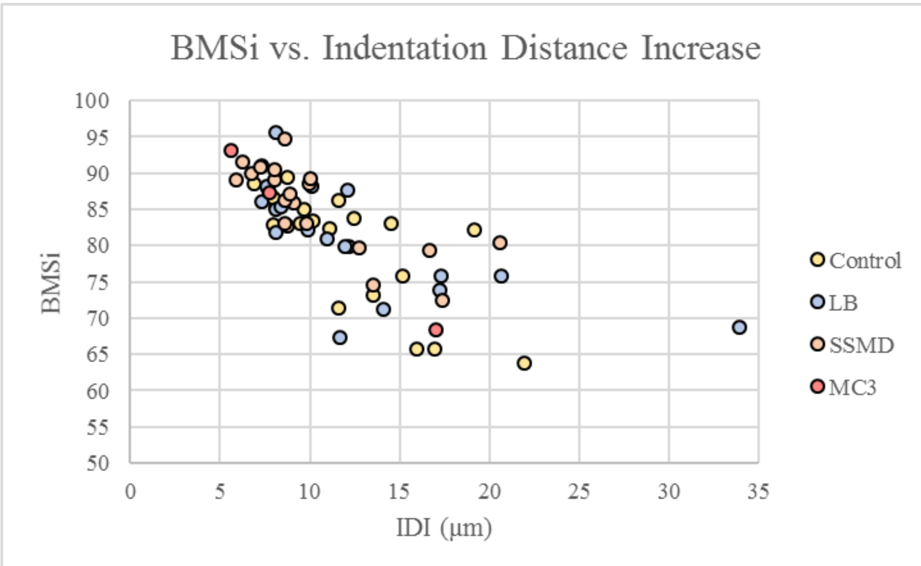

Group	R^2 Value
C	0.5709
LB	0.4653
SSMD	0.5866
MC3	0.9973
Total	0.5376

Figure 3.18. BMSi and IDI show a modest correlation in each experimental group

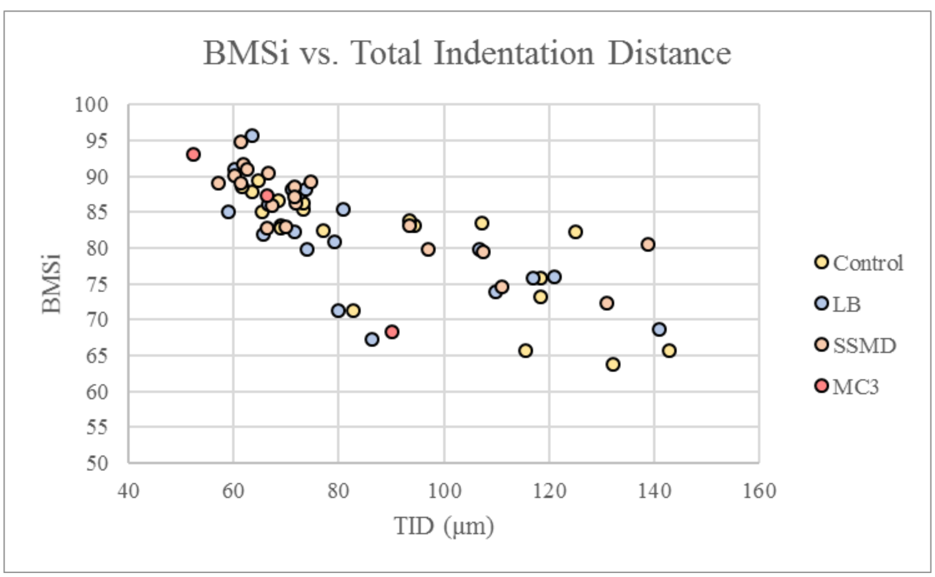

Group	R^2 Value
C	0.6259
LB	0.4900
SSMD	0.7057
MC3	0.9778
Total	0.5822

Figure 3.19. BMSi and TID show a modest correlation in each experimental group

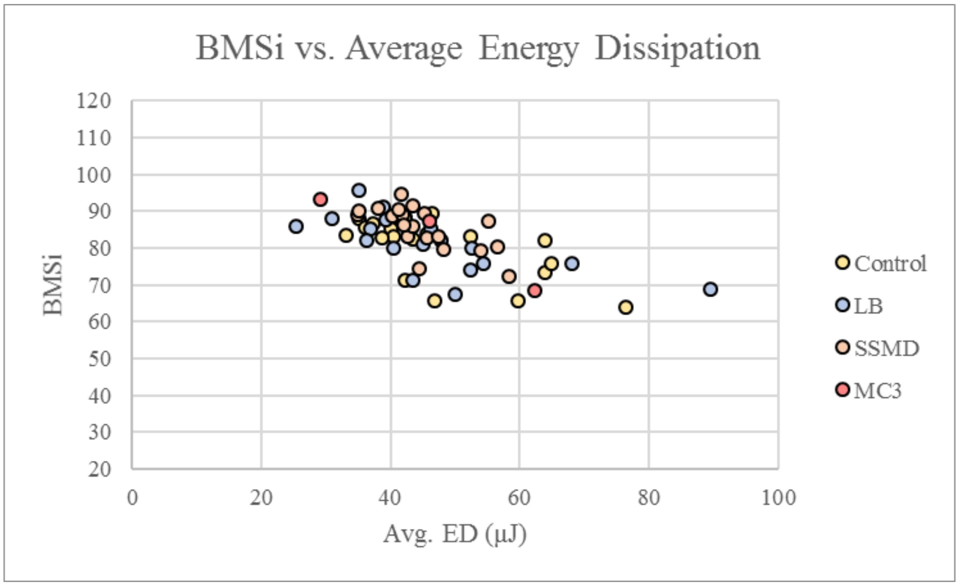

Group	R^2 Value
C	0.4191
LB	0.4545
SSMD	0.4381
MC3	0.9087
Total	0.4468

Figure 3.20. BMSi and avgED show a modest negative correlation in each experimental group.

3.4 Peripheral Quantitative Computed Tomography (pQCT)

Many parameters measured by pQCT reported significant differences, particularly significant site * group interactions. Contrary to other methodologies that were explored in this study, less differences and interactions were observed when the fracture groups are consolidated and compared against the control group. Though pQCT is a highly versatile methodology with many outputs (see Table 3.2), few will likely be considered candidates for predictor variables in the final regression model due to a lack of distinguishing ability or lack of perceived relevance.

After statistical analysis was performed, cortical thickness, cortical thickness standard deviation, endosteal circumference, and endosteal circumference (circular ring model) were found to have missing values. The results from these parameters are not accurate and should not be taken into consideration.

Table 3.2. Each parameter measured by pQCT testing. p-values for significant group differences and significant group * site interactions, when tested with all fracture groups or just Control compared against the combined Fracture group, bolded. Grayed-out values were found to have missing values after analysis and should not be considered.

Parameter	Abbreviation	All Fx Groups		C vs. Fx.	
		Group	Site * Group	Group	Site * Group
Cortical bone density (mg / cm^3)	CRT_DEN	***0.000***	***0.006***	0.068	0.143
Cortical & subcortical content per slice (mg / mm)	CRTSUB_CNT	***0.021***	***0.012***	0.332	0.143
Cortical & subcortical bone density (mg / cm^3)	CRTSUB_DEN	***0.007***	***0.001***	0.543	0.826
Total bone density (mg / cm^3)	TOT_DEN	***0.004***	***0.005***	0.100	0.235
Axial area moment of inertia (via circular ring model)	I_CIRC	0.837	***0.012***	0.608	0.378
Total bone area (mm^2)	TOT_A	0.973	***0.009***	0.762	0.331
Cortical thickness (via circular ring model) (mm)	CRT_THK_C	0.978	***0.048***	0.998	0.356
Periosteal circumference (via circular ring model) (mm)	PERI_C	0.994	***0.009***	0.848	0.309
Cortical & subcortical bone area (mm^2)	CRTSUB_A	0.100	***0.000***	0.391	***0.033***
Axial area moment of inertia of cortical area (x-axis)	IX_CRT_A	0.438	***0.000***	0.473	0.153
Axial area moment of inertia of cortical area (y-axis)	IY_CRT_A	0.644	***0.000***	0.548	0.468
Polar area moment of inertia of cortical area	IP_CRT_A	0.550	***0.000***	0.505	0.303
Cortical moment of resistance (x-axis)	RX_CRT_A	0.775	***0.002***	0.542	0.125
Cortical moment of resistance (y-axis)	RY_CRT_A	0.857	***0.043***	0.622	0.314
Polar moment of resistance	RP_CRT_A	0.898	***0.004***	0.753	0.197
Cortical bone area (mm^2)	CRT_A	0.893	***0.000***	0.680	0.185
Cortical content per slice (mg / mm)	CRT_CNT	0.437	0.189	0.510	0.647
Cortical thickness standard deviation	CRT_THK_SD	0.187	0.213	0.111	0.125
Mean cortical thickness (mm)	CRT_THK	0.125	0.169	0.124	0.111
Endosteal circumference (via circular ring model) (mm)	ENDO_C	0.867	0.962	0.606	0.966
Endosteal circumference (mm)	ENDO	0.315	0.147	0.403	0.696
Total bone content per slice (mg / mm)	TOT_CNT	0.364	0.422	0.448	0.704
Trabecular bone area (mm^2)	TRAB_A	0.061	0.088	0.762	0.331
Trabecular bone content per slice (mg / mm)	TRAB_CNT	0.384	0.901	0.448	0.704
Trabecular bone density (mg / cm^3)	TRAB_DEN	0.703	0.644	0.100	0.235

When considering gross mechanical properties of the bone, it is best to focus on cortical bone for its role in bearing loads and resisting fracture. Because of its ability to indicate bone health, BMD is also a factor of interest from these parameters. Therefore, taking also into consideration that many MC3 fractures occur in the distal part of the bone, one metric that was hypothesized to be valuable in assessing a bone's susceptibility to fracture is cortical & subcortical BMD at 90% length (see Figure 3.21).

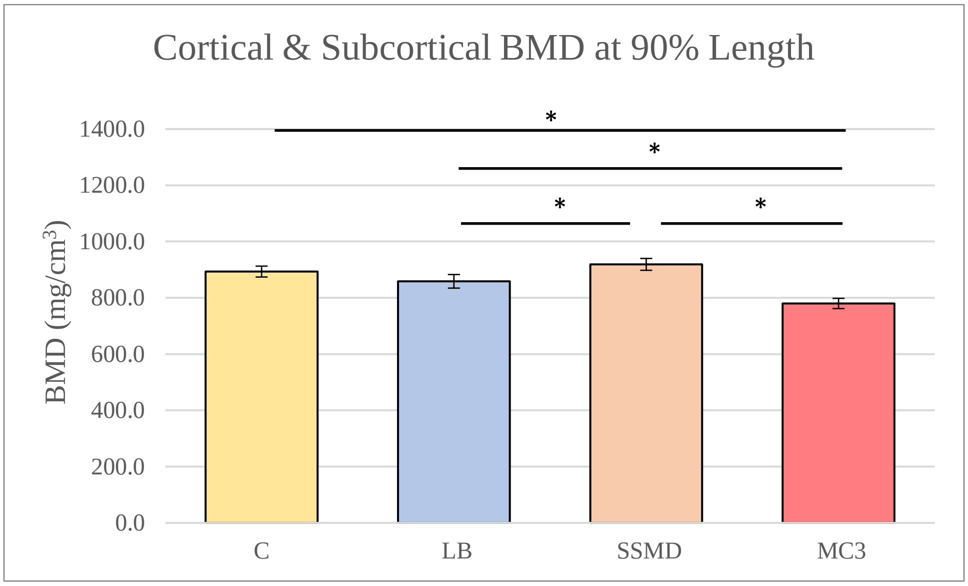

Figure 3.21. Bone mineral density in the cortical and subcortical bone significantly ($p < 0.05$) differs between the MC3 group and each other group, as well as in the SSMD group and LB group. ($n_C = 20$, $n_{LB} = 19$, $n_{SSMD} = 20$, $n_{MC3} = 5$). Bar and error bars represent mean ± 1 standard deviation.

The MC3 group had significantly lower BMD than each other group, and the SSMD group also had higher BMD than the LB group. The Control group did not distinguish itself from any fracture group beside MC3.

3.5 Micro-Computed Tomography (μCT)

Data from μCT testing performed on bones from the Control and LB groups were compared via independent sample t-tests. With Control n=10 and LB n=6, a significant difference in bone mineral density was discovered at the dorsal surface (p = 0.001), but not at the lateral and medial surfaces (p = 0.546 and p = 0.807, respectively). See Figure 3.22.

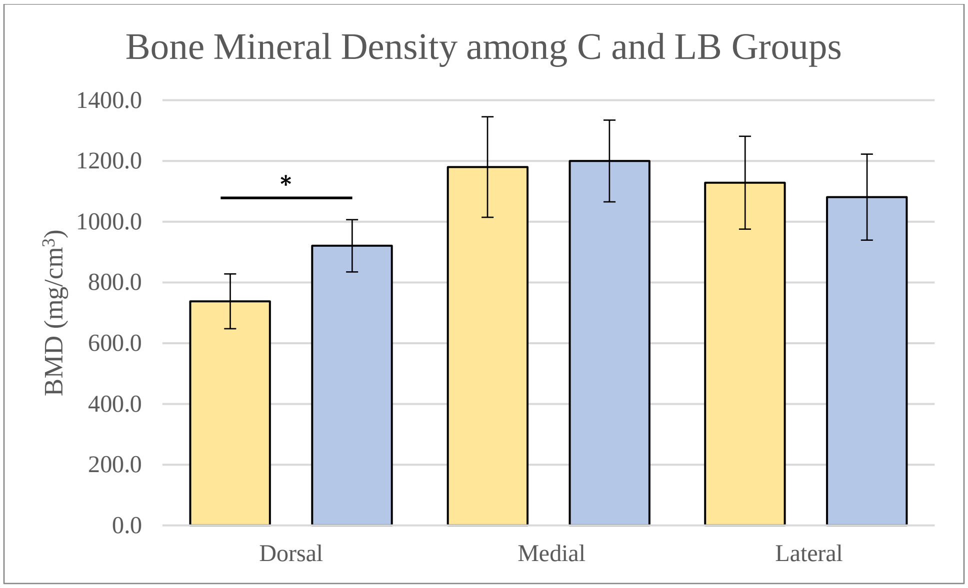

Figure 3.22. Only on the dorsal surface, the Control group (yellow) had a significantly ($p < 0.05$) lower BMD than the LB group (blue). ($n_C = 10$, $n_{LB} = 6$). Bar and error bars represent mean ± 1 standard deviation. Independent samples t-test.

While evaluating μCT images qualitatively, two irregularities were noted in select bones. In 5 out of 10 (50%) Control bones and 1 out of 6 (17%) of the LB group, a layer of low attenuation (i.e. darker coloring) is observed immediately below the surface of the bone (see Figure 3.23, left vs. center). In one bone from the LB group, the image has numerous dark spots within the cortex of the bone, indicating perhaps that the cortical bone in this region is porous (see Figure 3.23, right).

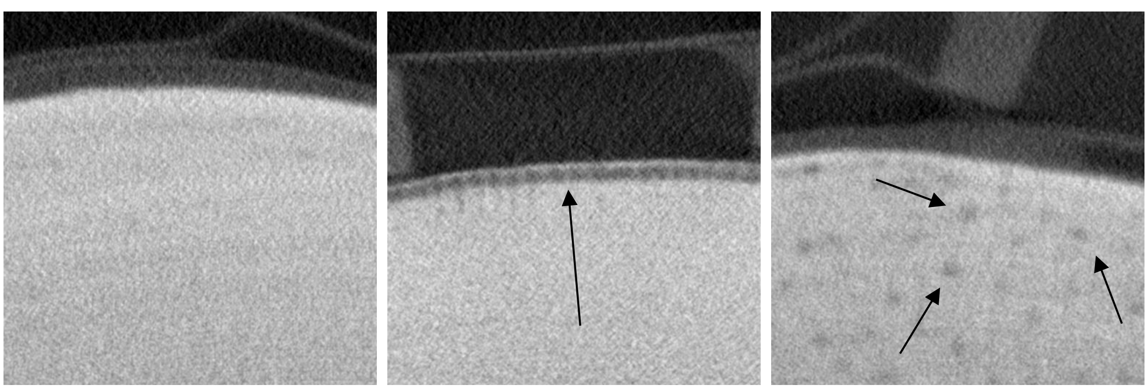

Figure 3.23. Left: a typical periosteal surface, seen here in a bone from the LB group. Center: a low-density strip is seen right below the bone surface, here in a bone from the Control group. Right: a bone apparently displaying abnormal porosity

3.6 Multivariable Model

3.6.1 Individual Analyses

In order to provide a different perspective than previous analyses that focused on difference in means, receiver operating characteristic (ROC) curves were created in MedCalc Statistical Software and their respective area under the curve (AUC) values were calculated to describe each parameter's ability to distinguish between bones from the Control group and those from the Fracture group. The ROC curves from four parameters that were deemed relevant at the 50% dorsal site are pictured in Figure 3.24.

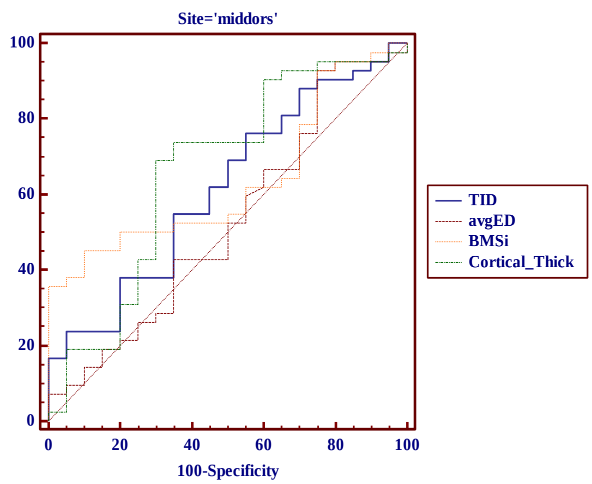

Figure 3.24. Individual parameters have low AUC values when modeled alone

Each individual parameter achieved an AUC above the minimum possible value of 0.50, though none achieved a value above 0.70. The corresponding AUC, 95% confidence interval, and standard error values are found in Table 3.3.

Table 3.3. The AUC, confidence interval, and SE values laid out for each individual parameter under consideration for the model. The low AUC values indicate that these variables don't have high capability to distinguish between healthy and at-risk bones. *Note: standard error not calculated for Average Loading Slope.*

Parameter	AUC	95% Confidence Interval	Standard Error
TID	0.617	0.484 – 0.737	0.0768
avgED	0.527	0.396 – 0.655	0.0826
BMSi	0.637	0.505 – 0.755	0.0718
Cortical Thickness	0.663	0.532 – 0.778	0.0803
ID1	0.621	0.489 – 0.742	0.0764
US1	0.563	0.431 – 0.688	0.0830
CID1	0.626	0.494 – 0.746	0.0731
IDI	0.581	0.449 – 0.705	0.0770
avgCID	0.577	0.445 – 0.702	0.0775
avgUS	0.555	0.423 – 0.681	0.0811
avgLS	0.526	0.395 – 0.654	-

When the same procedures were applied to a multivariable model containing parameters obtained data available at the time from x-rays, BioDent, and OsteoProbe at the 50% dorsal location, a more promising ROC curve was returned (Figure 3.25).

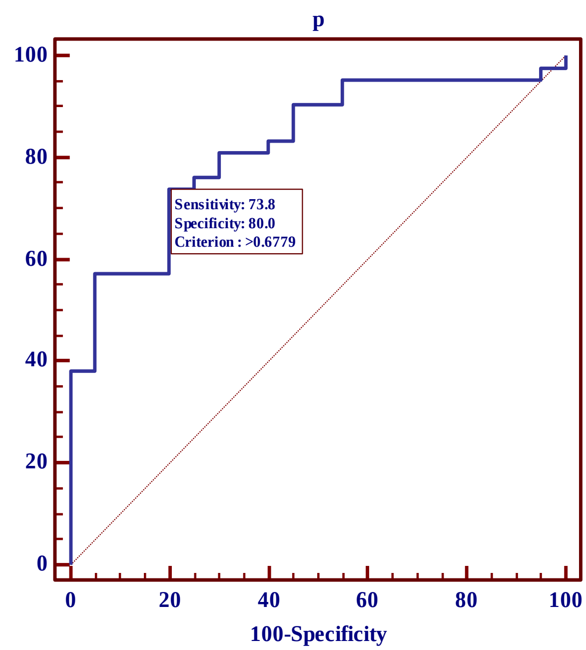

Figure 3.25. A model including TID, BMSi, avgED, and cortical thickness returns a fairly large AUC value of 0.82.

The AUC was found to be 0.82 with a 95% confidence interval of 0.71 – 0.91. The statistical optimal cutoff per the Youden index is at a specificity of 80.0 and sensitivity of 73.8, suggesting that the model has optimal distinguishing capacity at these levels.

When clinical practicality was taken into consideration, another model was created using only data from tests that can routinely be performed on live horses: BMSi, cortical thickness, and mass of the horse (Figure 3.26).

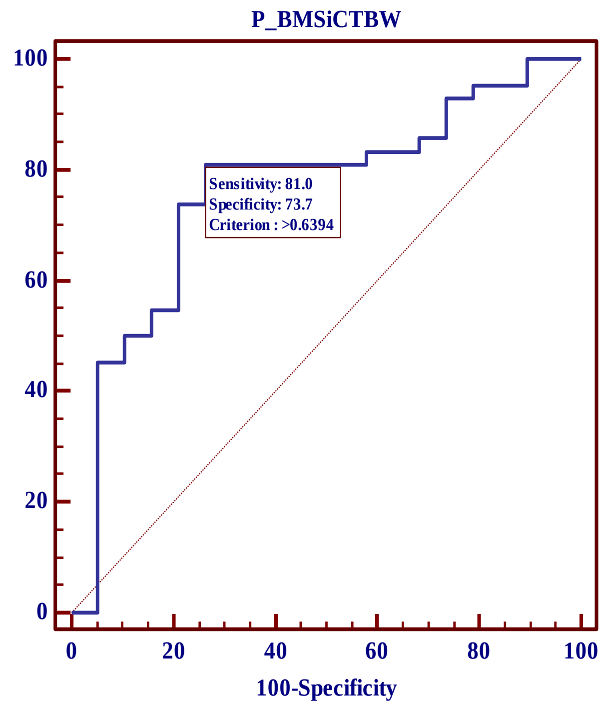

Figure 3.26. When only clinically relevant parameters (BMSi, cortical thickness, and mass) are included in the model, a returned AUC of 0.76 is still promising but not ideal

The AUC (0.761 with 95% confidence interval 0.634 – 0.861) was not as large as the previous model; however, it still suggests considerable distinguishing ability and reducing the number of predictor variables may help reduce the error inherent to the model.

Another model was created using three clinically-relevant parameters that were selected upon two primary criteria: uniqueness and utility. Cortical thickness at the 50% dorsal surface, bone mineral density of the cortex and subcortex at the 90% level, and the difference in percutaneous BMSi at the dorsolateral and medial surfaces at the 50% level. Each parameter displayed capability in distinguishing between experimental groups previously in the study, and each examined a unique property of the bone. Because data collected from the SSMD group appeared to be more similar to the C group throughout this study, and because the nature of logistic regression models only allows for a dichotomous response, only the C group and the combined LB / MC3 group were included in this model to achieve maximum potential predictive power.

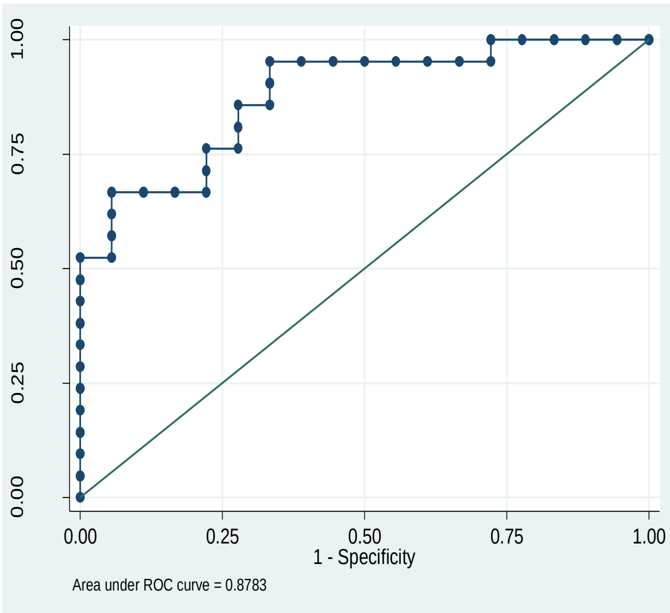

Figure 3.27. When the Control group and LB / MC3 group are included in the regression model with cortical thickness at the 50% dorsal surface, BMD at the 90% plane, and difference in BMSi between the dorsolateral and medial surfaces at 50% length, an area under the ROC curve of 0.88 is achieved.

This model returned an area under the ROC curve of 0.8783, with optimal sensitivity is 95.24% and specificity at 66.67%. Though the SSMD group is excluded from the model, it shows considerable promise in distinguishing between third metacarpal bones from horses that have experienced a long bone fracture and those that have not.

4. DISCUSSION

4.1 X-ray

Though prevalent differences in both geometry and fracture occurrence between right and left long bones in horses have been recorded [35][63][64], few discrepancies emerged between right and left cortical thicknesses at a given site within each group. As mentioned previously, the likelihood of type I errors increases when a high volume of hypothesis tests are performed concurrently; therefore, with the knowledge that the data's variance is large and that common controlling procedures would eliminate the significance of each observed difference, the mean of the data from each analogous location on right and left limbs was used in further analyses.

Cortical thickness was found to be significantly different between fracture groups along the dorsal surface of the bone, a clinically relevant site relating to the MC3's ability to adapt to exposure of compressive forces and strain [30]. Though the difference is indeed significant, it remains unclear how practical these findings will be in a clinical setting as the difference in means was on the order of 1 – 2 mm. Due to the potential for operator variation in the imaging and analysis of x-rays and the inherent high variability in MC3 geometry among racehorses [41], it is likely that the observed differences will have only marginal predictive applications when utilized in a univariate model. When considered in conjunction with data from other tests, however, it very well may bolster the predictive capability of the model.

4.2 OsteoProbe

Control bones did not distinguish themselves from any fracture group (or combination thereof) in pure BMSi measures through the skin or directly on the surface of the bone. However, the study provided insight to different test methods and potential differences in equine and human models.

The average standard deviation of measurements when taken percutaneously more than doubled that when taken on the same samples after having removed the skin and periosteum. While this doesn't disqualify the OsteoProbe as a potentially useful tool to clinically collect information on the material properties of bone, it does suggest that its capacity to distinguish between healthy and at-risk bones may be inversely related to its degree of noninvasiveness. Alternatively, it may be that factors other than the bone surface itself (such as the periosteum, which has been shown to exhibit different properties in patients with and without skeletal pathologies [65]), help differentiate between healthy and pathologic bones. This may be supported by the differences seen between the medial-minus-dorsolateral differences between the Control group, LB group, and MC3 group. Although the standard deviations are strikingly high, the results are consistent with what is expected in the Control group: a large discrepancy between the dorsal surface, which presumably may have a layer of more easily-indented primary bone, and the medial and lateral surfaces, which are not thought to be undergoing modeling. While the fact that the opposite trend was seen in the MC3 group cannot be ignored, the immense standard deviation values compared to the sample size (n = 5) does render the data unreliable.

It may also be that the OsteoProbe is a more useful tool in certain situations than others. While our data exhibits BMSi trending lower in the control group than the fracture group, human studies have concluded the opposite in studies examining both pathology and response to loading [55,56,66]. We hypothesize that a lower BMSi on the dorsal surface—an area associated with exercise-induced bone modeling—may be due to the indentation probe encountering woven bone. Woven bone is characterized by disorderly structure and is mechanically weaker than mature, lamellar bone. While its presence on the surface of bone may reduce its resistance to indentation, it is also likely an indicator of healthy response to loading. A surface more resistant to indentation may reveal a lack of immature bone and therefore a potential dysregulation in response to exercise, which may help explain the occurrence of fracture experienced in these horses.

OsteoProbe, despite not displaying significant differences in comparing means between control and fracture groups, did greatly enhance the apparent predictive capability of a logistic regression model including x-ray data. While BMSi and cortical thickness returned ROC area under the curve (AUC) values of 0.637 and 0.663, respectively, individually, the two parameters taken together with mass created a model with an AUC of 0.76. Though this AUC would not generally be regarded by clinicians as robust enough to use as a reliable diagnostic method, it lends credence to the possibility of creating a predictive model from a combination of subtle changes that might otherwise go unnoticed.

4.3 BioDent

While no significant differences emerged when comparing control bones to the three fracture groups, some trends did appear. Total indentation distance, for example, was 28% greater in the control group than the MC3 group at the midshaft dorsal site, though statistical significance was likely barred by the small sample size of the MC3 group.

When the three fracture groups were combined into one and compared against the control group, differences along the dorsal surface persisted. At the 50% dorsal site, total indentation distance was 11% greater in the control group than the fracture group and indentation distance increase was 6% greater. At the 75% dorsal site, average energy dissipated (avgED) was significantly greater in the control group. avgED is calculated by measuring the area under the force-displacement curve generated during testing. Consistent with the aforementioned BioDent trends and the BMSi trends seen in OsteoProbe measurements, a greater displacement per unit force may suggest a layer on the surface of bone that is less resistant to indentation, as may be expected from woven bone deposited on the periosteal surface.

Though the BioDent elucidated a significant difference between the control and fracture groups where the OsteoProbe did not, the OsteoProbe is still considered to be the more clinically-relevant microindenter between the two. The correlations between BMSi and most BioDent parameters are modest, though the trends among experimental groups are similar. Replacing 2 BioDent parameters in the multivariable logistic regression model with mass—a much more accessible metric—resulted in only a minor decrease in diagnostic ability of the model, according to the area under their respective ROC curves.

4.4 pQCT

Among the host of parameters that pQCT measures, many had significant site * group interactions when the four experimental groups were compared against one another. Among these, certain parameters can intuitively be expected to contribute more to the multivariable model than others. For example, geometric measurements may be somewhat redundant in the model if cortical thickness derived from x-rays is included. Alternatively, however, were pQCT to provide more reliable insight to fracture susceptibility than x-ray, a metric such as cortical area may be used in place of x-ray data. Bone mineral density (BMD) is looked upon as a valuable contribution from pQCT because of how distinct in nature it is from indentation and cortical thickness. Within the realm of BMD, cortical & subcortical measures at distal levels are deemed relevant due to the mechanical importance and common fracture incidence of these areas of bone.

It remains unclear whether pQCT should be classified as a clinically relevant tool. While standing pQCT has been successfully performed in standing horses before [67], it is not currently common practice and would likely be difficult to attain. Though it is not as practical as x-ray or OsteoProbe, it will not be disqualified from the potentially clinically applicable methodologies for the time being.

4.5 μCT

μCT testing was performed on a smaller and more selective sample size than the other test methods, but results were consistent with the running theory of bone modeling being evident on the dorsal surface of bones from horses without fracture diagnoses. Low BMD, in some cases, can be an indicator of pathology such as osteoporosis. While this may seem counterintuitive, as it was found that bones from the Control group had a lower surface BMD than bones from the fracture-afflicted group, the location of testing may play a significant role in interpreting the results. Just as the indentation testing and x-rays have suggested that modeling may be occurring on the dorsal surface of Control bones, the nature of μCT testing seems to also detect this immature bone. Woven bone has reduced mineral content compared to mature lamellar bone, which may explain why the BMD at the dorsal periosteal surface in Control bones is lower than that of LB bones despite LB bones having significantly lower cortical BMD per the pQCT results in this study (Table A.24).

The low-density layers found adjacent to the surface on the affected bones remain to be identified with certainty. Once again, it may be the case that disorganized, comparatively low-mineral primary bone that forms in response to exercise is lining the dorsal surface of the bone, creating an area of low attenuation that appears as a black strip in the radiographic image. The porous appearance of the bone pictured in Figure 3.23, however, likely exhibited another metabolic mechanism. It is possible that the increased porosity may be due to the resorption phase of the remodeling process, in which case the afflicted horse may have been undergoing healthy adaptation in the bone tissue but was simply left vulnerable to fracture due to decreased bone density and volume. Alternatively, the apparent porosity may have been pathological, making fracture essentially imminent. While the possibility of the apparent spots being caused by signal noise is not an impossibility, it is not being significantly considered given the surrounding portions of the image in conjunction with the other well-processed images in the set.

4.6 Multivariable Regression Model

The logistic regression analysis performed in this study was meant only to explore the field of predictive multivariable models, not to act as one. Predictive models of the sort for which we are aiming require statistical training sets much larger than our current sample size—depending on how many predictor variables and factors the model is to account for, hundreds of samples may be necessary. It is also worth noting that ROC curves and their corresponding AUC values are typically regarded as better predictors of diagnostic ability than comparison-of-mean tests such as t-tests or ANOVA. Because a large enough sample size could grant statistical significance to a difference on the order of a few osteons in a measure like cortical thickness, it is important not to draw any conclusions that are inappropriate for the nature of our testing.

At the same time, the results obtained from these preliminary models should not be discounted. Which predictive variables and potential covariates to use are yet to be optimized, and the working sample size is still relatively small. An AUC of 1.0 will never be achieved, but if the current model can be adjusted to a point where it can reliably predict the state of a bone, or the skeletal system as a whole, a vast majority of the time, it may find some important applications in equine or human fracture risk prediction.

When optimizing the model, sensitivity and specificity should also be considered. Horse owners, for example, may prefer a high sensitivity in the model, as allowing a period of rest may amount to a more economic decision than risking catastrophic breakdown and euthanasia.

4.7 Raman Spectroscopy and MRI

In a previous study that included a number of bones among this sample, Raman spectroscopy was used to determine the concentration of inorganic components in bone including phosphate, carbonate, and amide groups.

Raman spectroscopy was not utilized in this analysis due to the finding that bones exhibited different spectra than they did when measured in a previous study. Recent spectra suggest that bones have significantly higher carbonate than phosphate concentrations, when the opposite is known to be true and has been displayed in previous analyses of the same bones. While undergoing freeze-thaw cycles may have an effect on the organic composition of bone, it is not expected to cause any changes in the representation of inorganic components.

Figure 4.1. When previously obtained spectra ("Tony") were compared with recent samples ("Jon") and normalized by the height of the peak at ~970 cm^{-1}, other expected peaks (noted by vertical blue lines) were notably different between samples

A myriad of methods to remedy the discrepancies between previous and recent data were attempted. These revisions yielded spectra with distinct peaks at expected locations, though the magnitude of the peaks does not appear to be consistent with the known composition of bone.

A select number of bones in this study also underwent MRI testing. While cost and accessibility of MRI testing may exclude it from being considered as a clinically-relevant parameter in an equine model, it may be implemented in future iterations when human subjects are being considered.

4.8 Limitations

One conspicuous limitation of this study was the sample size of the MC3 experimental group. While grouping it together with the LB group didn't appear to have any adverse effects on the results, this experiment could not properly compare this subset of fractures to the other experimental groups. The overall sample size was also a limitation to the logistic regression model. In order to move forward with the model, a substantially greater sample size in each of the relevant fracture groups must be collected.

The relatively high standard deviations among the x-ray data may have stemmed from multiple factors. Bone geometries varied substantially: the length of the bones being analyzed ranged over 40 mm and standard deviations at certain sites within groups amounted to over 30% of the measurements themselves. Bone orientation during imaging may have also played a role, as small and potentially undetectable rotations of the bone would result in the projection of slightly different planes in the x-ray image. Additionally, human factors should be considered, as the calibration process allowed room for variability and the measurement process inherently relied on some judgement in distinguishing the interface between cortical and trabecular bone at the endosteal surface of the cortex.

While no significant results were discovered while using the OsteoProbe on a bare bone surface compared to when it was used percutaneously, the data collected percutaneously is less consistent. This tradeoff with clinical relevancy may be a drawback for the argument of the use of OsteoProbe in clinic.

5. CONCLUSIONS

Much was discovered in this study regarding which clinical and preclinical methods may be best suited for a predictive model and how to best focus future efforts. A lack of compelling evidence was found suggesting that any parameters significantly differ between left and right limbs, potentially eliminating the need for a dual-limb paradigm for each horse.

Cortical thickness, as determined by x-ray imaging, was found to be significantly different between the Control group and Fracture group at the mid- and distal-dorsal surfaces of third metacarpal bones. Bone material strength index (BMSi), while not significantly different between fracture groups, was found to potentially be able to detect primary bone deposition on the dorsal surface of healthy bones. BioDent measurements were able to detect that the average energy dissipated during cyclic indentation is higher in the Control group than in Fracture group on the distal dorsal surface, suggesting a less elastic surface more prone to permanent deformation. pQCT data suggested that overall cortical bone mineral density (BMD) may be lower in certain fracture groups than in the control group, and μCT found a significantly lower BMD on the dorsal surface—but not lateral or medial surfaces—of bones in the Control group compared to bones in the Long Bone group. Some μCT images show what appears to be immature primary bone on the surface of Control bones, which is consistent with other methodologies and suggests a healthy ability of the bone to adapt to training, which is consistent with the fracture history (or lack thereof) in this group.

While individual parameters exhibit poor ability to distinguish between control or fracture bones in a regression model, utilizing multiple parameters can establish a model with intriguing predictive potential. With a large sample size and an optimized set of independent variables, the prospect of a regression model with a clinically relevant ability to distinguish between healthy and at-risk bones appears promising.

6. FUTURE DIRECTIONS

The primary objective for the future of this project is to continue to increase the sample size. Once an adequate amount of data has been collected, a reliable predictive model can be created. In order to obtain the necessary sample size within practical bounds of time and cost, however, data will have to be collected more discriminately. A simple way to eliminate data collection resources by half is to only analyze one limb per horse. Given that the existing data does not exhibit any considerable differences between right and left limbs, a single-limb protocol can be implemented. Similarly, a majority of differences between the Control group and fracture groups are manifesting themselves at a select number of sites on the bone; if only these sites are tested, the process again becomes more efficient. Lastly, it may be prudent to only consider methodologies that are clinically relevant in either horses or humans. While data from sources such as Raman spectroscopy provide valuable insight to the composition of bones, the testing protocols are not at all conducive to or logistically feasible for live patients.

Considering the results from this study, it may be beneficial to move forward with the model without including the SSMD fracture group. Sesamoid bones are pointedly different from third metacarpals and other long bones, and sesamoid fractures may involve a distinct pathogenesis from their long bone counterparts. At many parameters and locations, bones from the SSMD group resemble the control bones more than the other two fracture groups; therefore, excluding them from the study may reveal more differences between bones in the Control group and those in the LB and MC3 groups. The inclusion of only the C, LB, and MC3 groups would also leave the regression model to distinguish only between bones from control horses and those from horses with long-bone fractures, which may lead to higher predictive values. To optimize which variables are included in the model, sensitivity analyses should be performed on each parameter collected thus far to establish which may have the best predictive capability when included in the model.

Additionally, a goal much further in the future is to translate a successful equine goal into one for humans. It will likely be most intuitive to transition the model from equine athletes to human athletes or soldiers, but being able to detect at-risk bones from pathologies such as osteoporosis are not out of the realm of this project in the long-term.

REFERENCES

[1] T. H. Witte, C. V. Hirst, and A. M. Wilson, “Effect of speed on stride parameters in racehorses at gallop in field conditions,” *Journal of Experimental Biology*, vol. 209, no. 21, pp. 4389–4397, Nov. 2006.

[2] A. C. Abraham, A. Agarwalla, A. Yadavalli, C. McAndrew, J. Y. Liu, and S. Y. Tang, “Multiscale Predictors of Femoral Neck In Situ Strength in Aging Women: Contributions of BMD, Cortical Porosity, Reference Point Indentation, and Nonenzymatic Glycation,” *J. Bone Miner. Res.*, vol. 30, no. 12, pp. 2207–2214, Dec. 2015.

[3] A. C. Abraham, A. Agarwalla, A. Yadavalli, J. Y. Liu, and S. Y. Tang, “Microstructural and compositional contributions towards the mechanical behavior of aging human bone measured by cyclic and impact reference point indentation,” Bone, vol. 87, pp. 37–43, 2016.

[3] L. McGlinchey, M. J. Hurley, C. M. Riggs, and S. M. Rosanowski, “Description of the incidence, clinical presentation and outcome of proximal limb and pelvic fractures in Hong Kong racehorses during 2003–2014,” *Equine Veterinary Journal*, vol. 49, no. 6, pp. 789–794, 2017.

[4] A. Beisser, S. McClure, G. Rezabek, K. H. Soring, and C. Wang, “Frequency of and risk factors associated with catastrophic musculoskeletal injuries in Quarter Horses at two Midwestern racetracks: 67 cases (2000–2011),” *Journal of the American Veterinary Medical Association*, vol. 245, no. 10, pp. 1160–1168, Oct. 2014.

[5] L. Estberg *et al.*, “Fatal musculoskeletal injuries incurred during racing and training in thoroughbreds,” *J. Am. Vet. Med. Assoc.*, vol. 208, no. 1, pp. 92–96, Jan. 1996.

[6] L. Estberg *et al.*, “Relationship between race start characteristics and risk of catastrophic injury in thoroughbreds: 78 cases (1992),” *J. Am. Vet. Med. Assoc.*, vol. 212, no. 4, pp. 544–549, Feb. 1998.

[7] J. Wolff, *The Law of Bone Remodelling*. Springer Science & Business Media, 2012.

[8] S. C. Blott *et al.*, “A genome-wide association study demonstrates significant genetic variation for fracture risk in Thoroughbred racehorses,” *BMC Genomics*, vol. 15, no. 1, p. 147, Feb. 2014.

[8] P. J. Prendergast and R. Huiskes, “The Biomechanics of Wolff’s law: Recent advances,” *I.J.M.S.*, vol. 164, no. 2, pp. 152–154, Apr. 1995.

[9] T. C. Lee and D. Taylor, “Bone remodelling: Should we cry wolff?,” *Ir. J. Med. Sci.*, vol. 168, no. 2, p. 102, Apr. 1999.

[10] A. C. Ahn and A. J. Grodzinsky, “Relevance of collagen piezoelectricity to ‘Wolff’s Law’: A critical review,” *Medical Engineering & Physics*, vol. 31, no. 7, pp. 733–741, Sep. 2009.

[11] S. Weinbaum, S. C. Cowin, and Y. Zeng, “A model for the excitation of osteocytes by mechanical loading-induced bone fluid shear stresses,” *Journal of Biomechanics*, vol. 27, no. 3, pp. 339–360, Mar. 1994.

[12] J. P. Bilezikian, L. G. Raisz, and T. J. Martin, “Principles of Bone Biology: Third Edition,” *Academic Press*. 2008.

[13] K. L. Bennell, S. A. Malcolm, J. D. Wark, and P. D. Brukner, “Models for the pathogenesis of stress fractures in athletes.,” *Br J Sports Med*, vol. 30, no. 3, pp. 200–204, Sep. 1996.

[14] R. C. Boston and D. M. Nunamaker, “Gait and speed as exercise components of risk factors associated with onset of fatigue injury of the third metacarpal bone in 2-year-old Thoroughbred racehorses,” American Journal of Veterinary Research, vol. 61, no. 6, pp. 602–608, Jun. 2000.

[15] K. L. P. Verheyen, W. E. Henley, J. S. Price, and J. L. N. Wood, “Training-related factors associated with dorsometacarpal disease in young Thoroughbred racehorses in the UK,” *Equine Veterinary Journal*, vol. 37, no. 5, pp. 442–448, 2005.

[16] N. Dalén and K. E. Olsson, “Bone Mineral Content and Physical Activity,” *Acta Orthopaedica Scandinavica*, vol. 45, no. 1–4, pp. 170–174, Jan. 1974.

[17] J. E. Smith, W. Reddan, and P. E. Smith, “Physical activity and calcium modalities for bone mineral increase in aged women.,” *Med Sci Sports Exerc*, vol. 13, no. 1, pp. 60–64, 1981.

[18] L. Gustafsson, B. Jacobson, and L. Kusoffsky, “X ray spectrophotometry for bone-mineral determinations,” *Med. & biol. Engng.*, vol. 12, no. 1, pp. 113–119, Jan. 1974.

[19] B. Jacobson, “X-RAY SPECTROPHOTOMETRY IN VIVO,” *Am. J. Roentgenol., Radium Therapy Nucl. Med.*, vol. Vol: 91, Jan. 1964.

[20] J. R. Cameron and J. Sorenson, “Measurement of bone mineral in vivo: an improved method,” *Salud pública Méx*, vol. 51, pp. s126–s131, 2009.

[21] Y. MAEDA, M. HANADA, and M. OIKAWA, “Epidemiology of racing injuries in Thoroughbred racehorses with special reference to bone fractures: Japanese experience from the 1980s to 2000s,” *J Equine Sci*, vol. 27, no. 3, pp. 81–97, 2016.

[22] M. A. Laskey, “Dual-energy X-ray absorptiometry and body composition,” Nutrition, vol. 12, no. 1, pp. 45–51, Jan. 1996.

[23] M. R. McClung *et al.*, “Romosozumab in Postmenopausal Women with Low Bone Mineral Density,” *New England Journal of Medicine*, vol. 370, no. 5, pp. 412–420, Jan. 2014.

[24] S. Kaul *et al.*, “Dual-Energy X-Ray Absorptiometry for Quantification of Visceral Fat,” *Obesity*, vol. 20, no. 6, pp. 1313–1318, 2012.

[25] T. Binkley, J. Johnson, L. Vogel, H. Kecskemethy, R. Henderson, and B. Specker, “Bone Measurements by Peripheral Quantitative Computed Tomography (pQCT) in Children with Cerebral Palsy,” The Journal of Pediatrics, vol. 147, no. 6, pp. 791–796, Dec. 2005.

[26] J. F. Griffith and H. K. Genant, “Bone mass and architecture determination: state of the art,” *Best Practice & Research Clinical Endocrinology & Metabolism*, vol. 22, no. 5, pp. 737–764, Oct. 2008.

[27] P. Rossman, J. Zagzebski, C. Mesina, J. Sorenson, and R. Mazess, “Comparison of speed of sound and ultrasound attenuation in the os calcis to bone density of the radius, femur and lumbar spine,” *Clin. Phys. Physiol. Meas.*, vol. 10, no. 4, pp. 353–360, Nov. 1989.

[28] G. Haïat *et al.*, “Optimal Prediction of Bone Mineral Density with Ultrasonic Measurements in Excised Human Femur,” *Calcif Tissue Int*, vol. 77, no. 3, pp. 186–192, Sep. 2005.

[29] S. Casciaro, F. Conversano, P. Pisani, and M. Muratore, “New perspectives in echographic diagnosis of osteoporosis on hip and spine,” *Clin Cases Miner Bone Metab*, vol. 12, no. 2, pp. 142–150, 2015.

[30] E. C. Firth, C. W. Rogers, M. Doube, and N. B. Jopson, “Musculoskeletal responses of 2-year-old Thoroughbred horses to early training. 6. Bone parameters in the third metacarpal and third metatarsal bones,” *New Zealand Veterinary Journal*, vol. 53, no. 2, pp. 101–112, Apr. 2005.

[31] P. Noble, E. R. Singer, and N. S. Jeffery, “Does subchondral bone of the equine proximal phalanx adapt to race training?,” *Journal of Anatomy*, vol. 229, no. 1, pp. 104–113, 2016.

[32] P. Tóth *et al.*, “Bone mineral density (BMD) and computer tomographic measurements of the equine proximal phalanx in correlation with breaking strength,” *Polish journal of veterinary sciences*, vol. 16, pp. 3–8, 2013.

[33] S. H. Bogers, C. W. Rogers, C. Bolwell, W. Roe, E. Gee, and C. W. McIlwraith, “Quantitative comparison of bone mineral density characteristics of the distal epiphysis of third metacarpal bones from Thoroughbred racehorses with or without condylar fracture,” *American Journal of Veterinary Research*, vol. 77, no. 1, pp. 32–38, Dec. 2015.

[34] S. Kumasaka, K. Asa, R. Kawamata, T. Okada, M. Miyake, and I. Kashima, “Relationship between bone mineral density and bone stiffness in bone fracture,” *Oral Radiol*, vol. 21, no. 1, pp. 38–40, Jun. 2005.

[35] K. M. Watson, D. J. Stitson, and H. M. S. Davies, “Third metacarpal bone length and skeletal asymmetry in the Thoroughbred racehorse,” *Equine Veterinary Journal*, vol. 35, no. 7, pp. 712–714, 2003.

[36] H. M. S. Davies, S. M. Gale, and I. D. C. Baker, “Radiographic measures of bone shape in young Thoroughbreds during training for racing,” *Equine Veterinary Journal*, vol. 31, no. S30, pp. 262–265, 1999.

[37] H. Davies and K. Watson, “Third metacarpal bone laterality asymmetry and midshaft dimensions in Thoroughbred racehorses,” *Australian Veterinary Journal*, vol. 83, no. 4, pp. 224–226, 2005.

[38] R. M. Embertson, L. R. Bramlage, D. S. Herring, and A. A. Gabel, “Physeal Fractures in the Horse:I. Classification and Incidence,” *Veterinary Surgery*, vol. 15, no. 3, pp. 223–229, 1986.

[39] V. S. Mackey, D. R. Trout, D. M. Meagher, and W. J. Hornof, “Stress Fractures of the Humerus, Radius, and Tibia in Horses,” *Veterinary Radiology*, vol. 28, no. 1, pp. 26–31, 1987.

[40] M. Hasegawa, M. Kaneko, M. Oikawa, T. Yoshihara, and R. Wada, “Pathological Studies on Distal Third Tibial Fractures on the Plantar Side in Racehorses,” Bull. Equine Res. Inst., vol. 1988, no. 25, pp. 6–14, Dec. 1988.

[41] P. D. Hanson and M. D. Markel, “Radiographic geometric variation of equine long bones.,” *Am J Vet Res*, vol. 55, no. 9, pp. 1220–1227, Sep. 1994.

[41] D. M. Nunamaker, D. M. Butterweck, and M. T. Provost, “Some geometric properties of the third metacarpal bone: A comparison between the thoroughbred and standardbred racehorse,” *Journal of Biomechanics*, vol. 22, no. 2, pp. 129–134, Jan. 1989.

[42] M. Oikawa and K. Shimazu, “In Vitro Measurement of the Bone Mineral Density of the Third Metacarpal Bone by Dual Energy X-Ray Absorptiometry in Racehorses-Comparison with Single Photon Absorptiometry.,” *Journal of Equine Science*, vol. 7, no. 4, pp. 93–96, 1996.

[42] K. L. Thomson, G. D. Potter, K. J. Terrell, E. L. Morris, and K. J. Mathiason-Kochan, “Cortical Bone Width in Juvenile Race Horses Treated with Exogenous Somatotropin,” *Professional animal scientists*, 2002.

[43] L. Gaschen and D. J. Burba, “Musculoskeletal Injury in Thoroughbred Racehorses,” *Veterinary Clinics of North America: Equine Practice*, vol. 28, no. 3, pp. 539–561, Dec. 2012.

[44] “Johan August Brinell | Swedish engineer,” *Encyclopedia Britannica*. [Online]. Available: https://www.britannica.com/biography/Johan-August-Brinell. [Accessed: 30-Sep-2019].

[45] K. L. Johnson, “The correlation of indentation experiments,” *Journal of the Mechanics and Physics of Solids*, vol. 18, no. 2, pp. 115–126, Apr. 1970.

[46] N. A. Sakharova, J. V. Fernandes, J. M. Antunes, and M. C. Oliveira, “Comparison between Berkovich, Vickers and conical indentation tests: A three-dimensional numerical simulation study,” International Journal of Solids and Structures, vol. 46, no. 5, pp. 1095–1104, Mar. 2009.

[47] D. L. Joslin and W. C. Oliver, "A new method for analyzing data from continuous depth-sensing microindentation tests," *Journal of Materials Research*, vol. 5, no. 1, pp. 123–126, Jan. 1990.

[48] F.-J. Ulm, M. Vandamme, C. Bobko, J. A. Ortega, K. Tai, and C. Ortiz, "Statistical Indentation Techniques for Hydrated Nanocomposites: Concrete, Bone, and Shale," *Journal of the American Ceramic Society*, vol. 90, no. 9, pp. 2677–2692, 2007.

[49] J. B. Thompson, J. H. Kindt, B. Drake, H. G. Hansma, D. E. Morse, and P. K. Hansma, "Bone indentation recovery time correlates with bond reforming time," *Nature*, vol. 414, no. 6865, pp. 773–776, Dec. 2001.

[49] J. Y. Rho, P. Zioupos, J. D. Currey, and G. M. Pharr, "Microstructural elasticity and regional heterogeneity in human femoral bone of various ages examined by nano-indentation," Journal of Biomechanics, vol. 35, no. 2, pp. 189–198, Feb. 2002.

[50] L. Feng, M. Chittenden, J. Schirer, M. Dickinson, and I. Jasiuk, "Mechanical properties of porcine femoral cortical bone measured by nanoindentation," Journal of Biomechanics, vol. 45, no. 10, pp. 1775–1782, Jun. 2012.

[51] A. Chang, G. W. Easson, and S. Y. Tang, "Clinical Measurements of Bone Tissue Mechanical Behavior Using Reference Point Indentation," *Clinic Rev Bone Miner Metab*, vol. 16, no. 3, pp. 87–94, Sep. 2018.

[52] ALSi, "Disruptive medical device for bone quality, OsteoProbe®, now in clinical use in Europe – Active Life Scientific, Inc." .

[53] J. N. Farr, M. T. Drake, S. Amin, L. J. Melton, L. K. McCready, and S. Khosla, "In Vivo Assessment of Bone Quality in Postmenopausal Women with Type 2 Diabetes," *J Bone Miner Res*, vol. 29, no. 4, pp. 787–795, Apr. 2014.

[53] S. Uppuganti *et al.*, "Differences in sensitivity to microstructure between cyclic- and impact-based microindentation of human cortical bone," *J. Orthop. Res.*, vol. 35, no. 7, pp. 1442–1452, 2017.

[54] J. R. Furst *et al.*, "Advanced Glycation Endproducts and Bone Material Strength in Type 2 Diabetes," *None*, vol. 101, no. 6, pp. 2502–2510, Jun. 2016.

[55] F. Malgo, N. A. T. Hamdy, S. E. Papapoulos, and N. M. Appelman-Dijkstra, "Bone Material Strength as Measured by Microindentation In Vivo Is Decreased in Patients With Fragility Fractures Independently of Bone Mineral Density," *J Clin Endocrinol Metab*, vol. 100, no. 5, pp. 2039–2045, May 2015.

[56] D. D. Sosa and E. F. Eriksen, "Reduced Bone Material Strength is Associated with Increased Risk and Severity of Osteoporotic Fractures. An Impact Microindentation Study," *Calcif Tissue Int*, vol. 101, no. 1, pp. 34–42, Jul. 2017.

[57] M. J. Pérez-Sáez *et al.*, “Bone density, microarchitecture, and material strength in chronic kidney disease patients at the time of kidney transplantation,” *Osteoporos Int*, vol. 28, no. 9, pp. 2723–2727, Sep. 2017.

[58] “BioDent Calculations – Active Life Scientific, Inc. – Research.” [Online]. Available: http://research.activelifescientific.com/biodent-calculations/

[59] R. C. Güerri-Fernández *et al.*, “Microindentation for in vivo measurement of bone tissue material properties in atypical femoral fracture patients and controls,” *Journal of Bone and Mineral Research*, vol. 28, no. 1, pp. 162–168, 2013.

[60] A. J. Williamson, N. A. Sims, C. D. L. Thomas, P. V. S. Lee, M. A. Stevenson, and R. C. Whitton, “Biomechanical testing of the calcified metacarpal articular surface and its association with subchondral bone microstructure in Thoroughbred racehorses,” *Equine Veterinary Journal*, vol. 50, no. 2, pp. 255–260, 2018.

[61] “Multiple Linear Regression.” [Online]. Available: http://www.stat.yale.edu/Courses/1997-98/101/linmult.htm. [Accessed: 01-Oct-2019].

[62] L. A. Anthenill, S. M. Stover, I. A. Gardner, and A. E. Hill, “Risk factors for proximal sesamoid bone fractures associated with exercise history and horseshoe characteristics in Thoroughbred racehorses,” *American Journal of Veterinary Research*, vol. 68, no. 7, pp. 760–771, Jul. 2007.

[63] G. Pearce, S. May-Davis, and D. Greaves, “Femoral asymmetry in the Thoroughbred racehorse,” *Australian Veterinary Journal*, vol. 83, no. 6, pp. 367–370, 2005.

[64] T. D. H. Parkin et al., “Catastrophic fracture of the lateral condyle of the third metacarpus/metatarsus in UK racehorses – fracture descriptions and pre-existing pathology,” The Veterinary Journal, vol. 171, no. 1, pp. 157–165, Jan. 2006.

[65] B. Hermanns-Sachweh et al., “Vascular changes in the periosteum of congenital pseudarthrosis of the tibia,” Pathology - Research and Practice, vol. 201, no. 4, pp. 305–312, May 2005.

[66] D. Sundh et al., “High-Impact Mechanical Loading Increases Bone Material Strength in Postmenopausal Women-A 3-Month Intervention Study,” J. Bone Miner. Res., vol. 33, no. 7, pp. 1242–1251, 2018.

[67] F. G. Desbrosse et al., “A technique for computed tomography (CT) of the foot in the standing horse,” Equine Veterinary Education, vol. 20, no. 2, pp. 93–98, 2008.

[68] A. Diez-Perez et al., “Microindentation for in vivo measurement of bone tissue mechanical properties in humans,” J. Bone Miner. Res., vol. 25, no. 8, pp. 1877–1885, Aug. 2010.

[69] A. E. Waller, J. L. Daniels, N. L. Weaver, and P. Robinson, “Jockey Injuries in the United States,” JAMA, vol. 283, no. 10, pp. 1326–1328, Mar. 2000.

[70] D. B. Burr, R. B. Martin, M. B. Schaffler, and E. L. Radin, “Bone remodeling in response to in vivo fatigue microdamage,” Journal of Biomechanics, vol. 18, no. 3, pp. 189–200, Jan. 1985.

[71] T. L. Bredbenner, R. L. Mason, L. M. Havill, E. S. Orwoll, and D. P. Nicolella, “Fracture Risk Predictions based on Statistical Shape and Density Modeling of the Proximal Femur,” J Bone Miner Res, vol. 29, no. 9, pp. 2090–2100, Sep. 2014.

[72] D. M. Black et al., “An Assessment Tool for Predicting Fracture Risk in Postmenopausal Women,” Osteoporos Int, vol. 12, no. 7, pp. 519–528, Aug. 2001.

[73] B. Kaye, C. Randall, D. Walsh, and P. K. Hansma, “The Effects of Freezing on the Mechanical Properties of Bone,” 2012.

APPENDIX

Horse Information List

Table A.1. Sex, age, mass, fracture group, and cause of death listed for each horse. (Sex: M = male, F = female, G = gelding, C = colt).

Horse ID	Sex	Age (yrs)	Mass (kg)	Fx Group	Cause of Death
A13-13503	M	3	514	C	Exercise-induced pulmonary embolism
A13-14144	F	4	410	C	
A14-0419	F	3	398	C	Diarrhea, Lethargy
A14-14702	F	5	488	C	Possible ruptured aorta
A14-15808	F	4	425	C	Ruptured right-front superior digital flexor tendon
A15-1229	F	3	485	C	Right-hind fetlock laceration / soft tissue injury
A15-1432	G	5	518	C	Severe osteoarthritis, right-front radiocarpal joing injury
A15-2920	F	3		C	Pneumonia, severe colitis
A15-4789	F	2	433	C	Colic
A16-1177	G	4	458	C	Exercise-induced pulmonary hemorrhage
A16-2118	G	4	432	C	Enterocolitis
A16-2293	M	2	494	C	Pastern joint luxation
A16-3336	G	3	532	C	Sudden death at end of race
A17-3709	G	4	527	C	Suspected colic
A18-15218	F	3	491	C	Possible colic
A18-17727	F	3	527	C	Sudden death at end of race
A18-584	G	3	450	C	Right-hind hoof avulsion
A19-4449	C	4	503	C	Laminitis
A19-5963	G	5	491	C	Open dislocation of left carpus
A19-7032	G	3	548	C	Suspected cardiovascular event
A14-1356	F	2	459	LB	Left radius fracture
A14-15954	G	5	514	LB	Left ulna olecranon tubercle fracture
A14-1818	F	3	525	LB	Comminuted right carpus fracture
A15-13734	F	3	480	LB	Comminuted right scapula fracture
A15-14441	G	3	515	LB	Comminuted left tibia fracture
A15-4293	F	2	459	LB	Right front long pastern bone fracture
A15-4869	M	4	493	LB	Left radius fracture
A15-5258	M	3	517	LB	3rd and 4th carpal fractures
A16-16656	F	6	552	LB	Scapula fracture
A16-2964	G	3	541	LB	Scapula fracture
A16-647	F	3	503	LB	Radial carpal bone fracture

Table A.1, continued

A18-1274	G	3	500	LB	Left scapula fracture
A18-15243	G	4	505	LB	Left 3rd carpal bone fracture
A18-15426	F	3	495	LB	Comminuted left humerus fracture
A18-3846	G	3	442	LB	Left-front scapula fracture
A18-6100	F	4	450	LB	Left humerus fracture
A19-16901	F	4	465	LB	Right-hind third metatarsal & long pastern bone fractures
A19-4350	G	4	622	LB	Comminuted left-front third carpal fracture
A19-998	G	3	476	LB	Comminuted right scapula fracture
A13-13148	F	3	433	SSMD	Both left-front sesamoid fracture
A14-0498	F	5	490	SSMD	Both left-front sesamoid fracture
A14-14416	M	4	526	SSMD	Both left-front sesamoid fracture
A14-15391	F	3	425	SSMD	Both left-front sesamoid fracture
A14-15834	G	4	503	SSMD	Both left-front sesamoid fracture
A14-1972	G	4	570	SSMD	Both left-front sesamoid fracture
A14-3323	M	5	575	SSMD	Both left-front sesamoid fracture
A14-4991	F	4	485	SSMD	Both left-front sesamoid fracture
A14-4992	G	5	441	SSMD	Both left-front sesamoid fracture
A16-1925	F	5	514	SSMD	Both right-front sesamoid fracture
A16-2635	G	4	541	SSMD	Both right-front sesamoid fracture
A16-9	F	6	463	SSMD	Both left-front sesamoid fracture
A17-13458	F	4	468	SSMD	Left-front sesamoid fracture, luxated fetlock
A17-18109	G	3	527	SSMD	Both left-front sesamoid fracture
A17-5101	G	3	440	SSMD	Left-front medial sesamoid fracture, flexor tendon rupture, DLS rupture
A19-1548	G	3	548	SSMD	Both right-front sesamoid fracture
A19-1718	G	3	491	SSMD	Both right-front sesamoid fracture
A19-2036	F	4	527	SSMD	Both right-front sesamoid fracture
A19-4679	F	6	489	SSMD	Left-front medial sesamoid fracture
A19-488	G	6	584	SSMD	Both left-front sesamoid fracture
391-187	G	5	480	MC3	Right condylar MC3 fracture
A14-14505	G	5	498	MC3	Left comminuted midshaft MC3 fracture
A15-4375	F	2	439	MC3	Left comminuted MC3 fracture
A17-14797	G	2	498	MC3	Left transverse MC3 fracture
A18-6468	F	3	481	MC3	Left comminuted midshaft MC3 fracture

Mixed Linear Model Result Tables

X-ray

Table A.2. Cortical thickness was not found to be significant ($p < 0.05$) between groups or in site * group interactions.

Type III Tests of Fixed Effects[a]

Source	Numerator df	Denominator df	F	Sig.
Intercept	1	61.082	6359.164	.000
site	11	665.502	148.665	.000
group	3	61.175	1.226	.308
site * group	33	665.587	1.282	.136

a. Dependent Variable: thickness.

Table A.3. Cortical thickness (normalized by mass of horse) was not found to be significant ($p < 0.05$) between groups or in site * group interactions.

Type III Tests of Fixed Effects[a]

Source	Numerator df	Denominator df	F	Sig.
Intercept	1	60.062	3293.937	.000
site	11	654.304	146.181	.000
group	3	60.120	1.112	.351
site * group	33	654.357	1.186	.221

a. Dependent Variable: thickness_norm_mass.

Table A.4. Cortical thickness (normalized by length of MC3 bone) was not found to be significant ($p < 0.05$) between groups or in site * group interactions.

Type III Tests of Fixed Effects[a]

Source	Numerator df	Denominator df	F	Sig.
Intercept	1	61.058	6716.450	.000
site	11	665.495	149.268	.000
group	3	61.154	1.628	.192
site * group	33	665.582	1.274	.142

a. Dependent Variable: thickness_norm_length.

Table A.5. Cortical thickness was found to be significant ($p < 0.05$) in site * group interactions when the LB and MC3 experimental groups were combined.

Type III Tests of Fixed Effects[a]

Source	Numerator df	Denominator df	F	Sig.
Intercept	1	62.319	9199.826	.000
site	11	676.729	213.207	.000
group	2	62.304	1.708	.190
site * group	22	676.708	1.560	.049

a. Dependent Variable: thickness.

Table A.6. Cortical thickness was found to be significant ($p < 0.05$) in site * group interactions when the LB, SSMD, and MC3 experimental groups were combined and compared against the C group in the mixed linear model. Post-hoc analysis revealed significant differences at the 50% and 75% dorsal sites.

Type III Tests of Fixed Effects[a]

Source	Numerator df	Denominator df	F	Sig.
Intercept	1	62.976	7667.165	.000
site	11	687.389	186.144	.000
group	1	62.976	.161	.690
site * group	11	687.389	1.889	.038

a. Dependent Variable: thickness.

OsteoProbe

Skin-on

Table A.7. BMSi was found to be significantly ($p < 0.05$) in site * group interactions.

Type III Tests of Fixed Effects[a]

Source	Numerator df	Denominator df	F	Sig.
Intercept	1	58.944	1579.594	.000
site	11	625.195	6.167	.000
group	3	59.143	.573	.635
site * group	33	625.456	1.957	.001

a. Dependent Variable: bmsi.

Table A.8. BMSi was found to be significantly ($p < 0.05$) in site * group interactions when the LB and MC3 experimental groups were combined.

Type III Tests of Fixed Effects[a]

Source	Numerator df	Denominator df	F	Sig.
Intercept	1	60.475	2253.061	.000
site	11	636.824	11.272	.000
group	2	60.433	.745	.479
site * group	22	636.746	1.978	.005

a. Dependent Variable: bmsi.

No Skin

Table A.9. BMSi was not found to be significant ($p < 0.05$) between groups or in site * group interactions.

Type III Tests of Fixed Effects[a]

Source	Numerator df	Denominator df	F	Sig.
Intercept	1	60.000	19440.801	.000
site	11	660.000	50.837	.000
group	3	60	1.489	.227
site * group	33	660.000	1.312	.116

a. Dependent Variable: bmsi.

Table A.10. BMSi was not found to be significant ($p < 0.05$) between groups or in site * group interactions when the LB and MC3 experimental groups were combined.

Type III Tests of Fixed Effects[a]

Source	Numerator df	Denominator df	F	Sig.
Intercept	1	61	27482.411	.000
site	11	671.000	75.605	.000
group	2	61	1.624	.205
site * group	22	671.000	1.518	.061

a. Dependent Variable: bmsi.

BioDent

Table A.11. Total Indentation Distance was not found to be significant ($p < 0.05$) between groups or in site * group interactions.

Type III Tests of Fixed Effects[a]

Source	Numerator df	Denominator df	F	Sig.
Intercept	1	63.209	2666.509	.000
site	8	455.805	24.535	.000
group	3	60.669	.497	.686
site * group	24	454.052	.859	.660

a. Dependent Variable: TID.

Table A.12. Indentation Distance Increase was not found to be significant ($p < 0.05$) between groups or in site * group interactions.

Type III Tests of Fixed Effects[a]

Source	Numerator df	Denominator df	F	Sig.
Intercept	1	63.927	1545.501	.000
site	8	456.493	23.262	.000
group	3	61.350	1.823	.152
site * group	24	454.752	.773	.772

a. Dependent Variable: IDI.

Table A.13. Average Energy Dissipated was not found to be significant ($p < 0.05$) between groups or in site * group interactions.

Type III Tests of Fixed Effects[a]

Source	Numerator df	Denominator df	F	Sig.
Intercept	1	64.354	4163.483	.000
site	8	456.941	37.704	.000
group	3	61.752	.746	.529
site * group	24	455.206	1.103	.336

a. Dependent Variable: avgED.

Table A.14. Initial Indentation Distance was not found to be significant ($p < 0.05$) between groups or in site * group interactions.

Type III Tests of Fixed Effects[a]

Source	Numerator df	Denominator df	F	Sig.
Intercept	1	62.973	2683.871	.000
site	8	455.614	23.430	.000
group	3	60.438	.456	.714
site * group	24	453.853	.858	.661

a. Dependent Variable: ID1.

Table A.15. Average Unloading Slope was not found to be significant ($p < 0.05$) between groups or in site * group interactions.

Type III Tests of Fixed Effects[a]

Source	Numerator df	Denominator df	F	Sig.
Intercept	1	61.258	18926.768	.000
site	8	453.257	14.346	.000
group	3	59.564	1.026	.388
site * group	24	451.972	1.189	.246

a. Dependent Variable: avgUS.

Table A.16. 1st-Cycle Unloading Slope was not found to be significant ($p < 0.05$) between groups or in site * group interactions.

Type III Tests of Fixed Effects[a]

Source	Numerator df	Denominator df	F	Sig.
Intercept	1	62.440	19112.689	.000
site	8	454.145	16.735	.000
group	3	60.626	1.549	.211
site * group	24	452.816	1.377	.112

a. Dependent Variable: US1.

Table A.17. 1st-Cycle Creep Indentation Distance was not found to be significant ($p < 0.05$) between groups or in site * group interactions.

Type III Tests of Fixed Effects[a]

Source	Numerator df	Denominator df	F	Sig.
Intercept	1	63.526	1986.372	.000
site	8	456.114	30.539	.000
group	3	60.968	.934	.430
site * group	24	454.366	.892	.614

a. Dependent Variable: CID1.

Table A.18. Average Creep Indentation Distance was not found to be significant ($p < 0.05$) between groups or in site * group interactions.

Type III Tests of Fixed Effects[a]

Source	Numerator df	Denominator df	F	Sig.
Intercept	1	63.598	3146.191	.000
site	8	456.246	40.305	.000
group	3	61.028	.354	.786
site * group	24	454.495	.946	.538

a. Dependent Variable: avgCID.

Table A.19. Average Loading Slope was not found to be significant ($p < 0.05$) between groups or in site * group interactions.

Type III Tests of Fixed Effects[a]

Source	Numerator df	Denominator df	F	Sig.
Intercept	1	62.392	18424.770	.000
site	8	454.674	44.277	.000
group	3	60.295	1.915	.137
site * group	24	453.160	1.140	.295

a. Dependent Variable: avgLS.

Table A.20. BioDent summary table including all p-values for site, group, and site * group interactions when all experimental groups are included in the linear mixed model.

Metric	Site	Group	Site * Group
TID	0.000	0.686	0.660
IDI	0.000	0.152	0.772
avg ED	0.000	0.529	0.336
ID1	0.000	0.714	0.661
avg US	0.000	0.388	0.246
US1	0.000	0.211	0.112
CID1	0.000	0.430	0.614
avg CID	0.000	0.786	0.538
avg LS	0.000	0.137	0.295

Table A.21. BioDent summary table including all p-values for site, group, and site * group interactions when the LB and MC3 groups are combined and compared against the C and SSMD groups in the linear mixed model

Metric	Site	Group	Site * Group
TID	0.000	0.666	0.622
IDI	0.000	0.073	0.655
avg ED	0.000	0.321	0.093
ID1	0.000	0.721	0.593
avg US	0.000	0.348	0.212
US1	0.000	0.153	0.212
CID1	0.000	0.266	0.317
avg CID	0.000	0.586	0.231
avg LS	0.000	0.064	0.217

Table A.22. BioDent summary table including all p-values for site, group, and site * group interactions when all the LB, MC3, and SSMD groups are combined and compared against the C group in the linear mixed model

Metric	Site	Group	Site * Group
TID	0.000	0.547	0.126
IDI	0.000	0.939	0.395
avg ED	0.000	0.433	**0.046**
ID1	0.000	0.494	0.107

avg US	0.000	0.368	0.359
US1	0.000	0.500	0.330
CID1	0.000	0.538	0.065
avg CID	0.000	0.884	0.095
avg LS	0.000	0.760	0.252

BioDent / OsteoProbe Correlations

Table A.23. R^2 values of no-skin BMSi compared with each BioDent parameter at each site. The 50% dorsal site, achieved by averaging together dorsolateral and dorsomedial BMSi measurements, consistently displays relatively high correlation values.

	25 Med	**50 Med**	**75 Med**	**25 Dors**	**50 Dors**	**75 Dors**	**25 Lat**	**50 Lat**	**75 Lat**
Initial Indentation Distance	0.305862	0.075273	0.157515	0.283154	**0.561892**	0.250936	0.042826	0.002449	0.032099
Total Indentation Distance	0.320588	0.078343	0.145904	0.29009	**0.582224**	0.271427	0.062476	0.004231	0.031863
Indentation Distance Increase	0.246358	0.059795	0.080039	0.317028	**0.537587**	0.334848	0.131853	0.062217	0.034911
Avg. CID	0.349406	0.235461	0.145012	0.369369	**0.575954**	0.382922	0.233675	0.132688	0.075463
Avg. ED	0.227203	0.188592	0.02954	0.200816	**0.446797**	0.097634	0.050333	0.003218	0.016083
Avg. US	0.222036	0.225556	0.004757	0.018106	**0.032446**	0.003313	0.039977	0.05237	0.065617
Avg. LS	0.304272	0.291006	0.062505	0.086505	**0.253977**	0.09293	0.048363	0.027182	0.098403

Detailed pQCT Results

Table A.24. Group differences in cortical BMD. 1 = Control, 2 = LB, 3 = SSMD, 4 = MC3.

Estimates[a]

1:CTRL, 2:LB, 3:SSMD, 4: MC3	Mean	Std. Error	df	95% Confidence Interval Lower Bound	95% Confidence Interval Upper Bound
1	969.171	5.297	61	958.579	979.763
2	947.783	5.297	61	937.191	958.376
3	971.834	5.297	61	961.242	982.426
4	922.329	10.594	61.000	901.145	943.514

a. Dependent Variable: CRT_DEN.

Pairwise Comparisons[a]

(I) 1:CTRL, 2:LB, 3:SSMD, 4:MC3	(J) 1:CTRL, 2:LB, 3: SSMD, 4:MC3	Mean Difference (I-J)	Std. Error	df	Sig.[c]	95% Confidence Interval for Difference[c] Lower Bound	95% Confidence Interval for Difference[c] Upper Bound
1	2	21.388*	7.491	61	.035	.959	41.816
	3	-2.663	7.491	61	1.000	-23.092	17.766
	4	46.842*	11.845	61.000	.001	14.541	79.142
2	1	-21.388*	7.491	61	.035	-41.816	-.959
	3	-24.051*	7.491	61	.013	-44.479	-3.622
	4	25.454	11.845	61.000	.214	-6.846	57.755
3	1	2.663	7.491	61	1.000	-17.766	23.092
	2	24.051*	7.491	61	.013	3.622	44.479
	4	49.505*	11.845	61.000	.001	17.204	81.805
4	1	-46.842*	11.845	61.000	.001	-79.142	-14.541
	2	-25.454	11.845	61.000	.214	-57.755	6.846
	3	-49.505*	11.845	61.000	.001	-81.805	-17.204

Based on estimated marginal means

*. The mean difference is significant at the .05 level.

a. Dependent Variable: CRT_DEN.

c. Adjustment for multiple comparisons: Bonferroni.

Table A.25. Group differences in cortical and subcortical mineral BMC. 1 = Control, 2 = LB, 3 = SSMD, 4 = MC3.

Estimates[a]

1:CTRL, 2:LB, 3:SSMD, 4: MC3	Mean	Std. Error	df	95% Confidence Interval	
				Lower Bound	Upper Bound
1	794.596	15.278	61	764.047	825.146
2	760.486	15.278	61	729.937	791.036
3	806.557	15.278	61	776.008	837.107
4	712.293	30.555	61	651.194	773.392

a. Dependent Variable: CRTSUB_CNT.

Pairwise Comparisons[a]

(I) 1:CTRL, 2:LB, 3:SSMD, 4:MC3	(J) 1:CTRL, 2:LB, 3: SSMD, 4:MC3	Mean Difference (I-J)	Std. Error	df	Sig.[c]	95% Confidence Interval for Difference[c]	
						Lower Bound	Upper Bound
1	2	34.110	21.606	61	.717	-24.809	93.029
	3	-11.961	21.606	61	1.000	-70.880	46.958
	4	82.303	34.162	61	.114	-10.856	175.463
2	1	-34.110	21.606	61	.717	-93.029	24.809
	3	-46.071	21.606	61	.222	-104.990	12.848
	4	48.193	34.162	61	.980	-44.966	141.353
3	1	11.961	21.606	61	1.000	-46.958	70.880
	2	46.071	21.606	61	.222	-12.848	104.990
	4	94.264*	34.162	61	.046	1.105	187.424
4	1	-82.303	34.162	61	.114	-175.463	10.856
	2	-48.193	34.162	61	.980	-141.353	44.966
	3	-94.264*	34.162	61	.046	-187.424	-1.105

Based on estimated marginal means

*. The mean difference is significant at the .05 level.

a. Dependent Variable: CRTSUB_CNT.

c. Adjustment for multiple comparisons: Bonferroni.

Table A.26. Group differences in cortical and subcortical BMD. 1 = Control, 2 = LB, 3 = SSMD, 4 = MC3.

Estimates[a]

1:CTRL, 2:LB, 3:SSMD, 4: MC3	Mean	Std. Error	df	95% Confidence Interval	
				Lower Bound	Upper Bound
1	1114.151	5.439	61.000	1103.275	1125.028
2	1105.256	5.439	61.000	1094.379	1116.133
3	1121.785	5.439	61.000	1110.908	1132.661
4	1080.226	10.879	61	1058.472	1101.979

a. Dependent Variable: CRTSUB_DEN.

Pairwise Comparisons[a]

(I) 1:CTRL, 2:LB, 3:SSMD, 4:MC3	(J) 1:CTRL, 2:LB, 3: SSMD, 4:MC3	Mean Difference (I-J)	Std. Error	df	Sig.[c]	95% Confidence Interval for Difference[c]	
						Lower Bound	Upper Bound
1	2	8.895	7.692	61.000	1.000	-12.082	29.873
	3	-7.633	7.692	61.000	1.000	-28.611	13.344
	4	33.926*	12.163	61	.042	.757	67.094
2	1	-8.895	7.692	61.000	1.000	-29.873	12.082
	3	-16.528	7.692	61.000	.214	-37.506	4.449
	4	25.030	12.163	61	.263	-8.138	58.199
3	1	7.633	7.692	61.000	1.000	-13.344	28.611
	2	16.528	7.692	61.000	.214	-4.449	37.506
	4	41.559*	12.163	61	.007	8.390	74.727
4	1	-33.926*	12.163	61	.042	-67.094	-.757
	2	-25.030	12.163	61	.263	-58.199	8.138
	3	-41.559*	12.163	61	.007	-74.727	-8.390

Based on estimated marginal means

*. The mean difference is significant at the .05 level.

a. Dependent Variable: CRTSUB_DEN.

c. Adjustment for multiple comparisons: Bonferroni.

Table A.27. Group differences in total BMD. 1 = Control, 2 = LB, 3 = SSMD, 4 = MC3.

Estimates[a]

1:CTRL, 2:LB, 3:SSMD, 4:MC3	Mean	Std. Error	df	95% Confidence Interval Lower Bound	95% Confidence Interval Upper Bound
1	885.170	7.490	61	870.191	900.148
2	862.322	7.490	61.000	847.344	877.301
3	884.962	7.490	61.000	869.984	899.940
4	832.537	14.981	61	802.580	862.493

a. Dependent Variable: TOT_DEN.

Pairwise Comparisons[a]

(I) 1:CTRL, 2:LB, 3:SSMD, 4:MC3	(J) 1:CTRL, 2:LB, 3:SSMD, 4:MC3	Mean Difference (I-J)	Std. Error	df	Sig.[c]	95% Confidence Interval for Difference[c] Lower Bound	95% Confidence Interval for Difference[c] Upper Bound
1	2	22.847	10.593	61.000	.210	-6.041	51.735
	3	.207	10.593	61.000	1.000	-28.680	29.095
	4	52.633*	16.749	61	.016	6.958	98.308
2	1	-22.847	10.593	61.000	.210	-51.735	6.041
	3	-22.640	10.593	61.000	.220	-51.527	6.248
	4	29.786	16.749	61	.482	-15.889	75.461
3	1	-.207	10.593	61.000	1.000	-29.095	28.680
	2	22.640	10.593	61.000	.220	-6.248	51.527
	4	52.426*	16.749	61	.016	6.750	98.101
4	1	-52.633*	16.749	61	.016	-98.308	-6.958
	2	-29.786	16.749	61	.482	-75.461	15.889
	3	-52.426*	16.749	61	.016	-98.101	-6.750

Based on estimated marginal means

*. The mean difference is significant at the .05 level.

a. Dependent Variable: TOT_DEN.

c. Adjustment for multiple comparisons: Bonferroni.

Table A.28. Site * group interactions in cortical BMD. 1 = Control, 2 = LB, 3 = SSMD, 4 = MC3.

site	(I) 1:CTRL, 2:LB, 3:SSMD, 4:MC3	(J) 1:CTRL, 2:LB, 3: SSMD, 4:MC3	Mean Difference (I-J)	Std. Error	df	Sig.[c]	95% Confidence Interval for Difference[c] Lower Bound	Upper Bound
10	1	2	46.096*	13.506	284.412	.004	10.212	81.981
		3	15.195	13.506	284.412	1.000	-20.690	51.079
		4	48.435	21.356	284.412	.144	-8.304	105.174
	2	1	-46.096*	13.506	284.412	.004	-81.981	-10.212
		3	-30.902	13.506	284.412	.137	-66.786	4.983
		4	2.339	21.356	284.412	1.000	-54.400	59.077
	3	1	-15.195	13.506	284.412	1.000	-51.079	20.690
		2	30.902	13.506	284.412	.137	-4.983	66.786
		4	33.240	21.356	284.412	.724	-23.498	89.979
	4	1	-48.435	21.356	284.412	.144	-105.174	8.304
		2	-2.339	21.356	284.412	1.000	-59.077	54.400
		3	-33.240	21.356	284.412	.724	-89.979	23.498
25	1	2	3.510	13.506	284.412	1.000	-32.375	39.395
		3	-1.260	13.506	284.412	1.000	-37.145	34.625
		4	13.650	21.356	284.412	1.000	-43.089	70.389
	2	1	-3.510	13.506	284.412	1.000	-39.395	32.375
		3	-4.770	13.506	284.412	1.000	-40.655	31.115
		4	10.140	21.356	284.412	1.000	-46.599	66.879
	3	1	1.260	13.506	284.412	1.000	-34.625	37.145
		2	4.770	13.506	284.412	1.000	-31.115	40.655
		4	14.910	21.356	284.412	1.000	-41.829	71.649
	4	1	-13.650	21.356	284.412	1.000	-70.389	43.089
		2	-10.140	21.356	284.412	1.000	-66.879	46.599
		3	-14.910	21.356	284.412	1.000	-71.649	41.829
50	1	2	-1.225	13.506	284.412	1.000	-37.110	34.660
		3	-5.080	13.506	284.412	1.000	-40.965	30.805
		4	8.950	21.356	284.412	1.000	-47.789	65.689
	2	1	1.225	13.506	284.412	1.000	-34.660	37.110
		3	-3.855	13.506	284.412	1.000	-39.740	32.030
		4	10.175	21.356	284.412	1.000	-46.564	66.914
	3	1	5.080	13.506	284.412	1.000	-30.805	40.965
		2	3.855	13.506	284.412	1.000	-32.030	39.740
		4	14.030	21.356	284.412	1.000	-42.709	70.769
	4	1	-8.950	21.356	284.412	1.000	-65.689	47.789
		2	-10.175	21.356	284.412	1.000	-66.914	46.564
		3	-14.030	21.356	284.412	1.000	-70.769	42.709
75	1	2	25.755	13.506	284.412	.345	-10.130	61.640
		3	-22.470	13.506	284.412	.584	-58.355	13.415
		4	82.255*	21.356	284.412	.001	25.516	138.994
	2	1	-25.755	13.506	284.412	.345	-61.640	10.130
		3	-48.225*	13.506	284.412	.003	-84.110	-12.340
		4	56.500	21.356	284.412	.052	-.239	113.239
	3	1	22.470	13.506	284.412	.584	-13.415	58.355
		2	48.225*	13.506	284.412	.003	12.340	84.110
		4	104.725*	21.356	284.412	.000	47.986	161.464
	4	1	-82.255*	21.356	284.412	.001	-138.994	-25.516
		2	-56.500	21.356	284.412	.052	-113.239	.239
		3	-104.725*	21.356	284.412	.000	-161.464	-47.986
90	1	2	32.802	13.506	284.412	.095	-3.083	68.686
		3	.300	13.506	284.412	1.000	-35.585	36.185
		4	80.919*	21.356	284.412	.001	24.180	137.657
	2	1	-32.802	13.506	284.412	.095	-68.686	3.083
		3	-32.502	13.506	284.412	.101	-68.386	3.383
		4	48.117	21.356	284.412	.150	-8.621	104.856
	3	1	-.300	13.506	284.412	1.000	-36.185	35.585
		2	32.502	13.506	284.412	.101	-3.383	68.386
		4	80.619*	21.356	284.412	.001	23.880	137.357
	4	1	-80.919*	21.356	284.412	.001	-137.657	-24.180
		2	-48.117	21.356	284.412	.150	-104.856	8.621
		3	-80.619*	21.356	284.412	.001	-137.357	-23.880

Based on estimated marginal means

*. The mean difference is significant at the .05 level.

a. Dependent Variable: CRT_DEN.

c. Adjustment for multiple comparisons: Bonferroni.

Table A.29. Site * group interactions in cortical and subcortical BMC. 1 = Control, 2 = LB, 3 = SSMD, 4 = MC3.

							95% Confidence Interval for Difference[c]	
site	(I) 1:CTRL, 2:LB, 3:SSMD, 4:MC3	(J) 1:CTRL, 2:LB, 3: SSMD, 4:MC3	Mean Difference (I-J)	Std. Error	df	Sig.[c]	Lower Bound	Upper Bound
10	1	2	64.597	26.030	122.277	.087	-5.211	134.405
		3	10.780	26.030	122.277	1.000	-59.028	80.588
		4	100.398	41.156	122.277	.097	-9.977	210.774
	2	1	-64.597	26.030	122.277	.087	-134.405	5.211
		3	-53.817	26.030	122.277	.245	-123.625	15.991
		4	35.801	41.156	122.277	1.000	-74.574	146.177
	3	1	-10.780	26.030	122.277	1.000	-80.588	59.028
		2	53.817	26.030	122.277	.245	-15.991	123.625
		4	89.618	41.156	122.277	.188	-20.757	199.994
	4	1	-100.398	41.156	122.277	.097	-210.774	9.977
		2	-35.801	41.156	122.277	1.000	-146.177	74.574
		3	-89.618	41.156	122.277	.188	-199.994	20.757
25	1	2	11.555	26.030	122.277	1.000	-58.253	81.363
		3	-7.736	26.030	122.277	1.000	-77.543	62.072
		4	54.216	41.156	122.277	1.000	-56.160	164.591
	2	1	-11.555	26.030	122.277	1.000	-81.363	58.253
		3	-19.291	26.030	122.277	1.000	-89.098	50.517
		4	42.661	41.156	122.277	1.000	-67.715	153.036
	3	1	7.736	26.030	122.277	1.000	-62.072	77.543
		2	19.291	26.030	122.277	1.000	-50.517	89.098
		4	61.951	41.156	122.277	.809	-48.425	172.327
	4	1	-54.216	41.156	122.277	1.000	-164.591	56.160
		2	-42.661	41.156	122.277	1.000	-153.036	67.715
		3	-61.951	41.156	122.277	.809	-172.327	48.425
50	1	2	35.466	26.030	122.277	1.000	-34.342	105.274
		3	-1.069	26.030	122.277	1.000	-70.877	68.739
		4	83.946	41.156	122.277	.261	-26.430	194.322
	2	1	-35.466	26.030	122.277	1.000	-105.274	34.342
		3	-36.535	26.030	122.277	.978	-106.343	33.273
		4	48.480	41.156	122.277	1.000	-61.896	158.856
	3	1	1.069	26.030	122.277	1.000	-68.739	70.877
		2	36.535	26.030	122.277	.978	-33.273	106.343
		4	85.015	41.156	122.277	.246	-25.361	195.391
	4	1	-83.946	41.156	122.277	.261	-194.322	26.430
		2	-48.480	41.156	122.277	1.000	-158.856	61.896
		3	-85.015	41.156	122.277	.246	-195.391	25.361
75	1	2	54.863	26.030	122.277	.223	-14.945	124.671
		3	-37.756	26.030	122.277	.897	-107.564	32.052
		4	133.295*	41.156	122.277	.009	22.919	243.670
	2	1	-54.863	26.030	122.277	.223	-124.671	14.945
		3	-92.619*	26.030	122.277	.003	-162.427	-22.811
		4	78.432	41.156	122.277	.354	-31.944	188.807
	3	1	37.756	26.030	122.277	.897	-32.052	107.564
		2	92.619*	26.030	122.277	.003	22.811	162.427
		4	171.051*	41.156	122.277	.000	60.675	281.426
	4	1	-133.295*	41.156	122.277	.009	-243.670	-22.919
		2	-78.432	41.156	122.277	.354	-188.807	31.944
		3	-171.051*	41.156	122.277	.000	-281.426	-60.675
90	1	2	4.069	26.030	122.277	1.000	-65.739	73.877
		3	-24.024	26.030	122.277	1.000	-93.832	45.783
		4	39.663	41.156	122.277	1.000	-70.713	150.038
	2	1	-4.069	26.030	122.277	1.000	-73.877	65.739
		3	-28.093	26.030	122.277	1.000	-97.901	41.714
		4	35.594	41.156	122.277	1.000	-74.782	145.969
	3	1	24.024	26.030	122.277	1.000	-45.783	93.832
		2	28.093	26.030	122.277	1.000	-41.714	97.901
		4	63.687	41.156	122.277	.746	-46.689	174.063
	4	1	-39.663	41.156	122.277	1.000	-150.038	70.713
		2	-35.594	41.156	122.277	1.000	-145.969	74.782
		3	-63.687	41.156	122.277	.746	-174.063	46.689

Based on estimated marginal means

*. The mean difference is significant at the .05 level.

a. Dependent Variable: CRTSUB_CNT.

c. Adjustment for multiple comparisons: Bonferroni.

Table A.30. Site * group interactions in cortical and subcortical BMD. 1 = Control, 2 = LB, 3 = SSMD, 4 = MC3.

site	(I) 1:CTRL, 2:LB, 3:SSMD, 4:MC3	(J) 1:CTRL, 2:LB, 3: SSMD, 4:MC3	Mean Difference (I-J)	Std. Error	df	Sig.[c]	95% Confidence Interval for Difference[c] Lower Bound	Upper Bound
10	1	2	4.814	13.951	285.668	1.000	-32.249	41.877
		3	-.995	13.951	285.668	1.000	-38.058	36.068
		4	6.969	22.058	285.668	1.000	-51.633	65.571
	2	1	-4.814	13.951	285.668	1.000	-41.877	32.249
		3	-5.808	13.951	285.668	1.000	-42.872	31.255
		4	2.155	22.058	285.668	1.000	-56.447	60.757
	3	1	.995	13.951	285.668	1.000	-36.068	38.058
		2	5.808	13.951	285.668	1.000	-31.255	42.872
		4	7.963	22.058	285.668	1.000	-50.639	66.565
	4	1	-6.969	22.058	285.668	1.000	-65.571	51.633
		2	-2.155	22.058	285.668	1.000	-60.757	56.447
		3	-7.963	22.058	285.668	1.000	-66.565	50.639
25	1	2	3.510	13.951	285.668	1.000	-33.553	40.573
		3	-1.260	13.951	285.668	1.000	-38.323	35.803
		4	13.650	22.058	285.668	1.000	-44.952	72.252
	2	1	-3.510	13.951	285.668	1.000	-40.573	33.553
		3	-4.770	13.951	285.668	1.000	-41.833	32.293
		4	10.140	22.058	285.668	1.000	-48.462	68.742
	3	1	1.260	13.951	285.668	1.000	-35.803	38.323
		2	4.770	13.951	285.668	1.000	-32.293	41.833
		4	14.910	22.058	285.668	1.000	-43.692	73.512
	4	1	-13.650	22.058	285.668	1.000	-72.252	44.952
		2	-10.140	22.058	285.668	1.000	-68.742	48.462
		3	-14.910	22.058	285.668	1.000	-73.512	43.692
50	1	2	-1.225	13.951	285.668	1.000	-38.288	35.838
		3	-5.080	13.951	285.668	1.000	-42.143	31.983
		4	8.950	22.058	285.668	1.000	-49.652	67.552
	2	1	1.225	13.951	285.668	1.000	-35.838	38.288
		3	-3.855	13.951	285.668	1.000	-40.918	33.208
		4	10.175	22.058	285.668	1.000	-48.427	68.777
	3	1	5.080	13.951	285.668	1.000	-31.983	42.143
		2	3.855	13.951	285.668	1.000	-33.208	40.918
		4	14.030	22.058	285.668	1.000	-44.572	72.632
	4	1	-8.950	22.058	285.668	1.000	-67.552	49.652
		2	-10.175	22.058	285.668	1.000	-68.777	48.427
		3	-14.030	22.058	285.668	1.000	-72.632	44.572
75	1	2	2.720	13.951	285.668	1.000	-34.343	39.783
		3	-5.240	13.951	285.668	1.000	-42.303	31.823
		4	26.600	22.058	285.668	1.000	-32.002	85.202
	2	1	-2.720	13.951	285.668	1.000	-39.783	34.343
		3	-7.960	13.951	285.668	1.000	-45.023	29.103
		4	23.880	22.058	285.668	1.000	-34.722	82.482
	3	1	5.240	13.951	285.668	1.000	-31.823	42.303
		2	7.960	13.951	285.668	1.000	-29.103	45.023
		4	31.840	22.058	285.668	.900	-26.762	90.442
	4	1	-26.600	22.058	285.668	1.000	-85.202	32.002
		2	-23.880	22.058	285.668	1.000	-82.482	34.722
		3	-31.840	22.058	285.668	.900	-90.442	26.762
90	1	2	34.657	13.951	285.668	.081	-2.406	71.720
		3	-25.591	13.951	285.668	.406	-62.655	11.472
		4	113.459*	22.058	285.668	.000	54.857	172.061
	2	1	-34.657	13.951	285.668	.081	-71.720	2.406
		3	-60.248*	13.951	285.668	.000	-97.311	-23.185
		4	78.802*	22.058	285.668	.002	20.200	137.404
	3	1	25.591	13.951	285.668	.406	-11.472	62.655
		2	60.248*	13.951	285.668	.000	23.185	97.311
		4	139.050*	22.058	285.668	.000	80.448	197.652
	4	1	-113.459*	22.058	285.668	.000	-172.061	-54.857
		2	-78.802*	22.058	285.668	.002	-137.404	-20.200
		3	-139.050*	22.058	285.668	.000	-197.652	-80.448

Based on estimated marginal means

*. The mean difference is significant at the .05 level.

a. Dependent Variable: CRTSUB_DEN.

c. Adjustment for multiple comparisons: Bonferroni.

Table A.31. Site * group interactions in total BMD. 1 = Control, 2 = LB, 3 = SSMD, 4 = MC3.

site	(I) 1:CTRL, 2:LB, 3:SSMD, 4:MC3	(J) 1:CTRL, 2:LB, 3: SSMD, 4:MC3	Mean Difference (I-J)	Std. Error	df	Sig.[c]	95% Confidence Interval for Difference[c]	
							Lower Bound	Upper Bound
10	1	2	47.819*	14.918	193.214	.009	8.054	87.585
		3	16.203	14.918	193.214	1.000	-23.562	55.969
		4	50.476	23.587	193.214	.202	-12.399	113.352
	2	1	-47.819*	14.918	193.214	.009	-87.585	-8.054
		3	-31.616	14.918	193.214	.212	-71.382	8.150
		4	2.657	23.587	193.214	1.000	-60.218	65.532
	3	1	-16.203	14.918	193.214	1.000	-55.969	23.562
		2	31.616	14.918	193.214	.212	-8.150	71.382
		4	34.273	23.587	193.214	.887	-28.602	97.148
	4	1	-50.476	23.587	193.214	.202	-113.352	12.399
		2	-2.657	23.587	193.214	1.000	-65.532	60.218
		3	-34.273	23.587	193.214	.887	-97.148	28.602
25	1	2	6.240	14.918	193.214	1.000	-33.526	46.006
		3	3.970	14.918	193.214	1.000	-35.796	43.736
		4	17.935	23.587	193.214	1.000	-44.940	80.810
	2	1	-6.240	14.918	193.214	1.000	-46.006	33.526
		3	-2.270	14.918	193.214	1.000	-42.036	37.496
		4	11.695	23.587	193.214	1.000	-51.180	74.570
	3	1	-3.970	14.918	193.214	1.000	-43.736	35.796
		2	2.270	14.918	193.214	1.000	-37.496	42.036
		4	13.965	23.587	193.214	1.000	-48.910	76.840
	4	1	-17.935	23.587	193.214	1.000	-80.810	44.940
		2	-11.695	23.587	193.214	1.000	-74.570	51.180
		3	-13.965	23.587	193.214	1.000	-76.840	48.910
50	1	2	1.910	14.918	193.214	1.000	-37.856	41.676
		3	.960	14.918	193.214	1.000	-38.806	40.726
		4	37.065	23.587	193.214	.706	-25.810	99.940
	2	1	-1.910	14.918	193.214	1.000	-41.676	37.856
		3	-.950	14.918	193.214	1.000	-40.716	38.816
		4	35.155	23.587	193.214	.826	-27.720	98.030
	3	1	-.960	14.918	193.214	1.000	-40.726	38.806
		2	.950	14.918	193.214	1.000	-38.816	40.716
		4	36.105	23.587	193.214	.765	-26.770	98.980
	4	1	-37.065	23.587	193.214	.706	-99.940	25.810
		2	-35.155	23.587	193.214	.826	-98.030	27.720
		3	-36.105	23.587	193.214	.765	-98.980	26.770
75	1	2	27.205	14.918	193.214	.418	-12.561	66.971
		3	-22.125	14.918	193.214	.838	-61.891	17.641
		4	85.695*	23.587	193.214	.002	22.820	148.570
	2	1	-27.205	14.918	193.214	.418	-66.971	12.561
		3	-49.330*	14.918	193.214	.007	-89.096	-9.564
		4	58.490	23.587	193.214	.084	-4.385	121.365
	3	1	22.125	14.918	193.214	.838	-17.641	61.891
		2	49.330*	14.918	193.214	.007	9.564	89.096
		4	107.820*	23.587	193.214	.000	44.945	170.695
	4	1	-85.695*	23.587	193.214	.002	-148.570	-22.820
		2	-58.490	23.587	193.214	.084	-121.365	4.385
		3	-107.820*	23.587	193.214	.000	-170.695	-44.945
90	1	2	31.061	14.918	193.214	.232	-8.705	70.827
		3	2.028	14.918	193.214	1.000	-37.737	41.794
		4	71.993*	23.587	193.214	.016	9.118	134.869
	2	1	-31.061	14.918	193.214	.232	-70.827	8.705
		3	-29.032	14.918	193.214	.319	-68.798	10.734
		4	40.933	23.587	193.214	.506	-21.943	103.808
	3	1	-2.028	14.918	193.214	1.000	-41.794	37.737
		2	29.032	14.918	193.214	.319	-10.734	68.798
		4	69.965*	23.587	193.214	.020	7.090	132.840
	4	1	-71.993*	23.587	193.214	.016	-134.869	-9.118
		2	-40.933	23.587	193.214	.506	-103.808	21.943
		3	-69.965*	23.587	193.214	.020	-132.840	-7.090

Based on estimated marginal means

*. The mean difference is significant at the .05 level.

a. Dependent Variable: TOT_DEN.

c. Adjustment for multiple comparisons: Bonferroni.

Table A.32. Site * group interactions in axial area moment of inertia. 1 = Control, 2 = LB, 3 = SSMD, 4 = MC3.

site	(I) 1:CTRL, 2:LB, 3:SSMD, 4:MC3	(J) 1:CTRL, 2:LB, 3: SSMD, 4:MC3	Mean Difference (I-J)	Std. Error	df	Sig.[c]	95% Confidence Interval for Difference[c] Lower Bound	Upper Bound
10	1	2	-3771.700	10279.633	257.400	1.000	-31103.226	23559.826
		3	-3484.599	10279.633	257.400	1.000	-30816.126	23846.927
		4	12217.317	16253.526	257.400	1.000	-30997.621	55432.255
	2	1	3771.700	10279.633	257.400	1.000	-23559.826	31103.226
		3	287.101	10279.633	257.400	1.000	-27044.426	27618.627
		4	15989.017	16253.526	257.400	1.000	-27225.921	59203.955
	3	1	3484.599	10279.633	257.400	1.000	-23846.927	30816.126
		2	-287.101	10279.633	257.400	1.000	-27618.627	27044.426
		4	15701.916	16253.526	257.400	1.000	-27513.021	58916.854
	4	1	-12217.317	16253.526	257.400	1.000	-55432.255	30997.621
		2	-15989.017	16253.526	257.400	1.000	-59203.955	27225.921
		3	-15701.916	16253.526	257.400	1.000	-58916.854	27513.021
25	1	2	474.700	10279.633	257.400	1.000	-26856.826	27806.226
		3	-1999.850	10279.633	257.400	1.000	-29331.376	25331.676
		4	5726.450	16253.526	257.400	1.000	-37488.488	48941.388
	2	1	-474.700	10279.633	257.400	1.000	-27806.226	26856.826
		3	-2474.550	10279.633	257.400	1.000	-29806.076	24856.976
		4	5251.750	16253.526	257.400	1.000	-37963.188	48466.688
	3	1	1999.850	10279.633	257.400	1.000	-25331.676	29331.376
		2	2474.550	10279.633	257.400	1.000	-24856.976	29806.076
		4	7726.300	16253.526	257.400	1.000	-35488.638	50941.238
	4	1	-5726.450	16253.526	257.400	1.000	-48941.388	37488.488
		2	-5251.750	16253.526	257.400	1.000	-48466.688	37963.188
		3	-7726.300	16253.526	257.400	1.000	-50941.238	35488.638
50	1	2	4770.800	10279.633	257.400	1.000	-22560.726	32102.326
		3	80.450	10279.633	257.400	1.000	-27251.076	27411.976
		4	7905.300	16253.526	257.400	1.000	-35309.638	51120.238
	2	1	-4770.800	10279.633	257.400	1.000	-32102.326	22560.726
		3	-4690.350	10279.633	257.400	1.000	-32021.876	22641.176
		4	3134.500	16253.526	257.400	1.000	-40080.438	46349.438
	3	1	-80.450	10279.633	257.400	1.000	-27411.976	27251.076
		2	4690.350	10279.633	257.400	1.000	-22641.176	32021.876
		4	7824.850	16253.526	257.400	1.000	-35390.088	51039.788
	4	1	-7905.300	16253.526	257.400	1.000	-51120.238	35309.638
		2	-3134.500	16253.526	257.400	1.000	-46349.438	40080.438
		3	-7824.850	16253.526	257.400	1.000	-51039.788	35390.088
75	1	2	2261.100	10279.633	257.400	1.000	-25070.426	29592.626
		3	1904.600	10279.633	257.400	1.000	-25426.926	29236.126
		4	3347.800	16253.526	257.400	1.000	-39867.138	46562.738
	2	1	-2261.100	10279.633	257.400	1.000	-29592.626	25070.426
		3	-356.500	10279.633	257.400	1.000	-27688.026	26975.026
		4	1086.700	16253.526	257.400	1.000	-42128.238	44301.638
	3	1	-1904.600	10279.633	257.400	1.000	-29236.126	25426.926
		2	356.500	10279.633	257.400	1.000	-26975.026	27688.026
		4	1443.200	16253.526	257.400	1.000	-41771.738	44658.138
	4	1	-3347.800	16253.526	257.400	1.000	-46562.738	39867.138
		2	-1086.700	16253.526	257.400	1.000	-44301.638	42128.238
		3	-1443.200	16253.526	257.400	1.000	-44658.138	41771.738
90	1	2	-25804.108	10279.633	257.400	.076	-53135.634	1527.419
		3	2366.934	10279.633	257.400	1.000	-24964.593	29698.460
		4	-58758.550*	16253.526	257.400	.002	-101973.488	-15543.613
	2	1	25804.108	10279.633	257.400	.076	-1527.419	53135.634
		3	28171.041*	10279.633	257.400	.039	839.515	55502.568
		4	-32954.443	16253.526	257.400	.262	-76169.380	10260.495
	3	1	-2366.934	10279.633	257.400	1.000	-29698.460	24964.593
		2	-28171.041*	10279.633	257.400	.039	-55502.568	-839.515
		4	-61125.484*	16253.526	257.400	.001	-104340.422	-17910.546
	4	1	58758.550*	16253.526	257.400	.002	15543.613	101973.488
		2	32954.443	16253.526	257.400	.262	-10260.495	76169.380
		3	61125.484*	16253.526	257.400	.001	17910.546	104340.422

Based on estimated marginal means

*. The mean difference is significant at the .05 level.

a. Dependent Variable: I_CIRC.

c. Adjustment for multiple comparisons: Bonferroni.

Table A.33. Site * group interactions in total bone area. 1 = Control, 2 = LB, 3 = SSMD, 4 = MC3.

site	(I) 1:CTRL, 2:LB, 3:SSMD, 4:MC3	(J) 1:CTRL, 2:LB, 3: SSMD, 4:MC3	Mean Difference (I-J)	Std. Error	df	Sig.[c]	95% Confidence Interval for Difference[c]	
							Lower Bound	Upper Bound
10	1	2	-17.180	44.280	210.473	1.000	-135.117	100.757
		3	-16.070	44.280	210.473	1.000	-134.007	101.867
		4	64.890	70.013	210.473	1.000	-121.585	251.364
	2	1	17.180	44.280	210.473	1.000	-100.757	135.117
		3	1.110	44.280	210.473	1.000	-116.827	119.047
		4	82.070	70.013	210.473	1.000	-104.405	268.545
	3	1	16.070	44.280	210.473	1.000	-101.867	134.007
		2	-1.110	44.280	210.473	1.000	-119.047	116.827
		4	80.960	70.013	210.473	1.000	-105.515	267.434
	4	1	-64.890	70.013	210.473	1.000	-251.364	121.585
		2	-82.070	70.013	210.473	1.000	-268.545	104.405
		3	-80.960	70.013	210.473	1.000	-267.434	105.515
25	1	2	5.280	44.280	210.473	1.000	-112.657	123.217
		3	-12.280	44.280	210.473	1.000	-130.217	105.657
		4	36.794	70.013	210.473	1.000	-149.681	223.269
	2	1	-5.280	44.280	210.473	1.000	-123.217	112.657
		3	-17.560	44.280	210.473	1.000	-135.497	100.377
		4	31.514	70.013	210.473	1.000	-154.961	217.989
	3	1	12.280	44.280	210.473	1.000	-105.657	130.217
		2	17.560	44.280	210.473	1.000	-100.377	135.497
		4	49.074	70.013	210.473	1.000	-137.401	235.549
	4	1	-36.794	70.013	210.473	1.000	-223.269	149.681
		2	-31.514	70.013	210.473	1.000	-217.989	154.961
		3	-49.074	70.013	210.473	1.000	-235.549	137.401
50	1	2	31.634	44.280	210.473	1.000	-86.303	149.571
		3	.934	44.280	210.473	1.000	-117.003	118.871
		4	44.812	70.013	210.473	1.000	-141.663	231.287
	2	1	-31.634	44.280	210.473	1.000	-149.571	86.303
		3	-30.700	44.280	210.473	1.000	-148.637	87.237
		4	13.178	70.013	210.473	1.000	-173.297	199.653
	3	1	-.934	44.280	210.473	1.000	-118.871	117.003
		2	30.700	44.280	210.473	1.000	-87.237	148.637
		4	43.878	70.013	210.473	1.000	-142.597	230.353
	4	1	-44.812	70.013	210.473	1.000	-231.287	141.663
		2	-13.178	70.013	210.473	1.000	-199.653	173.297
		3	-43.878	70.013	210.473	1.000	-230.353	142.597
75	1	2	15.530	44.280	210.473	1.000	-102.407	133.467
		3	11.506	44.280	210.473	1.000	-106.431	129.443
		4	17.308	70.013	210.473	1.000	-169.167	203.783
	2	1	-15.530	44.280	210.473	1.000	-133.467	102.407
		3	-4.024	44.280	210.473	1.000	-121.961	113.913
		4	1.778	70.013	210.473	1.000	-184.697	188.253
	3	1	-11.506	44.280	210.473	1.000	-129.443	106.431
		2	4.024	44.280	210.473	1.000	-113.913	121.961
		4	5.802	70.013	210.473	1.000	-180.673	192.277
	4	1	-17.308	70.013	210.473	1.000	-203.783	169.167
		2	-1.778	70.013	210.473	1.000	-188.253	184.697
		3	-5.802	70.013	210.473	1.000	-192.277	180.673
90	1	2	-98.644	44.280	210.473	.162	-216.581	19.292
		3	6.746	44.280	210.473	1.000	-111.191	124.683
		4	-220.116*	70.013	210.473	.011	-406.590	-33.641
	2	1	98.644	44.280	210.473	.162	-19.292	216.581
		3	105.391	44.280	210.473	.109	-12.546	223.328
		4	-121.471	70.013	210.473	.505	-307.946	65.003
	3	1	-6.746	44.280	210.473	1.000	-124.683	111.191
		2	-105.391	44.280	210.473	.109	-223.328	12.546
		4	-226.862*	70.013	210.473	.008	-413.337	-40.388
	4	1	220.116*	70.013	210.473	.011	33.641	406.590
		2	121.471	70.013	210.473	.505	-65.003	307.946
		3	226.862*	70.013	210.473	.008	40.388	413.337

Based on estimated marginal means

*. The mean difference is significant at the .05 level.

a. Dependent Variable: TOT_A.

c. Adjustment for multiple comparisons: Bonferroni.

Table A.34. Site * group interactions in cortical thickness (circular ring model). 1 = Control, 2 = LB, 3 = SSMD, 4 = MC3.

site	(I) 1:CTRL, 2:LB, 3:SSMD, 4:MC3	(J) 1:CTRL, 2:LB, 3: SSMD, 4:MC3	Mean Difference (I-J)	Std. Error	df	Sig.[c]	95% Confidence Interval for Difference[c] Lower Bound	Upper Bound
10	1	2	-.128	.341	234.231	1.000	-1.035	.778
		3	-.122	.341	234.231	1.000	-1.029	.785
		4	.535	.539	234.231	1.000	-.898	1.969
	2	1	.128	.341	234.231	1.000	-.778	1.035
		3	.006	.341	234.231	1.000	-.900	.913
		4	.664	.539	234.231	1.000	-.770	2.097
	3	1	.122	.341	234.231	1.000	-.785	1.029
		2	-.006	.341	234.231	1.000	-.913	.900
		4	.657	.539	234.231	1.000	-.776	2.091
	4	1	-.535	.539	234.231	1.000	-1.969	.898
		2	-.664	.539	234.231	1.000	-2.097	.770
		3	-.657	.539	234.231	1.000	-2.091	.776
25	1	2	.123	.341	234.231	1.000	-.784	1.029
		3	.046	.341	234.231	1.000	-.861	.952
		4	.349	.539	234.231	1.000	-1.084	1.783
	2	1	-.123	.341	234.231	1.000	-1.029	.784
		3	-.077	.341	234.231	1.000	-.984	.830
		4	.227	.539	234.231	1.000	-1.207	1.660
	3	1	-.046	.341	234.231	1.000	-.952	.861
		2	.077	.341	234.231	1.000	-.830	.984
		4	.304	.539	234.231	1.000	-1.130	1.737
	4	1	-.349	.539	234.231	1.000	-1.783	1.084
		2	-.227	.539	234.231	1.000	-1.660	1.207
		3	-.304	.539	234.231	1.000	-1.737	1.130
50	1	2	.278	.341	234.231	1.000	-.629	1.185
		3	.065	.341	234.231	1.000	-.841	.972
		4	.825	.539	234.231	.761	-.608	2.259
	2	1	-.278	.341	234.231	1.000	-1.185	.629
		3	-.213	.341	234.231	1.000	-1.119	.694
		4	.547	.539	234.231	1.000	-.886	1.981
	3	1	-.065	.341	234.231	1.000	-.972	.841
		2	.213	.341	234.231	1.000	-.694	1.119
		4	.760	.539	234.231	.958	-.674	2.194
	4	1	-.825	.539	234.231	.761	-2.259	.608
		2	-.547	.539	234.231	1.000	-1.981	.886
		3	-.760	.539	234.231	.958	-2.194	.674
75	1	2	.144	.341	234.231	1.000	-.763	1.051
		3	.101	.341	234.231	1.000	-.806	1.008
		4	.140	.539	234.231	1.000	-1.294	1.574
	2	1	-.144	.341	234.231	1.000	-1.051	.763
		3	-.043	.341	234.231	1.000	-.950	.864
		4	-.004	.539	234.231	1.000	-1.438	1.430
	3	1	-.101	.341	234.231	1.000	-1.008	.806
		2	.043	.341	234.231	1.000	-.864	.950
		4	.039	.539	234.231	1.000	-1.395	1.473
	4	1	-.140	.539	234.231	1.000	-1.574	1.294
		2	.004	.539	234.231	1.000	-1.430	1.438
		3	-.039	.539	234.231	1.000	-1.473	1.395
90	1	2	-.655	.341	234.231	.335	-1.562	.252
		3	.036	.341	234.231	1.000	-.871	.942
		4	-1.416	.539	234.231	.055	-2.850	.017
	2	1	.655	.341	234.231	.335	-.252	1.562
		3	.691	.341	234.231	.263	-.216	1.597
		4	-.761	.539	234.231	.954	-2.195	.672
	3	1	-.036	.341	234.231	1.000	-.942	.871
		2	-.691	.341	234.231	.263	-1.597	.216
		4	-1.452*	.539	234.231	.045	-2.886	-.018
	4	1	1.416	.539	234.231	.055	-.017	2.850
		2	.761	.539	234.231	.954	-.672	2.195
		3	1.452*	.539	234.231	.045	.018	2.886

Based on estimated marginal means

*. The mean difference is significant at the .05 level.

a. Dependent Variable: CRT_THK_C.

c. Adjustment for multiple comparisons: Bonferroni.

Table A.35. Site * group interactions in periosteal circumference (circular ring model). 1 = Control, 2 = LB, 3 = SSMD, 4 = MC3.

site	(I) 1:CTRL, 2:LB, 3:SSMD, 4:MC3	(J) 1:CTRL, 2:LB, 3: SSMD, 4:MC3	Mean Difference (I-J)	Std. Error	df	Sig.[c]	95% Confidence Interval for Difference[c] Lower Bound	Upper Bound
10	1	2	-.816	2.128	187.068	1.000	-6.491	4.859
		3	-.773	2.128	187.068	1.000	-6.448	4.903
		4	3.352	3.365	187.068	1.000	-5.621	12.325
	2	1	.816	2.128	187.068	1.000	-4.859	6.491
		3	.043	2.128	187.068	1.000	-5.632	5.719
		4	4.168	3.365	187.068	1.000	-4.805	13.141
	3	1	.773	2.128	187.068	1.000	-4.903	6.448
		2	-.043	2.128	187.068	1.000	-5.719	5.632
		4	4.125	3.365	187.068	1.000	-4.849	13.098
	4	1	-3.352	3.365	187.068	1.000	-12.325	5.621
		2	-4.168	3.365	187.068	1.000	-13.141	4.805
		3	-4.125	3.365	187.068	1.000	-13.098	4.849
25	1	2	.370	2.128	187.068	1.000	-5.305	6.045
		3	-.660	2.128	187.068	1.000	-6.335	5.015
		4	2.066	3.365	187.068	1.000	-6.907	11.039
	2	1	-.370	2.128	187.068	1.000	-6.045	5.305
		3	-1.030	2.128	187.068	1.000	-6.705	4.645
		4	1.696	3.365	187.068	1.000	-7.277	10.669
	3	1	.660	2.128	187.068	1.000	-5.015	6.335
		2	1.030	2.128	187.068	1.000	-4.645	6.705
		4	2.726	3.365	187.068	1.000	-6.247	11.699
	4	1	-2.066	3.365	187.068	1.000	-11.039	6.907
		2	-1.696	3.365	187.068	1.000	-10.669	7.277
		3	-2.726	3.365	187.068	1.000	-11.699	6.247
50	1	2	1.825	2.128	187.068	1.000	-3.851	7.500
		3	.065	2.128	187.068	1.000	-5.611	5.740
		4	2.470	3.365	187.068	1.000	-6.503	11.443
	2	1	-1.825	2.128	187.068	1.000	-7.500	3.851
		3	-1.760	2.128	187.068	1.000	-7.435	3.915
		4	.646	3.365	187.068	1.000	-8.327	9.619
	3	1	-.065	2.128	187.068	1.000	-5.740	5.611
		2	1.760	2.128	187.068	1.000	-3.915	7.435
		4	2.406	3.365	187.068	1.000	-6.567	11.379
	4	1	-2.470	3.365	187.068	1.000	-11.443	6.503
		2	-.646	3.365	187.068	1.000	-9.619	8.327
		3	-2.406	3.365	187.068	1.000	-11.379	6.567
75	1	2	.906	2.128	187.068	1.000	-4.769	6.581
		3	.634	2.128	187.068	1.000	-5.041	6.309
		4	.878	3.365	187.068	1.000	-8.095	9.852
	2	1	-.906	2.128	187.068	1.000	-6.581	4.769
		3	-.272	2.128	187.068	1.000	-5.947	5.403
		4	-.028	3.365	187.068	1.000	-9.001	8.945
	3	1	-.634	2.128	187.068	1.000	-6.309	5.041
		2	.272	2.128	187.068	1.000	-5.403	5.947
		4	.244	3.365	187.068	1.000	-8.729	9.218
	4	1	-.878	3.365	187.068	1.000	-9.852	8.095
		2	.028	3.365	187.068	1.000	-8.945	9.001
		3	-.244	3.365	187.068	1.000	-9.218	8.729
90	1	2	-4.336	2.128	187.068	.258	-10.011	1.339
		3	.226	2.128	187.068	1.000	-5.449	5.901
		4	-9.590*	3.365	187.068	.029	-18.564	-.617
	2	1	4.336	2.128	187.068	.258	-1.339	10.011
		3	4.562	2.128	187.068	.200	-1.113	10.237
		4	-5.254	3.365	187.068	.721	-14.228	3.719
	3	1	-.226	2.128	187.068	1.000	-5.901	5.449
		2	-4.562	2.128	187.068	.200	-10.237	1.113
		4	-9.816*	3.365	187.068	.024	-18.790	-.843
	4	1	9.590*	3.365	187.068	.029	.617	18.564
		2	5.254	3.365	187.068	.721	-3.719	14.228
		3	9.816*	3.365	187.068	.024	.843	18.790

Based on estimated marginal means

*. The mean difference is significant at the .05 level.

a. Dependent Variable: PERI_C.

c. Adjustment for multiple comparisons: Bonferroni.

Table A.36. Site * group interactions in cortical and subcortical area. 1 = Control, 2 = LB, 3 = SSMD, 4 = MC3.

site	(I) 1:CTRL, 2:LB, 3:SSMD, 4:MC3	(J) 1:CTRL, 2:LB, 3: SSMD, 4:MC3	Mean Difference (I-J)	Std. Error	df	Sig.[c]	95% Confidence Interval for Difference[c] Lower Bound	Upper Bound
10	1	2	55.004	22.106	122.743	.085	-4.276	114.285
		3	10.191	22.106	122.743	1.000	-49.090	69.472
		4	85.232	34.952	122.743	.097	-8.499	178.963
	2	1	-55.004	22.106	122.743	.085	-114.285	4.276
		3	-44.814	22.106	122.743	.269	-104.095	14.467
		4	30.227	34.952	122.743	1.000	-63.504	123.959
	3	1	-10.191	22.106	122.743	1.000	-69.472	49.090
		2	44.814	22.106	122.743	.269	-14.467	104.095
		4	75.041	34.952	122.743	.203	-18.690	168.772
	4	1	-85.232	34.952	122.743	.097	-178.963	8.499
		2	-30.227	34.952	122.743	1.000	-123.959	63.504
		3	-75.041	34.952	122.743	.203	-168.772	18.690
25	1	2	7.840	22.106	122.743	1.000	-51.441	67.121
		3	-5.800	22.106	122.743	1.000	-65.081	53.481
		4	36.224	34.952	122.743	1.000	-57.507	129.955
	2	1	-7.840	22.106	122.743	1.000	-67.121	51.441
		3	-13.640	22.106	122.743	1.000	-72.921	45.641
		4	28.384	34.952	122.743	1.000	-65.347	122.115
	3	1	5.800	22.106	122.743	1.000	-53.481	65.081
		2	13.640	22.106	122.743	1.000	-45.641	72.921
		4	42.024	34.952	122.743	1.000	-51.707	135.755
	4	1	-36.224	34.952	122.743	1.000	-129.955	57.507
		2	-28.384	34.952	122.743	1.000	-122.115	65.347
		3	-42.024	34.952	122.743	1.000	-135.755	51.707
50	1	2	31.158	22.106	122.743	.967	-28.123	90.439
		3	2.776	22.106	122.743	1.000	-56.505	62.057
		4	64.428	34.952	122.743	.406	-29.303	158.159
	2	1	-31.158	22.106	122.743	.967	-90.439	28.123
		3	-28.382	22.106	122.743	1.000	-87.663	30.899
		4	33.270	34.952	122.743	1.000	-60.461	127.001
	3	1	-2.776	22.106	122.743	1.000	-62.057	56.505
		2	28.382	22.106	122.743	1.000	-30.899	87.663
		4	61.652	34.952	122.743	.481	-32.079	155.383
	4	1	-64.428	34.952	122.743	.406	-158.159	29.303
		2	-33.270	34.952	122.743	1.000	-127.001	60.461
		3	-61.652	34.952	122.743	.481	-155.383	32.079
75	1	2	46.460	22.106	122.743	.226	-12.821	105.741
		3	-30.580	22.106	122.743	1.000	-89.861	28.701
		4	103.870*	34.952	122.743	.021	10.139	197.601
	2	1	-46.460	22.106	122.743	.226	-105.741	12.821
		3	-77.040*	22.106	122.743	.004	-136.321	-17.759
		4	57.410	34.952	122.743	.618	-36.321	151.141
	3	1	30.580	22.106	122.743	1.000	-28.701	89.861
		2	77.040*	22.106	122.743	.004	17.759	136.321
		4	134.450*	34.952	122.743	.001	40.719	228.181
	4	1	-103.870*	34.952	122.743	.021	-197.601	-10.139
		2	-57.410	34.952	122.743	.618	-151.141	36.321
		3	-134.450*	34.952	122.743	.001	-228.181	-40.719
90	1	2	-15.955	22.106	122.743	1.000	-75.236	43.326
		3	-12.528	22.106	122.743	1.000	-71.809	46.753
		4	-21.244	34.952	122.743	1.000	-114.976	72.487
	2	1	15.955	22.106	122.743	1.000	-43.326	75.236
		3	3.427	22.106	122.743	1.000	-55.854	62.708
		4	-5.289	34.952	122.743	1.000	-99.021	88.442
	3	1	12.528	22.106	122.743	1.000	-46.753	71.809
		2	-3.427	22.106	122.743	1.000	-62.708	55.854
		4	-8.716	34.952	122.743	1.000	-102.447	85.015
	4	1	21.244	34.952	122.743	1.000	-72.487	114.976
		2	5.289	34.952	122.743	1.000	-88.442	99.021
		3	8.716	34.952	122.743	1.000	-85.015	102.447

Based on estimated marginal means

*. The mean difference is significant at the .05 level.

a. Dependent Variable: CRTSUB_A.

c. Adjustment for multiple comparisons: Bonferroni.

Table A.37. Site * group interactions in axial moment of inertia of cortical area (x-axis). 1 = Control, 2 = LB, 3 = SSMD, 4 = MC3.

site	(I) 1:CTRL, 2:LB, 3:SSMD, 4:MC3	(J) 1:CTRL, 2:LB, 3: SSMD, 4:MC3	Mean Difference (I-J)	Std. Error	df	Sig.[c]	95% Confidence Interval for Difference[c] Lower Bound	Upper Bound
10	1	2	-3922.168	8690.880	269.274	1.000	-27021.585	19177.249
		3	-4423.209	8690.880	269.274	1.000	-27522.625	18676.208
		4	7199.543	13741.488	269.274	1.000	-29323.841	43722.928
	2	1	3922.168	8690.880	269.274	1.000	-19177.249	27021.585
		3	-501.041	8690.880	269.274	1.000	-23600.457	22598.376
		4	11121.711	13741.488	269.274	1.000	-25401.673	47645.096
	3	1	4423.209	8690.880	269.274	1.000	-18676.208	27522.625
		2	501.041	8690.880	269.274	1.000	-22598.376	23600.457
		4	11622.752	13741.488	269.274	1.000	-24900.633	48146.137
	4	1	-7199.543	13741.488	269.274	1.000	-43722.928	29323.841
		2	-11121.711	13741.488	269.274	1.000	-47645.096	25401.673
		3	-11622.752	13741.488	269.274	1.000	-48146.137	24900.633
25	1	2	628.475	8690.880	269.274	1.000	-22470.942	23727.891
		3	-1290.308	8690.880	269.274	1.000	-24389.724	21809.109
		4	1553.512	13741.488	269.274	1.000	-34969.872	38076.897
	2	1	-628.475	8690.880	269.274	1.000	-23727.891	22470.942
		3	-1918.782	8690.880	269.274	1.000	-25018.199	21180.634
		4	925.038	13741.488	269.274	1.000	-35598.347	37448.422
	3	1	1290.308	8690.880	269.274	1.000	-21809.109	24389.724
		2	1918.782	8690.880	269.274	1.000	-21180.634	25018.199
		4	2843.820	13741.488	269.274	1.000	-33679.565	39367.205
	4	1	-1553.512	13741.488	269.274	1.000	-38076.897	34969.872
		2	-925.038	13741.488	269.274	1.000	-37448.422	35598.347
		3	-2843.820	13741.488	269.274	1.000	-39367.205	33679.565
50	1	2	6280.249	8690.880	269.274	1.000	-16819.168	29379.665
		3	2334.076	8690.880	269.274	1.000	-20765.341	25433.493
		4	6490.273	13741.488	269.274	1.000	-30033.112	43013.657
	2	1	-6280.249	8690.880	269.274	1.000	-29379.665	16819.168
		3	-3946.173	8690.880	269.274	1.000	-27045.590	19153.244
		4	210.024	13741.488	269.274	1.000	-36313.361	36733.409
	3	1	-2334.076	8690.880	269.274	1.000	-25433.493	20765.341
		2	3946.173	8690.880	269.274	1.000	-19153.244	27045.590
		4	4156.197	13741.488	269.274	1.000	-32367.188	40679.581
	4	1	-6490.273	13741.488	269.274	1.000	-43013.657	30033.112
		2	-210.024	13741.488	269.274	1.000	-36733.409	36313.361
		3	-4156.197	13741.488	269.274	1.000	-40679.581	32367.188
75	1	2	2526.918	8690.880	269.274	1.000	-20572.499	25626.335
		3	1141.243	8690.880	269.274	1.000	-21958.173	24240.660
		4	-466.178	13741.488	269.274	1.000	-36989.562	36057.207
	2	1	-2526.918	8690.880	269.274	1.000	-25626.335	20572.499
		3	-1385.675	8690.880	269.274	1.000	-24485.091	21713.742
		4	-2993.096	13741.488	269.274	1.000	-39516.481	33530.289
	3	1	-1141.243	8690.880	269.274	1.000	-24240.660	21958.173
		2	1385.675	8690.880	269.274	1.000	-21713.742	24485.091
		4	-1607.421	13741.488	269.274	1.000	-38130.806	34915.964
	4	1	466.178	13741.488	269.274	1.000	-36057.207	36989.562
		2	2993.096	13741.488	269.274	1.000	-33530.289	39516.481
		3	1607.421	13741.488	269.274	1.000	-34915.964	38130.806
90	1	2	-24451.318*	8690.880	269.274	.032	-47550.734	-1351.901
		3	1033.370	8690.880	269.274	1.000	-22066.047	24132.787
		4	-75508.534*	13741.488	269.274	.000	-112031.919	-38985.150
	2	1	24451.318*	8690.880	269.274	.032	1351.901	47550.734
		3	25484.688*	8690.880	269.274	.022	2385.271	48584.105
		4	-51057.217*	13741.488	269.274	.001	-87580.601	-14533.832
	3	1	-1033.370	8690.880	269.274	1.000	-24132.787	22066.047
		2	-25484.688*	8690.880	269.274	.022	-48584.105	-2385.271
		4	-76541.904*	13741.488	269.274	.000	-113065.289	-40018.520
	4	1	75508.534*	13741.488	269.274	.000	38985.150	112031.919
		2	51057.217*	13741.488	269.274	.001	14533.832	87580.601
		3	76541.904*	13741.488	269.274	.000	40018.520	113065.289

Based on estimated marginal means

*. The mean difference is significant at the .05 level.

a. Dependent Variable: IX_CRT_A.

c. Adjustment for multiple comparisons: Bonferroni.

Table A.38. Site * group interactions in axial moment of inertia of cortical area (y-axis). 1 = Control, 2 = LB, 3 = SSMD, 4 = MC3.

site	(I) 1:CTRL, 2:LB, 3:SSMD, 4:MC3	(J) 1:CTRL, 2:LB, 3: SSMD, 4:MC3	Mean Difference (I-J)	Std. Error	df	Sig.[c]	95% Confidence Interval for Difference[c] Lower Bound	Upper Bound
10	1	2	-6696.827	15143.183	241.924	1.000	-46979.638	33585.984
		3	-4217.472	15143.183	241.924	1.000	-44500.283	36065.339
		4	19324.853	23943.475	241.924	1.000	-44367.863	83017.570
	2	1	6696.827	15143.183	241.924	1.000	-33585.984	46979.638
		3	2479.355	15143.183	241.924	1.000	-37803.456	42762.166
		4	26021.681	23943.475	241.924	1.000	-37671.036	89714.397
	3	1	4217.472	15143.183	241.924	1.000	-36065.339	44500.283
		2	-2479.355	15143.183	241.924	1.000	-42762.166	37803.456
		4	23542.325	23943.475	241.924	1.000	-40150.391	87235.042
	4	1	-19324.853	23943.475	241.924	1.000	-83017.570	44367.863
		2	-26021.681	23943.475	241.924	1.000	-89714.397	37671.036
		3	-23542.325	23943.475	241.924	1.000	-87235.042	40150.391
25	1	2	-1158.954	15143.183	241.924	1.000	-41441.765	39123.857
		3	-3013.939	15143.183	241.924	1.000	-43296.750	37268.872
		4	9723.042	23943.475	241.924	1.000	-53969.675	73415.758
	2	1	1158.954	15143.183	241.924	1.000	-39123.857	41441.765
		3	-1854.985	15143.183	241.924	1.000	-42137.796	38427.826
		4	10881.996	23943.475	241.924	1.000	-52810.721	74574.712
	3	1	3013.939	15143.183	241.924	1.000	-37268.872	43296.750
		2	1854.985	15143.183	241.924	1.000	-38427.826	42137.796
		4	12736.981	23943.475	241.924	1.000	-50955.736	76429.698
	4	1	-9723.042	23943.475	241.924	1.000	-73415.758	53969.675
		2	-10881.996	23943.475	241.924	1.000	-74574.712	52810.721
		3	-12736.981	23943.475	241.924	1.000	-76429.698	50955.736
50	1	2	1523.005	15143.183	241.924	1.000	-38759.806	41805.816
		3	-3191.130	15143.183	241.924	1.000	-43473.941	37091.681
		4	8409.491	23943.475	241.924	1.000	-55283.226	72102.207
	2	1	-1523.005	15143.183	241.924	1.000	-41805.816	38759.806
		3	-4714.135	15143.183	241.924	1.000	-44996.946	35568.676
		4	6886.486	23943.475	241.924	1.000	-56806.231	70579.202
	3	1	3191.130	15143.183	241.924	1.000	-37091.681	43473.941
		2	4714.135	15143.183	241.924	1.000	-35568.676	44996.946
		4	11600.620	23943.475	241.924	1.000	-52092.096	75293.337
	4	1	-8409.491	23943.475	241.924	1.000	-72102.207	55283.226
		2	-6886.486	23943.475	241.924	1.000	-70579.202	56806.231
		3	-11600.620	23943.475	241.924	1.000	-75293.337	52092.096
75	1	2	3302.833	15143.183	241.924	1.000	-36979.978	43585.644
		3	3942.759	15143.183	241.924	1.000	-36340.053	44225.570
		4	-1650.578	23943.475	241.924	1.000	-65343.295	62042.139
	2	1	-3302.833	15143.183	241.924	1.000	-43585.644	36979.978
		3	639.925	15143.183	241.924	1.000	-39642.886	40922.736
		4	-4953.411	23943.475	241.924	1.000	-68646.128	58739.306
	3	1	-3942.759	15143.183	241.924	1.000	-44225.570	36340.053
		2	-639.925	15143.183	241.924	1.000	-40922.736	39642.886
		4	-5593.336	23943.475	241.924	1.000	-69286.053	58099.380
	4	1	1650.578	23943.475	241.924	1.000	-62042.139	65343.295
		2	4953.411	23943.475	241.924	1.000	-58739.306	68646.128
		3	5593.336	23943.475	241.924	1.000	-58099.380	69286.053
90	1	2	-35967.680	15143.183	241.924	.110	-76250.491	4315.131
		3	8675.536	15143.183	241.924	1.000	-31607.275	48958.347
		4	-109524.166*	23943.475	241.924	.000	-173216.882	-45831.449
	2	1	35967.680	15143.183	241.924	.110	-4315.131	76250.491
		3	44643.216*	15143.183	241.924	.021	4360.405	84926.027
		4	-73556.486*	23943.475	241.924	.014	-137249.202	-9863.769
	3	1	-8675.536	15143.183	241.924	1.000	-48958.347	31607.275
		2	-44643.216*	15143.183	241.924	.021	-84926.027	-4360.405
		4	-118199.702*	23943.475	241.924	.000	-181892.418	-54506.985
	4	1	109524.166*	23943.475	241.924	.000	45831.449	173216.882
		2	73556.486*	23943.475	241.924	.014	9863.769	137249.202
		3	118199.702*	23943.475	241.924	.000	54506.985	181892.418

Based on estimated marginal means

*. The mean difference is significant at the .05 level.

a. Dependent Variable: IY_CRT_A.

c. Adjustment for multiple comparisons: Bonferroni.

Table A.39. Site * group interactions in polar moment of inertia of cortical area. 1 = Control, 2 = LB, 3 = SSMD, 4 = MC3.

site	(I) 1:CTRL, 2:LB, 3:SSMD, 4:MC3	(J) 1:CTRL, 2:LB, 3: SSMD, 4:MC3	Mean Difference (I-J)	Std. Error	df	Sig.[c]	95% Confidence Interval for Difference[c] Lower Bound	Upper Bound
10	1	2	-10618.995	22985.249	253.415	1.000	-71739.744	50501.755
		3	-8640.680	22985.249	253.415	1.000	-69761.430	52480.069
		4	26524.395	36342.870	253.415	1.000	-70115.995	123164.785
	2	1	10618.995	22985.249	253.415	1.000	-50501.755	71739.744
		3	1978.314	22985.249	253.415	1.000	-59142.435	63099.064
		4	37143.390	36342.870	253.415	1.000	-59497.000	133783.780
	3	1	8640.680	22985.249	253.415	1.000	-52480.069	69761.430
		2	-1978.314	22985.249	253.415	1.000	-63099.064	59142.435
		4	35165.075	36342.870	253.415	1.000	-61475.315	131805.465
	4	1	-26524.395	36342.870	253.415	1.000	-123164.785	70115.995
		2	-37143.390	36342.870	253.415	1.000	-133783.780	59497.000
		3	-35165.075	36342.870	253.415	1.000	-131805.465	61475.315
25	1	2	-530.479	22985.249	253.415	1.000	-61651.228	60590.270
		3	-4304.247	22985.249	253.415	1.000	-65424.996	56816.502
		4	11276.554	36342.870	253.415	1.000	-85363.836	107916.944
	2	1	530.479	22985.249	253.415	1.000	-60590.270	61651.228
		3	-3773.768	22985.249	253.415	1.000	-64894.517	57346.982
		4	11807.033	36342.870	253.415	1.000	-84833.357	108447.423
	3	1	4304.247	22985.249	253.415	1.000	-56816.502	65424.996
		2	3773.768	22985.249	253.415	1.000	-57346.982	64894.517
		4	15580.801	36342.870	253.415	1.000	-81059.589	112221.191
	4	1	-11276.554	36342.870	253.415	1.000	-107916.944	85363.836
		2	-11807.033	36342.870	253.415	1.000	-108447.423	84833.357
		3	-15580.801	36342.870	253.415	1.000	-112221.191	81059.589
50	1	2	7803.254	22985.249	253.415	1.000	-53317.495	68924.003
		3	-857.053	22985.249	253.415	1.000	-61977.803	60263.696
		4	14899.764	36342.870	253.415	1.000	-81740.626	111540.154
	2	1	-7803.254	22985.249	253.415	1.000	-68924.003	53317.495
		3	-8660.307	22985.249	253.415	1.000	-69781.057	52460.442
		4	7096.509	36342.870	253.415	1.000	-89543.881	103736.899
	3	1	857.053	22985.249	253.415	1.000	-60263.696	61977.803
		2	8660.307	22985.249	253.415	1.000	-52460.442	69781.057
		4	15756.817	36342.870	253.415	1.000	-80883.573	112397.207
	4	1	-14899.764	36342.870	253.415	1.000	-111540.154	81740.626
		2	-7096.509	36342.870	253.415	1.000	-103736.899	89543.881
		3	-15756.817	36342.870	253.415	1.000	-112397.207	80883.573
75	1	2	5829.751	22985.249	253.415	1.000	-55290.998	66950.500
		3	5084.002	22985.249	253.415	1.000	-56036.748	66204.751
		4	-2116.755	36342.870	253.415	1.000	-98757.145	94523.635
	2	1	-5829.751	22985.249	253.415	1.000	-66950.500	55290.998
		3	-745.749	22985.249	253.415	1.000	-61866.499	60375.000
		4	-7946.506	36342.870	253.415	1.000	-104586.896	88693.884
	3	1	-5084.002	22985.249	253.415	1.000	-66204.751	56036.748
		2	745.749	22985.249	253.415	1.000	-60375.000	61866.499
		4	-7200.757	36342.870	253.415	1.000	-103841.147	89439.633
	4	1	2116.755	36342.870	253.415	1.000	-94523.635	98757.145
		2	7946.506	36342.870	253.415	1.000	-88693.884	104586.896
		3	7200.757	36342.870	253.415	1.000	-89439.633	103841.147
90	1	2	-60418.997	22985.249	253.415	.055	-121539.747	701.752
		3	9708.908	22985.249	253.415	1.000	-51411.841	70829.657
		4	-185032.699*	36342.870	253.415	.000	-281673.089	-88392.309
	2	1	60418.997	22985.249	253.415	.055	-701.752	121539.747
		3	70127.905*	22985.249	253.415	.015	9007.156	131248.655
		4	-124613.702*	36342.870	253.415	.004	-221254.092	-27973.312
	3	1	-9708.908	22985.249	253.415	1.000	-70829.657	51411.841
		2	-70127.905*	22985.249	253.415	.015	-131248.655	-9007.156
		4	-194741.607*	36342.870	253.415	.000	-291381.997	-98101.217
	4	1	185032.699*	36342.870	253.415	.000	88392.309	281673.089
		2	124613.702*	36342.870	253.415	.004	27973.312	221254.092
		3	194741.607*	36342.870	253.415	.000	98101.217	291381.997

Based on estimated marginal means

*. The mean difference is significant at the .05 level.

a. Dependent Variable: IP_CRT_A.

c. Adjustment for multiple comparisons: Bonferroni.

Table A.40. Site * group interactions in cortical moment of resistance (x-axis). 1 = Control, 2 = LB, 3 = SSMD, 4 = MC3.

site	(I) 1:CTRL, 2:LB, 3:SSMD, 4:MC3	(J) 1:CTRL, 2:LB, 3: SSMD, 4:MC3	Mean Difference (I-J)	Std. Error	df	Sig.[c]	95% Confidence Interval for Difference[c] Lower Bound	Upper Bound
10	1	2	-148.681	317.560	264.808	1.000	-992.828	695.465
		3	-174.594	317.560	264.808	1.000	-1018.740	669.552
		4	421.302	502.107	264.808	1.000	-913.411	1756.014
	2	1	148.681	317.560	264.808	1.000	-695.465	992.828
		3	-25.913	317.560	264.808	1.000	-870.059	818.234
		4	569.983	502.107	264.808	1.000	-764.729	1904.695
	3	1	174.594	317.560	264.808	1.000	-669.552	1018.740
		2	25.913	317.560	264.808	1.000	-818.234	870.059
		4	595.896	502.107	264.808	1.000	-738.817	1930.608
	4	1	-421.302	502.107	264.808	1.000	-1756.014	913.411
		2	-569.983	502.107	264.808	1.000	-1904.695	764.729
		3	-595.896	502.107	264.808	1.000	-1930.608	738.817
25	1	2	43.698	317.560	264.808	1.000	-800.449	887.844
		3	-35.820	317.560	264.808	1.000	-879.966	808.327
		4	81.091	502.107	264.808	1.000	-1253.622	1415.803
	2	1	-43.698	317.560	264.808	1.000	-887.844	800.449
		3	-79.517	317.560	264.808	1.000	-923.664	764.629
		4	37.393	502.107	264.808	1.000	-1297.319	1372.106
	3	1	35.820	317.560	264.808	1.000	-808.327	879.966
		2	79.517	317.560	264.808	1.000	-764.629	923.664
		4	116.910	502.107	264.808	1.000	-1217.802	1451.623
	4	1	-81.091	502.107	264.808	1.000	-1415.803	1253.622
		2	-37.393	502.107	264.808	1.000	-1372.106	1297.319
		3	-116.910	502.107	264.808	1.000	-1451.623	1217.802
50	1	2	233.181	317.560	264.808	1.000	-610.965	1077.327
		3	70.812	317.560	264.808	1.000	-773.334	914.959
		4	218.238	502.107	264.808	1.000	-1116.474	1552.951
	2	1	-233.181	317.560	264.808	1.000	-1077.327	610.965
		3	-162.368	317.560	264.808	1.000	-1006.515	681.778
		4	-14.943	502.107	264.808	1.000	-1349.655	1319.770
	3	1	-70.812	317.560	264.808	1.000	-914.959	773.334
		2	162.368	317.560	264.808	1.000	-681.778	1006.515
		4	147.426	502.107	264.808	1.000	-1187.287	1482.138
	4	1	-218.238	502.107	264.808	1.000	-1552.951	1116.474
		2	14.943	502.107	264.808	1.000	-1319.770	1349.655
		3	-147.426	502.107	264.808	1.000	-1482.138	1187.287
75	1	2	139.938	317.560	264.808	1.000	-704.209	984.084
		3	88.413	317.560	264.808	1.000	-755.733	932.559
		4	87.786	502.107	264.808	1.000	-1246.926	1422.499
	2	1	-139.938	317.560	264.808	1.000	-984.084	704.209
		3	-51.525	317.560	264.808	1.000	-895.671	792.621
		4	-52.151	502.107	264.808	1.000	-1386.864	1282.561
	3	1	-88.413	317.560	264.808	1.000	-932.559	755.733
		2	51.525	317.560	264.808	1.000	-792.621	895.671
		4	-.626	502.107	264.808	1.000	-1335.339	1334.086
	4	1	-87.786	502.107	264.808	1.000	-1422.499	1246.926
		2	52.151	502.107	264.808	1.000	-1282.561	1386.864
		3	.626	502.107	264.808	1.000	-1334.086	1335.339
90	1	2	-899.889*	317.560	264.808	.030	-1744.035	-55.742
		3	-79.859	317.560	264.808	1.000	-924.005	764.287
		4	-2153.299*	502.107	264.808	.000	-3488.012	-818.587
	2	1	899.889*	317.560	264.808	.030	55.742	1744.035
		3	820.030	317.560	264.808	.062	-24.117	1664.176
		4	-1253.411	502.107	264.808	.079	-2588.123	81.302
	3	1	79.859	317.560	264.808	1.000	-764.287	924.005
		2	-820.030	317.560	264.808	.062	-1664.176	24.117
		4	-2073.440*	502.107	264.808	.000	-3408.153	-738.728
	4	1	2153.299*	502.107	264.808	.000	818.587	3488.012
		2	1253.411	502.107	264.808	.079	-81.302	2588.123
		3	2073.440*	502.107	264.808	.000	738.728	3408.153

Based on estimated marginal means

*. The mean difference is significant at the .05 level.

a. Dependent Variable: RX_CRT_A.

c. Adjustment for multiple comparisons: Bonferroni.

Table A.41. Site * group interactions in cortical moment of resistance (y-axis). 1 = Control, 2 = LB, 3 = SSMD, 4 = MC3.

site	(I) 1:CTRL, 2:LB, 3:SSMD, 4:MC3	(J) 1:CTRL, 2:LB, 3: SSMD, 4:MC3	Mean Difference (I-J)	Std. Error	df	Sig.[c]	95% Confidence Interval for Difference[c] Lower Bound	Upper Bound
10	1	2	-238.960	420.329	235.009	1.000	-1357.364	879.443
		3	-102.133	420.329	235.009	1.000	-1220.536	1016.270
		4	532.460	664.599	235.009	1.000	-1235.891	2300.810
	2	1	238.960	420.329	235.009	1.000	-879.443	1357.364
		3	136.827	420.329	235.009	1.000	-981.576	1255.230
		4	771.420	664.599	235.009	1.000	-996.930	2539.771
	3	1	102.133	420.329	235.009	1.000	-1016.270	1220.536
		2	-136.827	420.329	235.009	1.000	-1255.230	981.576
		4	634.593	664.599	235.009	1.000	-1133.757	2402.944
	4	1	-532.460	664.599	235.009	1.000	-2300.810	1235.891
		2	-771.420	664.599	235.009	1.000	-2539.771	996.930
		3	-634.593	664.599	235.009	1.000	-2402.944	1133.757
25	1	2	-83.810	420.329	235.009	1.000	-1202.213	1034.593
		3	-70.038	420.329	235.009	1.000	-1188.441	1048.365
		4	269.921	664.599	235.009	1.000	-1498.429	2038.272
	2	1	83.810	420.329	235.009	1.000	-1034.593	1202.213
		3	13.772	420.329	235.009	1.000	-1104.632	1132.175
		4	353.731	664.599	235.009	1.000	-1414.620	2122.081
	3	1	70.038	420.329	235.009	1.000	-1048.365	1188.441
		2	-13.772	420.329	235.009	1.000	-1132.175	1104.632
		4	339.959	664.599	235.009	1.000	-1428.391	2108.310
	4	1	-269.921	664.599	235.009	1.000	-2038.272	1498.429
		2	-353.731	664.599	235.009	1.000	-2122.081	1414.620
		3	-339.959	664.599	235.009	1.000	-2108.310	1428.391
50	1	2	57.478	420.329	235.009	1.000	-1060.925	1175.881
		3	-67.884	420.329	235.009	1.000	-1186.287	1050.519
		4	289.133	664.599	235.009	1.000	-1479.217	2057.484
	2	1	-57.478	420.329	235.009	1.000	-1175.881	1060.925
		3	-125.362	420.329	235.009	1.000	-1243.765	993.041
		4	231.656	664.599	235.009	1.000	-1536.695	2000.006
	3	1	67.884	420.329	235.009	1.000	-1050.519	1186.287
		2	125.362	420.329	235.009	1.000	-993.041	1243.765
		4	357.017	664.599	235.009	1.000	-1411.333	2125.368
	4	1	-289.133	664.599	235.009	1.000	-2057.484	1479.217
		2	-231.656	664.599	235.009	1.000	-2000.006	1536.695
		3	-357.017	664.599	235.009	1.000	-2125.368	1411.333
75	1	2	212.521	420.329	235.009	1.000	-905.882	1330.924
		3	216.508	420.329	235.009	1.000	-901.895	1334.911
		4	260.749	664.599	235.009	1.000	-1507.602	2029.099
	2	1	-212.521	420.329	235.009	1.000	-1330.924	905.882
		3	3.987	420.329	235.009	1.000	-1114.416	1122.390
		4	48.228	664.599	235.009	1.000	-1720.123	1816.578
	3	1	-216.508	420.329	235.009	1.000	-1334.911	901.895
		2	-3.987	420.329	235.009	1.000	-1122.390	1114.416
		4	44.241	664.599	235.009	1.000	-1724.110	1812.591
	4	1	-260.749	664.599	235.009	1.000	-2029.099	1507.602
		2	-48.228	664.599	235.009	1.000	-1816.578	1720.123
		3	-44.241	664.599	235.009	1.000	-1812.591	1724.110
90	1	2	-977.021	420.329	235.009	.126	-2095.424	141.382
		3	-29.280	420.329	235.009	1.000	-1147.683	1089.123
		4	-2105.764*	664.599	235.009	.010	-3874.114	-337.413
	2	1	977.021	420.329	235.009	.126	-141.382	2095.424
		3	947.742	420.329	235.009	.150	-170.662	2066.145
		4	-1128.742	664.599	235.009	.545	-2897.093	639.608
	3	1	29.280	420.329	235.009	1.000	-1089.123	1147.683
		2	-947.742	420.329	235.009	.150	-2066.145	170.662
		4	-2076.484*	664.599	235.009	.012	-3844.834	-308.133
	4	1	2105.764*	664.599	235.009	.010	337.413	3874.114
		2	1128.742	664.599	235.009	.545	-639.608	2897.093
		3	2076.484*	664.599	235.009	.012	308.133	3844.834

Based on estimated marginal means

*. The mean difference is significant at the .05 level.

a. Dependent Variable: RY_CRT_A.

c. Adjustment for multiple comparisons: Bonferroni.

Table A.42. Site * group interactions in polar moment of resistance. 1 = Control, 2 = LB, 3 = SSMD, 4 = MC3.

site	(I) 1:CTRL, 2:LB, 3:SSMD, 4:MC3	(J) 1:CTRL, 2:LB, 3: SSMD, 4:MC3	Mean Difference (I-J)	Std. Error	df	Sig.[c]	95% Confidence Interval for Difference[c]	
							Lower Bound	Upper Bound
10	1	2	-223.949	605.161	236.675	1.000	-1834.051	1386.152
		3	-185.107	605.161	236.675	1.000	-1795.209	1424.994
		4	863.631	956.843	236.675	1.000	-1682.163	3409.425
	2	1	223.949	605.161	236.675	1.000	-1386.152	1834.051
		3	38.842	605.161	236.675	1.000	-1571.259	1648.943
		4	1087.580	956.843	236.675	1.000	-1458.214	3633.374
	3	1	185.107	605.161	236.675	1.000	-1424.994	1795.209
		2	-38.842	605.161	236.675	1.000	-1648.943	1571.259
		4	1048.738	956.843	236.675	1.000	-1497.056	3594.532
	4	1	-863.631	956.843	236.675	1.000	-3409.425	1682.163
		2	-1087.580	956.843	236.675	1.000	-3633.374	1458.214
		3	-1048.738	956.843	236.675	1.000	-3594.532	1497.056
25	1	2	-18.967	605.161	236.675	1.000	-1629.068	1591.134
		3	-38.033	605.161	236.675	1.000	-1648.134	1572.068
		4	357.260	956.843	236.675	1.000	-2188.534	2903.054
	2	1	18.967	605.161	236.675	1.000	-1591.134	1629.068
		3	-19.066	605.161	236.675	1.000	-1629.167	1591.035
		4	376.227	956.843	236.675	1.000	-2169.567	2922.021
	3	1	38.033	605.161	236.675	1.000	-1572.068	1648.134
		2	19.066	605.161	236.675	1.000	-1591.035	1629.167
		4	395.293	956.843	236.675	1.000	-2150.501	2941.087
	4	1	-357.260	956.843	236.675	1.000	-2903.054	2188.534
		2	-376.227	956.843	236.675	1.000	-2922.021	2169.567
		3	-395.293	956.843	236.675	1.000	-2941.087	2150.501
50	1	2	313.898	605.161	236.675	1.000	-1296.203	1923.999
		3	127.034	605.161	236.675	1.000	-1483.068	1737.135
		4	616.480	956.843	236.675	1.000	-1929.314	3162.273
	2	1	-313.898	605.161	236.675	1.000	-1923.999	1296.203
		3	-186.864	605.161	236.675	1.000	-1796.966	1423.237
		4	302.582	956.843	236.675	1.000	-2243.212	2848.375
	3	1	-127.034	605.161	236.675	1.000	-1737.135	1483.068
		2	186.864	605.161	236.675	1.000	-1423.237	1796.966
		4	489.446	956.843	236.675	1.000	-2056.348	3035.240
	4	1	-616.480	956.843	236.675	1.000	-3162.273	1929.314
		2	-302.582	956.843	236.675	1.000	-2848.375	2243.212
		3	-489.446	956.843	236.675	1.000	-3035.240	2056.348
75	1	2	342.107	605.161	236.675	1.000	-1267.994	1952.209
		3	301.281	605.161	236.675	1.000	-1308.821	1911.382
		4	509.914	956.843	236.675	1.000	-2035.880	3055.707
	2	1	-342.107	605.161	236.675	1.000	-1952.209	1267.994
		3	-40.827	605.161	236.675	1.000	-1650.928	1569.275
		4	167.806	956.843	236.675	1.000	-2377.988	2713.600
	3	1	-301.281	605.161	236.675	1.000	-1911.382	1308.821
		2	40.827	605.161	236.675	1.000	-1569.275	1650.928
		4	208.633	956.843	236.675	1.000	-2337.161	2754.427
	4	1	-509.914	956.843	236.675	1.000	-3055.707	2035.880
		2	-167.806	956.843	236.675	1.000	-2713.600	2377.988
		3	-208.633	956.843	236.675	1.000	-2754.427	2337.161
90	1	2	-1425.749	605.161	236.675	.116	-3035.851	184.352
		3	-11.525	605.161	236.675	1.000	-1621.627	1598.576
		4	-3724.253*	956.843	236.675	.001	-6270.046	-1178.459
	2	1	1425.749	605.161	236.675	.116	-184.352	3035.851
		3	1414.224	605.161	236.675	.122	-195.878	3024.325
		4	-2298.503	956.843	236.675	.102	-4844.297	247.290
	3	1	11.525	605.161	236.675	1.000	-1598.576	1621.627
		2	-1414.224	605.161	236.675	.122	-3024.325	195.878
		4	-3712.727*	956.843	236.675	.001	-6258.521	-1166.933
	4	1	3724.253*	956.843	236.675	.001	1178.459	6270.046
		2	2298.503	956.843	236.675	.102	-247.290	4844.297
		3	3712.727*	956.843	236.675	.001	1166.933	6258.521

Based on estimated marginal means

*. The mean difference is significant at the .05 level.

a. Dependent Variable: RP_CRT_A.

c. Adjustment for multiple comparisons: Bonferroni.

Table A.43. Site * group interactions in cortical area. 1 = Control, 2 = LB, 3 = SSMD, 4 = MC3.

site	(I) 1:CTRL, 2:LB, 3:SSMD, 4:MC3	(J) 1:CTRL, 2:LB, 3: SSMD, 4:MC3	Mean Difference (I-J)	Std. Error	df	Sig.[c]	95% Confidence Interval for Difference[c] Lower Bound	95% Confidence Interval for Difference[c] Upper Bound
10	1	2	-20.176	44.285	221.349	1.000	-138.070	97.718
		3	-18.253	44.285	221.349	1.000	-136.147	99.641
		4	68.561	70.021	221.349	1.000	-117.846	254.968
	2	1	20.176	44.285	221.349	1.000	-97.718	138.070
		3	1.923	44.285	221.349	1.000	-115.971	119.817
		4	88.737	70.021	221.349	1.000	-97.671	275.144
	3	1	18.253	44.285	221.349	1.000	-99.641	136.147
		2	-1.923	44.285	221.349	1.000	-119.817	115.971
		4	86.814	70.021	221.349	1.000	-99.593	273.221
	4	1	-68.561	70.021	221.349	1.000	-254.968	117.846
		2	-88.737	70.021	221.349	1.000	-275.144	97.671
		3	-86.814	70.021	221.349	1.000	-273.221	99.593
25	1	2	7.840	44.285	221.349	1.000	-110.054	125.734
		3	-5.800	44.285	221.349	1.000	-123.694	112.094
		4	36.224	70.021	221.349	1.000	-150.183	222.631
	2	1	-7.840	44.285	221.349	1.000	-125.734	110.054
		3	-13.640	44.285	221.349	1.000	-131.534	104.254
		4	28.384	70.021	221.349	1.000	-158.023	214.791
	3	1	5.800	44.285	221.349	1.000	-112.094	123.694
		2	13.640	44.285	221.349	1.000	-104.254	131.534
		4	42.024	70.021	221.349	1.000	-144.383	228.431
	4	1	-36.224	70.021	221.349	1.000	-222.631	150.183
		2	-28.384	70.021	221.349	1.000	-214.791	158.023
		3	-42.024	70.021	221.349	1.000	-228.431	144.383
50	1	2	31.158	44.285	221.349	1.000	-86.736	149.052
		3	2.776	44.285	221.349	1.000	-115.118	120.670
		4	64.428	70.021	221.349	1.000	-121.979	250.835
	2	1	-31.158	44.285	221.349	1.000	-149.052	86.736
		3	-28.382	44.285	221.349	1.000	-146.276	89.512
		4	33.270	70.021	221.349	1.000	-153.137	219.677
	3	1	-2.776	44.285	221.349	1.000	-120.670	115.118
		2	28.382	44.285	221.349	1.000	-89.512	146.276
		4	61.652	70.021	221.349	1.000	-124.755	248.059
	4	1	-64.428	70.021	221.349	1.000	-250.835	121.979
		2	-33.270	70.021	221.349	1.000	-219.677	153.137
		3	-61.652	70.021	221.349	1.000	-248.059	124.755
75	1	2	14.942	44.285	221.349	1.000	-102.952	132.836
		3	10.616	44.285	221.349	1.000	-107.278	128.510
		4	4.188	70.021	221.349	1.000	-182.219	190.595
	2	1	-14.942	44.285	221.349	1.000	-132.836	102.952
		3	-4.326	44.285	221.349	1.000	-122.220	113.568
		4	-10.754	70.021	221.349	1.000	-197.161	175.653
	3	1	-10.616	44.285	221.349	1.000	-128.510	107.278
		2	4.326	44.285	221.349	1.000	-113.568	122.220
		4	-6.428	70.021	221.349	1.000	-192.835	179.979
	4	1	-4.188	70.021	221.349	1.000	-190.595	182.219
		2	10.754	70.021	221.349	1.000	-175.653	197.161
		3	6.428	70.021	221.349	1.000	-179.979	192.835
90	1	2	-114.671	44.285	221.349	.062	-232.565	3.224
		3	8.473	44.285	221.349	1.000	-109.422	126.367
		4	-304.282*	70.021	221.349	.000	-490.690	-117.875
	2	1	114.671	44.285	221.349	.062	-3.224	232.565
		3	123.143*	44.285	221.349	.035	5.249	241.038
		4	-189.612*	70.021	221.349	.044	-376.019	-3.204
	3	1	-8.473	44.285	221.349	1.000	-126.367	109.422
		2	-123.143*	44.285	221.349	.035	-241.038	-5.249
		4	-312.755*	70.021	221.349	.000	-499.162	-126.348
	4	1	304.282*	70.021	221.349	.000	117.875	490.690
		2	189.612*	70.021	221.349	.044	3.204	376.019
		3	312.755*	70.021	221.349	.000	126.348	499.162

Based on estimated marginal means

*. The mean difference is significant at the .05 level.

a. Dependent Variable: CRT_A.

c. Adjustment for multiple comparisons: Bonferroni.